Computation of Multivariate Barrier Crossing Probability, and Its Applications in Finance

by

Joonghee Huh

A thesis
presented to the University of Waterloo
in fulfilment of the
thesis requirement for the degree of
Doctor of Philosophy
in
Statistics

Waterloo, Ontario, Canada, 2007

Author's Declaration for Electronic Submission of a Thesis

I hearby declare that I am the sole author of this thesis. This is a true copy of the thesis, including my required final revisions, as accepted by my examiners.

I understand that my thesis may be made electronically available to the public.

Acknowledgement

I praise God and my Lord Jesus Christ for enabling me to complete this thesis. Only by His grace, I have been able to come this far.

I would like to thank Dr. Adam Kolkiewicz for supervising my thesis research with patience. He has been a great mentor and a role model in my academic endeavours. He also provided me with generous financial supports. I appreciate committee members Dr. Don McLeish and Dr. Weidong Tian for providing me with constructive comments. I also thank external examiners Dr. Ken Vetzal and Dr. Reg Kulperger for taking time to examine this thesis.

I am greatly indebted to my parents for their continual endless love and support they have shown me, and my brother Woonghee for being a great friend and mentor.

I give special thanks to my wife Joohyun for love and friendship, and especially for putting up with my endless hours of studies even immediately after the honeymoon.

I thank SungChul, WooChul, and Hyuntae for friendships developed while I was in Waterloo. Also, I thank Waterloo Korean Church and YoungNak Presbyterian Church of Toronto for providing me with an environment where I could grow spiritually during eight years of my graduate studies.

Abstract

In this thesis, we consider computational methods of finding exit probabilities for a class of multivariate stochastic processes. While there is an abundance of results for one-dimensional processes, for multivariate processes one has to rely on approximations or simulation methods. We adopt a Large Deviations approach in order to estimate barrier crossing probabilities of a multivariate Brownian Bridge. We use this approach in conjunction with numerical techniques to propose an efficient method of obtaining barrier crossing probabilities of a multivariate Brownian motion. Using numerical examples, we demonstrate that our method works better than other existing methods. We present applications of the proposed method in addressing problems in finance such as estimating default probabilities of several credit risky entities and pricing credit default swaps. We also extend our computational method to efficiently estimate a barrier crossing probability of a sum of Geometric Brownian motions. This allows us to perform a portfolio selection by maximizing a path-dependent utility function.

Contents

Chapter 1

Preliminaries

1.1 Introduction

Suppose that the variables $\{\mathbf{X}(t) \in R^d, 0 \leq t \leq T\}$ follow a d-dimensional continuous-time stochastic process for $0 \leq t \leq T$. In this thesis, we investigate procedures to compute the probability that components of this continuous time processes $\mathbf{X}(t)$ cross or touch pre-specified barriers at some time between 0 and T.

This type of problem is very relevant in finance, especially in pricing barrier-style options and credit risk derivatives. In an up-and-in barrier option, as soon as the underlying asset value hits a pre-specified barrier, the barrier option starts behaving like an European option. Also, in pricing credit risk derivatives using a structural type approach, computation of probability that the credit worthiness index of a firm reaches a default threshold is a crucial element.

We typically assume that the underlying variable follows a d-dimensional Brownian Motion process,

$$d\mathbf{X}(t) = \mu dt + \Sigma d\mathbf{W}(t), \tag{1.1}$$

where $\mathbf{X}(t)$ is a d-dimensional vector, $\mathbf{W}(t)$ represents a d-dimensional vector of standard Brownian Motions, and Σ is a $d \times d$ definite matrix of constants corresponding to a square root of an instantaneous variance-covariance matrix. Also, μ is a d-dimensional vector of constants. Let us denote by $\mathbf{x}$ the initial value of $\mathbf{X}$. We consider the probability that any of the components of $\mathbf{X}$ breaches its respective corresponding barrier or all the components breach their corresponding barriers within a given time horizon.

Simulation methods designed to determine an exit probability of a continuous-time stochastic process typically use some form of a discrete-time approximation. In particular, if $\{\mathbf{X}(t),\ t \in [0,T]\}$ is a diffusion process, such a discretization may be based on the Euler's scheme with a time step of size ϵ. Suppose that τ denotes the first time the process $\{\mathbf{X}(t),\ t \in [0,T]\}$ crosses a pre-specified, possibly time-dependent, deterministic barrier $\{b(t) \in R^d,\ t \in [0,T]\}$. Let $\mathbf{X}(t) = [X_1(t), \ldots X_d(t)]$ and $b(t) = [b_1(t), \ldots, b_d(t)]$. We assume $X_i(0) > b_i(0)$ for all $i = 1, \ldots, d$. We can represent the barrier crossing time τ as

$$\tau = \min(\tau^1, \ldots, \tau^d)$$

where $\tau^i = \inf\{t \mid X_i(t) \leq b_i(t)\}$ for $i = 1, \ldots, d$. In a naive simulation approach, the barrier crossing time τ can be approximated by the first time the discretized

process reaches the barrier

$$\hat{\tau} = \min(\hat{\tau}^1, \ldots, \hat{\tau}^d)$$

where

$$\begin{aligned} \hat{\tau}^1 &= \min\{i\epsilon : \ X_1(i\epsilon) \leq b_1(i\epsilon), i = 1, 2, \ldots, M\}, \\ &\vdots \\ \hat{\tau}^d &= \min\{i\epsilon : \ X_d(i\epsilon) \leq b_d(i\epsilon), i = 1, 2, \ldots, M\}, \end{aligned}$$

and $M = T/\epsilon$. However, in this method the estimate $\hat{\tau}$ will be biased in a sense that $E(\hat{\tau}) < \tau$. This is due to the fact that even if we know that the values of all the components of $\mathbf{X}(i\epsilon)$ and $\mathbf{X}((i+1)\epsilon)$ are greater than the respective barriers, there is still possibility that the process $\mathbf{X}$ may breach the barrier at some time between $i\epsilon$ and $(i+1)\epsilon$. Ignoring this possibility leads to a slow convergence of $\hat{\tau}$ to τ as the number of time steps goes to infinity. In practice, this is manifested by a non-negligible approximation error for finite values of M.

In order to refine the discrete-time approximation of the exit probability, we need to determine the probability that the process $\mathbf{X}$ crosses the barrier between discrete simulation times. This problem involves computation of the exit probability of a Brownian Bridge process, which describes the dynamics of a Brownian Motion when its end values are known. Currently analytical representations of the exit probability for a Brownian Bridge exist only if the dimension of the process does not exceed two. For higher dimensions we have to rely on approximations. In this context, asymptotic results based on the theory of Large Deviations have proven

to be particularly useful (for example, Baldi (1995), Baldi et al. (1999), Baldi and Caramellino (2002)). The existing results, however, are not sufficient for the general application in finance, as they usually deal with a standard Brownian Motion. In the thesis we demonstrate that a direct extension of the result obtained by Baldi to a general multivariate Brownian Motion does not capture the covariance structure of the process. This finding was the motivation for the new method that we present in the thesis. Our approach still uses the Large Deviations Theory to approximate exit probabilities but is more accurate than the existing methods, and it captures the correlation structure of the process.

In conjunction with the proposed method for a multivariate Brownian Bridge, we suggest an accurate and time-efficient simulation algorithm for computing exit probabilities of a multivariate correlated Brownian Motion process. In typical applications in finance, the method requires only a small number of subintervals. The algorithm allows us to compute directly the probability that in a portfolio of defaultable instruments at least one obligor defaults. It can also be extended to deal with the problem of finding the complete distribution of number of defaults for a portfolio. Such information is required to price instruments such as first or n^{th} to default.

This thesis presents five related contributions to the domain of computation of a multivariate barrier crossing probability. Firstly, we extend Baldi's framework to a correlated multidimensional Brownian Motion process and show that the approximation based on Baldi's approach does not take account into the effect of covariance of underlying processes. Secondly, we propose a new procedure based on the Large

Deviations Theory and demonstrate that our method gives us a quite reasonable approximation of the true barrier crossing probability. The main strengths of our method is the reasonable accuracy and that it provides a framework which is extendible beyond dimensionality of two. Also, it reflects correlation of the underlying processes. Thirdly, we provide various applications of this procedure in valuations of financial instruments and risk managements. Fourthly, we further develop the ideas from Baldi (1995) and Baldi and Caramellino (2002) to address a related issue of computing a barrier crossing probability of a sum of correlated Geometric Brownian Motions. Fifthly, we introduce a path-dependent utility function which depends on a probability that a wealth level falls below a certain threshold level during a given time horizon.

This thesis is organized in the following way. In Chapter 1, we provide an overview of the Large Deviations Theory and outline Baldi's framework for computing exit probabilities for a d-dimensional uncorrelated Brownian Motion process. We also summarize recent work that shows how the Large Deviations are used to solve problems in portfolio management, ruin theory, and credit risk. In Chapter 2, we present approximations of exit probabilities of a Brownian Bridge for one interval. We discuss the method proposed by Baldi and show shortcomings of this method. Then we propose a method and demonstrate that it gives more accurate estimates. In Chapter 3, we extend the idea from Chapter 2 to propose an algorithm for computing an exit probability of a multivariate Brownian Motion process, and show various extensions and applications. In Chapter 4, we consider a problem of computing exit probabilities with curved boundaries. In particular, we develop a

method of computing an exit probability of a sum of several Geometric Brownian Motions. As an application, we introduce a path-dependent utility function and find an optimal portfolio that maximizes this utility function. Finally, we conclude in Chapter 5 with some directions of possible future research extensions.

1.2 Overview of Large Deviations Theory

In this section, we outline fundamental concepts of the Large Deviations Theory and some applications to stochastic processes, finance, and insurance problems.

1.2.1 Introduction

The Law of Large Numbers says that, as the sample size increases to infinity, the sample mean approaches the true mean. Suppose that $X_1, X_2, \ldots$ is a sequence of *i.i.d.* random variables with a finite mean $E[X] = \mu$. Let $S_n = \frac{1}{n}\sum_{j=1}^{n} X_j$, $n \geq 1$. Then the Strong Law of Large Numbers says that

$$P[\lim_{n\to\infty} S_n = \mu] = 1. \tag{1.2}$$

Hence, it states that the sample mean, S_n, converges to the true mean μ as n goes to ∞. In the Large Deviations Theory, we are interested in how fast the sample mean converges to the true mean. Let us state this more precisely. Suppose that we fix a number $a > \mu$. From the Law of Large Numbers, we know that $P(S_n \geq a) \to 0$, as n goes to ∞, because of (1.2). In the Large Deviations Theory, we would like to investigate the rate at which this probability $P(S_n \geq a)$ decays to zero.

To illustrate this concept, we consider the case where $X_1, X_2, \ldots$ are *i.i.d.* random variables. Let us define the following functions:

$$M(\theta) = E(e^{\theta X_1}) \tag{1.3}$$

$$\ell(a) = -\log(\inf_{\theta} e^{-\theta a} M(\theta)) = \sup_{\theta}(\theta a - \log M(\theta)). \tag{1.4}$$

$M(\theta)$ is the moment generating function of the random variable X_1. We have assumed that $M(\theta)$ exists in a neighbourhood of 0. The function $\ell(a)$ is often referred as a Legendre-Fenchel transform. Note that $\ell(a)$ is always non-negative, and this is evident by setting $\theta = 0$ in (1.4). Suppose that the supremum in (1.4) is attained at a point θ^* in the interior of the interval where $M(\theta)$ is finite. Then $M(\theta)$ is differentiable at θ^*, and we obtain

$$\ell(a) = -\log E(e^{\theta^*(X_1 - a)}). \tag{1.5}$$

Now we can state Cramér's theorem (Shwartz and Weiss (1995)).

Theorem 1.2.1 (Cramér's) *Consider a sequence $X_1, X_2, \ldots$ of i.i.d. random variables. For every $a > E(X_1)$ and positive integer n, we have*

$$P(\frac{X_1 + X_2 + \ldots + X_n}{n} \geq a) \leq e^{-n\ell(a)} \tag{1.6}$$

where $\ell(a)$ is defined in (1.4). Assume that $M(\theta) < \infty$ for θ in some neighbourhood of 0, and that (1.5) holds for some θ^* in the interior of that neighbourhood. Then, for every $\epsilon > 0$ there exists an integer n_0 such that whenever $n > n_0$,

$$P(\frac{X_1 + X_2 + \ldots + X_n}{n} \geq a) \geq e^{-n(\ell(a)+\epsilon)}. \tag{1.7}$$

In addition, (1.6) and (1.7) together imply that

$$P(\frac{X_1 + X_2 + \ldots + X_n}{n} \geq a) = e^{-n\ell(a)+o(n)}. \tag{1.8}$$

Proof of this theorem can be found, for example in Section 1.2 of Shwartz and Weiss (1995).

1.2.2 Large Deviations Principle

The Large Deviations Principle (LDP) characterizes the limiting behavior, as $\epsilon \to 0$, of a family of probability measures $\{\mu_\epsilon\}$ on $\{\mathcal{X}, \mathcal{B}\}$, where $\mathcal{X}$ is a topological space and $\mathcal{B}$ is a Borel σ-algebra. For any set Γ, we use the notations Γ° and $\overline{\Gamma}$ to denote the interior and closure of Γ, respectively. We now state the definition of Large Deviations Principle (Dembo and Zeitouni (1993)).

Definition 1.2.1 *$\{\mu_\epsilon\}$ satisfies the Large Deviations Principle with a rate function I if for all $\Gamma \in \mathcal{B}$,*

$$-\inf_{x\in\Gamma^\circ} I(x) \leq \liminf_{\epsilon\to 0} \epsilon \log \mu_\epsilon(\Gamma) \tag{1.9}$$

$$-\inf_{x\in\overline{\Gamma}} I(x) \geq \limsup_{\epsilon\to 0} \epsilon \log \mu_\epsilon(\Gamma). \tag{1.10}$$

The following lemma is trivial but useful later in this thesis.

Lemma 1.2.1 *Suppose that $\{\mu_\epsilon\}$ satisfies the Large Deviations Principle with a rate function I. Let $\Gamma_3 = \Gamma_1 \cap \Gamma_2$, where $\Gamma_1, \Gamma_2 \subseteq \mathcal{B}$. Then, the following inequality*

holds for Γ_3.

$$-\inf_{x\in\Gamma_3^\circ} I(x) \leq \liminf_{\epsilon\to 0} \epsilon \log \mu_\epsilon(\Gamma_3) \tag{1.11}$$

$$-\inf_{x\in\overline{\Gamma_3}} I(x) \geq \limsup_{\epsilon\to 0} \epsilon \log \mu_\epsilon(\Gamma_3) \tag{1.12}$$

This lemma is trivially proved by noting that $\Gamma_3 \subseteq \mathcal{B}$, because $\mathcal{B}$ is a σ-algebra. $\square$

1.2.3 Large Deviations Principle for Diffusion Processes

In this section, we provide a concise review of Large Deviations Theory that is relevant in computation of an exit probability of a diffusion process. Suppose that we have a d-dimensional stochastic process $\mathbf{X}(t)$ that satisfies

$$d\mathbf{X}(t) = b(\mathbf{X}(t), t)dt + \sqrt{\epsilon}\Sigma(\mathbf{X}(t), t)d\mathbf{W}(t), \tag{1.13}$$

where $b(\mathbf{X}(t), t)$ is Lipschitz continuous in $\mathbf{X}(t)$ and uniformly in t. Also, $\{\mathbf{W}(t), t \geq s\}$ is a d-dimensional standard Brownian Motion and s is the initial time, and ϵ is a real number.

Suppose that $\mathbf{X}(s) = \mathbf{x}$ and that the barriers are represented by $(d-1)$ dimensional hyperplanes, denoted by $B_i(t, x_1, \ldots, x_d) = 0$ for $i = 1, \ldots, n$, where n is the number of barriers and $(x_1, \ldots, x_d) \in R^d$. In the case $d = 2$, the barriers consist of a set of lines. When $d = 1$, a barrier is equivalent to a point in R^1. In the R^d space, we denote by D an open set defined by the $(d-1)$ dimensional hyperplanes

$B_i(t, x_1, \ldots, x_d) = 0$ for $i = 1, \ldots, n$. Assuming that the barriers are constant functions of time t, we can write

$$D = \{(x_1, \ldots, x_d) \in R^d \mid B_i(x_1, \ldots, x_d) > 0 \text{ for } i = 1, \ldots, n\}.$$

This set can be either bounded or unbounded depending on the barriers. Without loss of generality, we assume that $\mathbf{X}(s) = \mathbf{x}$ where $\mathbf{x} \in D$. Also we have $\tau = \inf\{t : \mathbf{X}(t) \notin D\}$, the first time the process $\mathbf{X}(t)$ goes outside of the region D. For the given diffusion process (1.13), we are interested in finding $P^{\epsilon}_{\mathbf{X},s}\{\tau \leq T\} = Prob\{\mathbf{X}(t) \notin D \text{ for some } t \in (s, T) \mid \mathbf{X}(s) = \mathbf{x}\}$. Here we have the notation $P^{\epsilon}_{\mathbf{X},s}\{\tau \leq T\}$ with a superscript ϵ to signify that the diffusion process of $\mathbf{X}(t)$ involves a parameter ϵ, and the asymptotic result from the Large Deviations Theory holds as $\epsilon \to 0$.

Theorem 2.1 and Theorem 4.4 in Baldi (1995) provide a general asymptotic formula for approximating this probability using the Large Deviation Theory as ϵ approaches 0.

Theorem 1.2.2 *We have*

$$\begin{aligned} P^{\epsilon}_{\mathbf{X},s}(\tau \leq T) &= \exp(-\frac{u(\mathbf{x}, s)}{\epsilon} \exp(-\omega(\mathbf{x}, s)) \\ &\times \quad (1 + \psi_1(\mathbf{x}, s)\epsilon + \ldots + \psi_m(\mathbf{x}, s)\epsilon^m + o(\epsilon^m)). \end{aligned}$$

with

$$\exp(-\omega(\mathbf{x}, s)) = (1 - s)^{(n-1)/2} \det((1 - s)I - (t(\mathbf{x}, s) - s)A^{-1}B)^{-1/2}$$

where A, B, and ψ's are defined in Baldi(1995).

With the assumption that the boundary is a hyperplane, the formula reduces to the following one

$$P^{\epsilon}_{\mathbf{X},s}\{\tau \leq T\} = \exp(-\frac{u(\mathbf{x},s)}{\epsilon})(1+o(\epsilon^m)) \tag{1.14}$$

for every $m > 0$, where

$$u(\mathbf{x},s) = \inf_{\gamma \in \Gamma_{\mathbf{x},s}} J_{s,T}(\gamma), \tag{1.15}$$

$$\begin{aligned}\Gamma_{\mathbf{x},s} \quad = \quad & \{\text{absolutely continuous functions } \gamma \in R^d \text{ on } [s,T] \text{ such that } \gamma(s) = \mathbf{x} \text{ and} \\ & \gamma(r) \in D^C \text{ for some } r \in (s,T)\},\end{aligned} \tag{1.16}$$

and D^C is the complement of D. Here $\Gamma_{\mathbf{x},s}$ represents a set of all absolutely continuous paths $\gamma(t), s < t < T$, such that $\gamma(s) = \mathbf{x}$ and γ goes outside of the open set D between s and T. $J_{s,T}(\gamma)$ in equation (1.15) is often referred as an action functional and is defined as follows:

$$J_{s,T}(\gamma) = \frac{1}{2}\int_s^T < A^{-1}(\gamma_t,t)(\gamma_t^{'} - b(\gamma_t,t)), \gamma_t^{'} - b(\gamma_t,t)) > \mathrm{d}t \tag{1.17}$$

$$A = \Sigma(\gamma_t,t)\Sigma(\gamma_t,t)^T. \tag{1.18}$$

The symbol $<,>$ denotes a dot product operation; If $\mathbf{v}$ and $\mathbf{z}$ are $n \times 1$ vectors, then $< \mathbf{v}, \mathbf{z} >= \mathbf{v}^T\mathbf{z}$. The variables $b(\gamma_t,t)$ and Σ are as defined in equation (1.13). If $\gamma(t), s < t < T$, is not absolutely continuous, then we have $J_{s,T}(\gamma) = \infty$ as shown in Baldi (1997). This is the reason that the infimum in (1.15) is taken over a set of absolutely continuous paths.

Moreover, if the minimizing path γ of $J_{s,T}$ is unique, then $P^{\epsilon}_{\mathbf{X},s}\{\tau \leq T\}$ is asymptotically the same as $P^{\epsilon}_{\mathbf{X},s}\{\tau \leq T, X(t) \in B_\delta(\gamma(t)) \text{ for } s \leq t \leq T\}$ as $\epsilon \to 0$, where

$B_\delta(\gamma(t))$ denotes the neighbourhood (a tube) of radius δ of $\gamma(t)$. This implies that the barrier hitting probability is asymptotically determined only by the portion of the barrier that this minimizing path goes through.

1.2.4 Large Deviations Principle for Uncorrelated Brownian Motion

In this section, we consider a d-dimensional pinned Brownian Motion process between times s and $T = s + \epsilon$, with fixed initial and terminal values to be $\mathbf{X}(s) = \mathbf{x} \in D$ and $\mathbf{X}(s + \epsilon) = \mathbf{y} \in D$. D, as described in the previous section, is an open set defined by the barriers, which are represented by a number of hyperplanes in the R^d space. All results in this section are attributed to Baldi (1995).

First of all, we assume that the drift term of the process is 0. We will consider the case where the drift term is non-zero in Section 2.2.2. However, as we will see, the value of the drift term does not have any effect when we consider a Brownian Motion process with fixed values at times s and $T = s+\epsilon$. Hence, the corresponding stochastic process is

$$d\mathbf{X}(t) = \Sigma d\mathbf{W}(t), \qquad \text{for} \qquad t \in [s, s + \epsilon]. \tag{1.19}$$

We should consider the case with $s = 0$, where $\mathbf{X}(0) = \mathbf{x} \in D$ and $\mathbf{X}(\epsilon) = \mathbf{y}$. Now, by an appropriate scaling of the time variable t by $t \to t/\epsilon$, we obtain

$$d\mathbf{X}(t) = \Sigma d\mathbf{W}(\epsilon t) \qquad \text{for} \qquad t \in [0, 1] \tag{1.20}$$

with $\mathbf{X}(0) = \mathbf{x}$ and $\mathbf{X}(1) = \mathbf{y}$. By using basic properties of a Brownian Motion, we notice $(\mathbf{W}(\epsilon t) - \mathbf{W}(0)) \sim \mathcal{N}(0, \epsilon t)$ and $\sqrt{\epsilon}(\mathbf{W}(t) - \mathbf{W}(0)) \sim \mathcal{N}(0, \epsilon t)$. Hence, we

obtain the following equivalent process

$$d\mathbf{X}(t) = \sqrt{\epsilon}\Sigma d\mathbf{W}(t) \qquad \text{for} \qquad t \in [0,1], \tag{1.21}$$

with $\mathbf{X}(0) = \mathbf{x}$ and $\mathbf{X}(1) = \mathbf{y}$.

The Brownian Motion process with fixed values at time 0 and 1 can be equivalently represented as the following Brownian Bridge process (Karlin and Taylor (1981))

$$d\mathbf{X}(t) = -\frac{\mathbf{X}(t) - \mathbf{y}}{1-t}dt + \sqrt{\epsilon}\Sigma d\mathbf{W}(t), \qquad \text{for} \qquad t \in [0,1), \tag{1.22}$$

with $\mathbf{X}(0) = \mathbf{x}$. We present a derivation of this result in Appendix B.1.

We can clearly see that the equation (1.22) is in the form of the equation (1.13), and hence the Large Deviations Theory is readily applicable to this setting. We now summarize Baldi (1995)'s approach to the problem of finding the probability that $\{\mathbf{X}(t), t \geq 0\}$ exits D during the time interval $[0,1]$.

Baldi (1995) assumes that drift term μ is zero and the instantaneous variance-covariance matrix Σ is an identity matrix. Hence, the underlying stochastic process is defined as in the equation (1.22) with $\Sigma = I$, I being a $d \times d$ identity matrix. The open set D and the set $\Gamma_{x,s}$ are defined as in the earlier section with $s = 0$ and $T = 1$.

By applying the general equations (1.15) and (1.17) to the specific diffusion process given by equation (1.22), we obtain the following formulae for $u(\mathbf{x}, 0)$ and the action functional $J_{0,1}(\gamma)$, where the subscript of J denotes the interval over which we find

$\gamma(t)$ such that the action functional J is minimized:

$$u(\mathbf{x},0) = \inf_{\gamma\in\Gamma_{\mathbf{x},0}} J_{0,1}(\gamma), \tag{1.23}$$

where

$$J_{0,1} = \frac{1}{2}\int_0^1 \|\gamma'(t)+\frac{\gamma(t)-\mathbf{y}}{1-t}\|^2 \mathrm{d}t \tag{1.24}$$

and $\|.\|$ is an Euclidean norm of a vector. i.e. if $\mathbf{z}=[z_1,z_2,\ldots,z_d]$, $\|\mathbf{z}\| = \sqrt{z_1^2+z_2^2+\ldots+z_d^2}$. As defined in (1.16), $\Gamma_{\mathbf{x},s}$ denotes the set of all absolutely continuous paths $\gamma(t)$ such that $\gamma(s)=\mathbf{x}$ and $\gamma(t)\in D^C$ for some $0<t<1$. Now we introduce lemmas that enable us to simplify the representation of $u(\mathbf{x},0)$ in (1.23).

Lemma 1.2.2 *Let us consider the following optimization problem*

$$u(\mathbf{x},s) = \inf_{\gamma\in\Gamma_{\mathbf{x},s}} J_{s,1}(\gamma) \tag{1.25}$$

$$= \inf_{\gamma\in\Gamma_{\mathbf{x},s}} \frac{1}{2}\int_s^1 \|\gamma'(r)+\frac{\gamma(r)-\mathbf{y}}{1-r}\|^2 \mathrm{d}r. \tag{1.26}$$

Then, the above problem is equivalent to the following problem:

$$u(\mathbf{x},s) = \inf_{s<t<1,\phi\in\delta D} \frac{1}{2}\{\frac{\|\mathbf{x}-\phi\|^2}{t-s}+\frac{\|\mathbf{y}-\phi\|^2}{1-t}-\frac{\|\mathbf{x}-\mathbf{y}\|^2}{1-s}\}, \tag{1.27}$$

where δD denotes the boundary of D.

Lemma 1.2.3 *If we focus on computing the infimum with respect to t in the following expression,*

$$u(\mathbf{x},s) = \inf_{\phi\in\delta D}\inf_{s<t<1} \frac{1}{2}\{\frac{\|\mathbf{x}-\phi\|^2}{t-s}+\frac{\|\mathbf{y}-\phi\|^2}{1-t}-\frac{\|\mathbf{x}-\mathbf{y}\|^2}{1-s}\}, \tag{1.28}$$

then the optimal value of t *can be represented as*

$$t^* = s + (1-s)\frac{\|\mathbf{x}-\phi\|}{\|\mathbf{x}-\phi\| + \|\mathbf{y}-\phi\|}, \tag{1.29}$$

which gives

$$u(\mathbf{x}, s) = \inf_{\phi \in \partial D} \frac{1}{2(1-s)}\{(\|\mathbf{x}-\phi\| + \|\mathbf{y}-\phi\|)^2 - \|\mathbf{x}-\mathbf{y}\|^2\}. \tag{1.30}$$

Now, by applying Lemma 1.2.2 and Lemma 1.2.3, we obtain the following theorem to which we will refer frequently throughout the thesis.

Theorem 1.2.3 *The solution of the following optimization problem*

$$\begin{aligned} u(\mathbf{x}, 0) &= \inf_{\gamma \in \Gamma_{\mathbf{x},0}} J_{0,1}(\gamma) && (1.31) \\ &= \inf_{\gamma \in \Gamma_{\mathbf{x},0}} \frac{1}{2}\int_0^1 \|\gamma'(r) + \frac{\gamma(r)-\mathbf{y}}{1-r}\|^2 \mathrm{d}r && (1.32) \end{aligned}$$

can be obtained by solving the equivalent optimization problem:

$$u(\mathbf{x}, 0) = \inf_{\phi \in \partial D} \frac{1}{2}\{(\|\mathbf{x}-\phi\| + \|\mathbf{y}-\phi\|)^2 - \|\mathbf{x}-\mathbf{y}\|^2\}. \tag{1.33}$$

In order to obtain $u(\mathbf{x}, 0)$ in (1.33), we obtain a point ϕ on the boundary of D such that $\|\mathbf{x}-\phi\| + \|\mathbf{y}-\phi\|$ is minimized. Since we apply the Large Deviations Theory to the process given by (1.22), we can obtain the exit probability by approximating $P^{\epsilon}_{\mathbf{X},0}(\tau \leq 1)$ using Theorem 1.2.2.

1.3 Application of Large Deviations Theory in Finance and Insurance

In this section, we discuss some examples of applications of Large Deviations theory in the fields of finance and actuarial science. Specifically, we look at the pricing of

general barrier options, portfolio management, computation of ruin probabilities in actuarial science, and credit risk modelling. Comprehensive overviews are provided in Pham (2007) and Boyle et al. (2005).

1.3.1 Pricing Double and Single Barrier Options

A barrier option is an option whose payoff depends on whether the path of the underlying asset has reached a barrier (i.e. a certain pre-determined level) during its lifetime.

In the standard Black-Scholes model, we assume that the underlying asset S follows:

$$dS(t) = \alpha S(t)dt + \sigma S(t)dW(t). \tag{1.34}$$

Suppose that a barrier level is given by $B_1 = b$. Using Ito's lemma, we apply log-transformation to (1.34) to obtain

$$d\ln S(t) = \left(\alpha - \frac{\sigma^2}{2}\right)dt + \sigma dW(t), \tag{1.35}$$

with a new barrier level $B = \ln b$. Hence, by setting $X(t) = \ln S(t), t \geq 0$, $\mu = \alpha - \frac{\sigma^2}{2}$, $c = \ln b$, we get a stochastic process $X(t)$ that follows a Brownian Motion

$$dX(t) = \mu dt + \sigma dW(t) \tag{1.36}$$

with a barrier level $B = c$. In a single barrier option, we have one barrier either above or below the initial value of the underlying, $S(0)$. In the case of a double barrier option, we have two barriers with one above and the other below $S(0)$. These barrier options can also be classified as either *knock-out options* or *knock-in*

options. A knock-out option ceases to exist when the underlying asset price hits the specified barrier level. A knock-in option comes into existence only when the underlying asset price reaches a barrier.

If we price barrier options by simulation, we simulate trajectories of the underlying and determine whether each simulated point breaches the barrier. However, to obtain the true probability of barriers crossing, we also have to consider the possibility that the barrier may be breached between the simulated times. Large Deviations Theory can be used to approximate the barrier crossing probability between the discrete simulation intervals as follows.

Suppose $t_1, t_2, \ldots, t_n$ is a sequence of discrete time points at which we evaluate the process. Hence, we want to compute the probability that the underlying process X breaches either upper or lower barrier between t_i and t_{i+1}, given that $X(t_i) = \zeta$ and $X(t_{i+1}) = y$ and that ζ and y are between barriers. Let us denote the length of time interval $t_{i+1} - t_i$ by ϵ. We assume that the underlying process follows a Brownian Motion process and the upper barrier and lower barrier are equal to U and L, respectively. By $p^{\epsilon}_{U,L}(T_i, \zeta, y)$ we denote the probability that the underlying process X breaches either upper or lower barrier between time t_i and t_{i+1}, given that $X(t_i) = \zeta$ and $X(t_{i+1}) = y$. The Large Deviations estimate of $p^{\epsilon}_{U,L}(T_i, \zeta, y)$ is shown to be of the form

$$p^{\epsilon}_{U,L}(T_i, \zeta, y) \approx \exp\{-\frac{Q_{U,L}(T_i, \zeta, y)}{\epsilon}\}$$

as $\epsilon \to 0$ where

$$Q_{U,L}(T_i, \zeta, y) = \begin{cases} \frac{2}{\sigma^2}(U - \zeta)(U - y) & , \text{ if } \zeta + y > U + L \\ \frac{2}{\sigma^2}(\zeta - L)(y - L) & , \text{ if } \zeta + y < U + L. \end{cases}$$

Now, if we choose $L = 0$ or $U = \infty$, we can obtain the probabilities of crossing the upper or lower barrier, respectively:

$$\begin{aligned} p_U^{\epsilon}(T_i, \zeta, y) &\approx \exp\{-\tfrac{2(U-\zeta)(U-y)}{\sigma^2\epsilon}\} \\ p_L^{\epsilon}(T_i, \zeta, y) &\approx \exp\{-\tfrac{2(\zeta-L)(y-L)}{\sigma^2\epsilon}\}. \end{aligned} \tag{1.37}$$

Baldi et al. (1999) obtains this result using the Large Deviations Theory. This result is identical to the exact analytic solution of the barrier-crossing probability in a single barrier case, as will be shown in (2.2).

1.3.2 Portfolio Management

Decay Rate Maximization

Large Deviations Theory has also applications in portfolio management. We assume that a portfolio consists of one risk-free asset and one risky asset, and by p we denote the proportion of the risk-free asset in the portfolio. Suppose that an investor has a target log growth rate, $\log r$, and that the objective of the investor is to maximize the probability that the portfolio's growth exceeds this target rate in his/her portfolio selection.

Suppose $W_T = W_0 \prod_{t=1}^{T} R_{pt}$, where W_0 and W_T are the amount of wealth at time 0 and T, respectively, and R_{pt}'s are the returns on the portfolio from time $t-1$ to t which are independently and identically distributed. Furthermore, let $\overline{\log R_p} = \frac{1}{T}\sum_{t=1}^{T} \log R_{pt}$, i.e. $\overline{\log R_p}$ is the average log return on portfolio from time 0 to T.

If we assume $\log R_{pt} \sim N(E[\log R_p], Var[\log R_p])$ and the return on each period is identical and independent from other periods, we have $\overline{\log R_p} \sim N(E[\log R_p], \frac{Var[\log R_p]}{T})$. Hence, the probability that the portfolio return does not exceed the target rate is represented as follows,

$$P[\overline{\log R_p} \leq \log r] = P[Z \leq \frac{\log r - E[\log R_p]}{\sqrt{Var[R_p]/T}}], \tag{1.38}$$

where Z is a standard normal random variable. We consider only portfolios such that $E[\log R_p] > \log r$. Recall that $\overline{\log R_p} = \frac{1}{T}\sum_{t=1}^{T} \log R_{pt}$, and $P[\overline{\log R_p} \leq \log r] \to 0$ as $T \to \infty$. Hence, this is the context in which we can apply Large Deviations Theory in order to obtain the rate at which $P[\overline{\log R_p} \leq \log r] \to 0$. If we assume R_{pt}, $t = 1, 2, \ldots, T$, are i.i.d, then we can use Cramér's theorem.

In the case when R_{pt}, $t = 1, 2, \ldots, T$, are i.i.d, Stutzer (2003) shows that the rate function of convergence, or *decay rate*, is given by

$$D_p(\log r) = \frac{1}{2}\left(\frac{\log r - E[\log R_p]}{\sqrt{Var[R_p]}}\right)^2. \tag{1.39}$$

This is the decay rate at which $P[\overline{\log R_p} \leq \log r] \to 0$. Hence, the proportion p of a risk-free asset in a portfolio can be chosen so that we maximize this decay rate. This decay rate is the same as $\ell()$ in Theorem 1.2.1. Maximizing the decay rate means minimizing the probability that we do not meet the target rate. Stutzer (2003) also shows that this maximization problem is equivalent to the utility maximization problem where the utility function is a power utility.

The dynamic continuous-time version of the portfolio management using decay rate is described in Pham (2003).

Utility Maximization

Gardiol et al. (2000) shows that the expected utility can be approximated to any degree of accuracy by a finite sum of tail probabilities. We assume that the utility function $U_T()$ is a differentiable strictly increasing and concave function.

$$\begin{aligned}
&\exists K \in N, (a_k, b_k) \in R^2, k = 1, \ldots, K \\
&E[U_T(W_0 R_T)] \simeq \sum_{k=1}^{K} a_k P(R_T > b_k) \\
&= \sum_{k=1}^{K} a_k (1_{[b_k \geq \text{med}]} P(R_T \geq b_k) + 1_{[b_k < \text{med}]} (1 - P(R_T < b_k))) \qquad (1.40)
\end{aligned}$$

where *med* is the median of the distribution of R_T. Because of the presence of indicator functions, $E[U_T(W_0 R_T)]$ is indeed a linear combination of tail probabilities. Here R_T is the return of the portfolio at time horizon T and $R_T = \prod_{t=1}^{T} R_t$. The tail probabilities $P(R_T < b_k)$ and $P(R_T > b_k)$ in (1.40) can be evaluated using the Large Deviations Theory, namely Cramér's Theorem.

1.3.3 Ruin Probabilities

In actuarial science, we model the process in which an insurance company's reserve changes over time. In a traditional risk model, an insurance company's wealth process is modelled by the following risk process,

$$X(t) = u + pt - S(t). \qquad (1.41)$$

where p is a continuous rate of premium received, u is an initial reserve, and $S(t)$ is a compound Poisson process with a rate parameter $\lambda > 0$. $S(t)$ represents the

aggregate loss due to the claim payments and can also be expressed as

$$S(t) = \sum_{j \geq 0} Y_j I_{\{T_j \leq t\}} \tag{1.42}$$

where $0 < T_1 < T_2 < \ldots$ are Poisson jump times and $Y_1, Y_2, \ldots,$ are positive independent and identically distributed random variables with a distribution function F. They represent successive jump sizes. In this section, we consider a more general process in which the amount of premium received varies over time. Hence, we have

$$X(t) = u + \int_0^t b(X(r))dr - S(t). \tag{1.43}$$

The event of "ruin" is said to occur when $X(t)$ falls below 0. This is the situation where the insurance company does not have sufficient funds to meet its contractual obligations. We define the time of ruin of X by

$$\tau = \inf\{t; X(t) < 0\}. \tag{1.44}$$

Now we introduce the following notation to represent the finite time ruin probability with the initial wealth of u:

$$\Psi(u, T) = P_u(\tau < T) \tag{1.45}$$

We also let Ω be a set of absolutely continuous functions on $[0, T]$. Let $\ell(.)$ be the Legendre-Fenchel transform of a compound Poisson variable. Let $J_T(x) = \int_0^T \ell(\dot{x}(t) + b(x(t)))dt$ if $x \in \Omega$ and $J_T(x) = -\infty$ if $x \notin \Omega$. Moreover, let $\Lambda_u = \{x \in \Omega; x(T) \geq u\}$. Then we have the following result from Djehiche (1993).

Theorem 1.3.1 *Assume that the premium function b is differentiable and non increasing. Then,* $\Psi(u, T) \leq \exp \sup_{\Lambda_u} J_T(x)$.

This theorem provides the upper bound for the finite time ruin probability. Here the Large Deviations Theory is applied to a compound Poisson process. As an extension, we can further research how the Large Deviations Theory can be applied to a multivariate compound Poisson process or more generally to a multivariate point process.

1.3.4 Credit Risk

Credit risk is the possibility of a financial loss due to a default event of a counterparty or migration of counterparty's credit rating. Hence, in credit risk, modelling the probability of occurrence of a default event either in a real or risk-neutral measure is crucially important. Credit risk models are classified into two major methodological groups: structural models and reduced-form models. In structural models, a default event is triggered by a firm's capital structure when the value of the firm falls below its financial obligation. Hence, the default event in the structural model is somewhat predictable. On the other hand, in the reduced-form models (also known as intensity-based models) default events are modelled with a point process that counts frequency of default events. Hence, for such models, a default event is not predictable at all. In this section, we explore how the Large Deviations Theory can be used in the context of the structural approach.

Initiated by the paper by Merton (1974), structural models use the evolution of firms' structural variables, such as asset and debt values, to determine the time of default. In Merton's model, a firm defaults if at the time of servicing the debt its assets are below the debt. The paper by Black and Cox (1976) provides an

essential extension of this approach by allowing the default to occur at any time between the inception of the contract and its maturity. It can be described as a first passage model, as it specifies the default time as the first time the firm's asset value hits a lower barrier. The barrier can be determined exogenously, as in Black and Cox (1976) and Longstaff and Schwartz (1995). Alternatively it can be determined endogenously, and then it corresponds to the level as the stockholders attempt to maximize the value of the firm (Leland (1994) and Leland and Toft (1996)).

In this approach, we model the value of the firm as a stochastic process, typically a Geometric Brownian Motion,

$$\frac{dV(t)}{V(t)} = \mu dt + \sigma dW(t), \tag{1.46}$$

where $V(t)$ is a value of the firm at time t, μ is a growth rate, and $W(t)$ is a Wiener process. We also have a certain default threshold level, D. We normally determine the threshold level by examining the firm's capital structure and accounting information. This level can be determined from the credit rating of the firm, which is provided by rating agencies such as Moody's or Standard & Poors. If the underlying process falls below this threshold, then a default event is triggered. The commercial products such as CreditMetrics and KMV are implemented based on this structural approach.

The problem of characterizing the default events is very similar to the one we had when pricing single and double barrier options, which was discussed in Section 1.3.1. When we compute the probability of default by the method of simulation, we generate many trajectories of values of $V(t)$ at the discrete times $t = t_1, t_2, \ldots$.

We also need to consider the probability that the trajectory may have breached the threshold between the discrete time intervals. Hence, a similar application of Large Deviations technique, as discussed in Section 1.3.1, can be potentially used.

Practitioners of credit risk management would be interested in understanding default behaviour of their credit risky portfolio. Under this circumstance, the value process in (1.46) will be represented by a correlated multivariate Brownian Motion process. The objective is to compute the probability of a default by each component as well as the probability of the joint default. This is the issue to be addressed in this thesis.

The existing literature provide variations of the structural model in credit risk. For instance, Zhou (1997) and Zhou (2001) add a jump term to the the value of the firm process, and Giesecke (2006) allows for incomplete information by letting the default threshold level to be uncertain. Further research is necessary to determine how the Large Deviations Theory can be utilized in these variations.

1.3.5 Other Relevant Literatures on Computation of Barrier Crossing Probability

We present some existing relevant results on the issue of computing a barrier crossing probability. Giraudo et al. (2001) propose a fully-simulation based algorithm for computing the barrier crossing probability of a pinned process. However, this method does not improve the computational time much more than the method where we take a very fine partition in the standard simulation technique. For each

interval $[t_i, t_{i+1}]$ of a simulation run, the authors suggest to perform a nested simulation of R runs over 8 subintervals within the given interval, in order to determine the barrier crossing probability between time t_i and t_{i+1}. This probability is then approximated by the proportion of R runs that breach the barrier.

The amount of research on the barrier crossing probability for two or higher dimensional processes is limited. He et al. (1998) provide a semi-closed form formula for the barrier crossing probability of a two-dimensional pinned Brownian Motion process. In Section 2.3, we use results of He et al. (1998) as a benchmark in evaluating accuracy of our approximation methods in two-dimensions. The drawback is that this formula involves an infinite sum of Bessel functions and that this result cannot readily be extended beyond two dimensions.

Broadie et al. (1997) provide a relationship between the price of a continuously monitored barrier option and the price of a discretely monitored barrier option when the underlying component follows a Geometric Brownian Motion. Their main result is given in the following theorem.

Theorem 1.3.2 *Let $V_m(H)$ be the price of a discretely monitored knock-in or knock-out down call or up put with barrier H, where m is the size of discretization. Let $V(H)$ be the price of the corresponding continuously monitored barrier option. Then,*

$$V_m(H) = V(He^{\pm\beta\sigma\sqrt{T/m}}) + o\left(\frac{1}{\sqrt{m}}\right) \tag{1.47}$$

where the sign + applies if the barrier is above the initial value of an underlying and the sign - applies otherwise. In addition, it is known that $\beta \approx 0.5826$.

According to this theorem, if we know the price of a continuously monitored barrier option, we can get a price of discretely monitored one, by shifting the barrier level, and vice versa. Therefore, the error due to discretizations is compensated by adjusting the barrier level. This result is derived for a one-dimension Brownian Motion. Future research may focus on extending this result to a higher dimensional process.

Chapter 2

Exit Probabilities for a Brownian Bridge Process

Suppose that the underlying process $\{W(t), t \geq 0\}$ follows a standard Brownian Motion process between time t_0 and t_1, with fixed values of $W(t_0) = 0$ and $W(t_1) = y$. This process is also referred as a Brownian Bridge process. Karatzas and Shreve (1991) show that the distribution of the maximum value of this Brownian Bridge is given by

$$P(\max_{t_0 \leq t \leq t_1} W(t) \geq \beta | W(t_1) = y) = e^{-2\beta(\beta - y)/h}, \tag{2.1}$$

where $h = t_1 - t_0 > 0$, $\beta > 0$, and $y \leq \beta$. The expression given in (2.1) is the probability that the Brownian Motion process with fixed values of 0 at time t_0 and y at time t_1 crosses the barrier β between the time t_0 and t_1.

We consider a slightly more general process $\{X_t, t \geq 0\}$ given by $X(t) = \sigma W(t)$ with fixed values $X(t_0) = \zeta$ and $X(t_1) = y$. We also have $h = t_1 - t_0 > 0$. Let

$p_a^h(\zeta, y)$ denote the probability that the process X breaches the barrier β between time t_0 and t_1. As a generalization of (2.1), $p_a^h(\zeta, y)$ is given by

$$p_a^h(\zeta, y) = \exp\{-\frac{2(\beta - \zeta)(\beta - y)}{\sigma^2 h}\}. \tag{2.2}$$

This expression is consistent with the Large Deviations representations in (1.37). The same expression is also derived using the first type Volterra integral equation by Giraudo and Sacerdote (1999).

The analytic representation of an exit probability for a multidimensional Brownian Bridge is not available. In this chapter, we develop an approximation method based on the Large Deviations Theory. In Section 2.1, we focus on computing an exit probability of a two-dimensional Brownian Bridge. In Section 2.2, we extend our method to a multidimensional Brownian Bridge and more general processes. Then we provide numerical examples in Section 2.3

2.1 Exit Probability of a Two-Dimensional Process

This section focuses on developing asymptotic approximation methods for computing an exit probability of a 2-dimensional Brownian Bridge process. This section is organized as follows. Section 2.1.1 shows relationship between marginal exit probabilities and joint exit probabilities using set theory. In Section 2.1.2, we propose an approximation method by extending Baldi (1995) and show some of its shortcomings. Then, in Section 2.1.3, we propose an alternative method based on the Large Deviations Theory that approximates the exit probability more accurately.

2.1.1 Discussions on Modelling in the Two-Dimensional Case

We use basic set theory in order to establish relationship between marginal barrier crossing probabilities and joint barrier crossing probabilities in the case of a 2-dimensional stochastic process. In particular, suppose that we have $\mathbf{X}(t) = (X_1(t), X_2(t))$ that follows a 2-dimensional correlated Brownian Bridge process. As shown in Section 1.2.4 and Appendix B.1, the Brownian Bridge process between $[s, s+\epsilon)$ can be equivalently written in the following way:

$$d\mathbf{X}(t) = -\frac{\mathbf{X}(t) - \mathbf{y}}{1-t}dt + \sqrt{\epsilon}\Sigma d\mathbf{W}(t) \qquad \text{for} \qquad t \in [0, 1), \tag{2.3}$$

where Σ is a 2×2 positive definite matrix, $\mathbf{y}$ is a 2×1 vector of terminal values, ϵ is length of the given interval. By $\mathbf{c} = (c_1, c_2)$, we denote a vector of the barrier levels for each component. We assume, without loss of generality, that $X_1(0) < c_1$, $X_2(0) < c_2$, $X_1(1) < c_1$ and $X_2(1) < c_2$.

We define two events E_1 and E_2 as follows:

$$E_1 = \{X_1(t) \geq c_1 \text{ for some t}, 0 \leq t \leq 1\} \tag{2.4}$$

$$E_2 = \{X_2(t) \geq c_2 \text{ for some t}, 0 \leq t \leq 1\}. \tag{2.5}$$

E_1 and E_2 are the events in which the first and the second component of the process cross their respective barriers. From the inclusion-exclusion principle of set theory, we have

$$P(E_1 \cup E_2) = P(E_1) + P(E_2) - P(E_1 \cap E_2). \tag{2.6}$$

Note that we can easily compute $P(E_1)$ and $P(E_2)$, as the exact analytic formula is given in (2.2). Hence, if we can approximate either $P(E_1 \cup E_2)$ or $P(E_1 \cap E_2)$, we can obtain an estimate of the other.

Baldi (1995)'s work provides a framework within which Large Deviations Theory can be applied to estimate the probability $P(E_1 \cup E_2)$, which is the probability that at least one of the two components cross its respective barrier. However, as we will show in the subsequent section, when we apply Baldi's approach to estimate $P(E_1 \cup E_2)$, the result does not depend on the correlation between two components. Moreover, we have $P(E_1 \cup E_2) = \max(P(E_1), P(E_2))$. In order to remedy this situation, in Section 2.1.3 we estimate $P(E_1 \cap E_2)$ directly and demonstrate that this estimate takes account of the correlation between components.

2.1.2 Approximation of $P(E_1 \cup E_2)$

In Section 1.2.4, we have described the recent work of Baldi (1995), where the author uses Large Deviations Theory to approximate a barrier-crossing probability for a standard multivariate Brownian Motion. In this section, we extend this methodology to the case with a general variance-covariance structure. We adopt the same line of reasoning as Baldi (1995) and extend his methodology to handle a two-dimensional correlated Brownian motion with zero drift.

First we consider the following lemma.

Lemma 2.1.1 *Suppose that* $\mathbf{P}$ *is a symmetric* $d \times d$ *matrix and* $\mathbf{m}$ *is a* $d \times 1$ *vector. Then* $< \mathbf{Pm}, \mathbf{Pm} > = < \mathbf{PP}^T\mathbf{m}, \mathbf{m} >$ *where* $<,>$ *is a dot product defined in Section 1.2.3.*

Proof.

$$\begin{aligned} < \mathbf{Pm}, \mathbf{Pm} > &= (\mathbf{Pm})^T(\mathbf{Pm}) = \mathbf{m}^T\mathbf{P}^T\mathbf{Pm} \\ &= \mathbf{m}^T\mathbf{PP}^T\mathbf{m} = (\mathbf{PP}^T\mathbf{m})^T\mathbf{m} \\ &= < \mathbf{PP}^T\mathbf{m}, \mathbf{m} > \\ \text{Therefore, } < \mathbf{Pm}, \mathbf{Pm} > &= < \mathbf{PP}^T\mathbf{m}, \mathbf{m} > \qquad \square \end{aligned}$$

Recall that $A = \Sigma\Sigma^T$ from (1.18), and let K be a $d \times d$ matrix such that $A^{-1} = KK^T$. In fact, $K = ((\Sigma\Sigma^T)^{-1})^{1/2}$ and existence of K can be shown using a singular value decomposition, because the matrix A is symmetric and positive definite.

For the diffusion process of (1.13), we have an expression for the action functional given by (1.17). By applying these formulas to the Brownian Bridge process (2.3), we obtain the following action functional:

$$\begin{aligned} J_{0,1}(\gamma) &= \frac{1}{2}\int_0^1 < A(\gamma_t, t)^{-1}(\gamma_t^{'} - b(\gamma_t, t)), \gamma_t^{'} - b(\gamma_t, t)) > \mathrm{d}t & (2.7) \\ &= \frac{1}{2}\int_0^1 < KK^T(\gamma_t^{'} - b(\gamma_t, t)), \gamma_t^{'} - b(\gamma_t, t)) > \mathrm{d}t & (2.8) \\ &= \frac{1}{2}\int_0^1 < K(\gamma_t^{'} - b(\gamma_t, t)), K(\gamma_t^{'} - b(\gamma_t, t))) > \mathrm{d}t & (2.9) \\ &= \frac{1}{2}\int_0^1 \|K(\gamma^{'}(t) + \frac{\gamma(t) - y}{1 - t})\|^2 \mathrm{d}t & (2.10) \\ &= \frac{1}{2}\int_0^1 \|K\gamma^{'}(t) + \frac{K\gamma(t) - Ky}{1 - t}\|^2 \mathrm{d}t & (2.11) \end{aligned}$$

$$= \frac{1}{2}\int_0^1 \|\eta^{'}(t) + \frac{\eta(t) - w}{1 - t}\|^2 \mathrm{d}t \qquad (2.12)$$

where $\eta(t) = K\gamma(t)$ and $w = Ky$.

We have obtained the first equality (2.7) from the equation (1.17), the second equality (2.8) using $K = ((\Sigma\Sigma^T)^{-1})^{1/2}$, the third equality (2.9) from Lemma 2.1.1, and the last equality (2.12) by introducing new vector variables $\eta(t)$ and w.

We use the same notations as in Section 1.2.3. We define a new open set F as

$$F = \{K\mathbf{x} | \text{all } \mathbf{x} \in D\}, \tag{2.13}$$

and a set $H_{K\mathbf{x},0}$ to be of the following form:

$$\begin{aligned} H_{K\mathbf{x},0} \quad = \quad & \{\text{absolutely continuous } \eta(t) \in R^d, 0 < t < 1 | \eta(0) = K\mathbf{x}, \eta(t) \in F^C \\ & \text{for some t, } 0 < t < 1\}. \end{aligned} \tag{2.14}$$

In other words, F is an open set that is transformed from the open set D by the transformation matrix K, and H is a set of all absolutely continuous paths $\{\eta(t), 0 < t < 1\}$ such that $\eta(0) = K\mathbf{x}$ and $\eta(t) \in F^C$ for some $0 < t < 1$. With the newly defined variables, we can reformulate the problem of computing $u(\mathbf{x}, 0)$ as follows:

$$u(\mathbf{x}, 0) = \inf_{\eta \in H_{K\mathbf{x},0}} J_{0,1}(\eta) \tag{2.15}$$

where

$$J_{0,1}(\eta) = \frac{1}{2} \int_0^1 \|\eta^{'}(t) + \frac{\eta(t) - w}{1 - t}\|^2 \mathrm{d}t. \tag{2.16}$$

The formulae in equations (2.15) and (2.16) are in the same form as in equations (1.23) and (1.24), except that the above equations make use of variables and sets

transformed by matrix K. Hence, the representations in (1.23) and (1.24) can indeed be viewed as a special case of (2.15) and (2.16) where we take $\Sigma = I$.

Since the computation of the exit probability under correlated multivariate Brownian Motion can be reduced to the setting with a standard multivariate Brownian Motion by an appropriate transformation, we now focus on solving the problem formulated in (2.15) and (2.16). Suppose that we are in the R^d space whose coordinates are denoted by $z_1, z_2, \ldots, z_d$. In expressions (1.23) and (1.24) in Section 1.2.4, the hyperplanes defining the barriers are in the form of $z_i = constant$. On the other hand, due to the transformation by the matrix K, in expressions (2.15) and (2.16), the barriers are expressed in the form of $a_1 z_1 + a_2 z_2 + \ldots + a_d z_d = constant$.

We need to find u in (2.15), which involves optimization. This problem is one of the standard problems in the domain of calculus of variations. It can be solved using Hamilton's principle in which we set up a corresponding Lagrange equation. See Arthurs (1975).

With some abuse of notations, from here on we will represent $K\mathbf{x}$ by $\mathbf{x}$, and w by $\mathbf{y}$ for the simplicity of representation of the formulae to follow.

By applying Lemma 1.2.2 and 1.2.3, the equation (2.15) can be expressed as

$$u(\mathbf{x}, 0) = \inf_{\phi \in \partial F} \{\frac{1}{2}\{(\|\mathbf{x} - \phi\| + \|\mathbf{y} - \phi\|)^2 - \|\mathbf{x} - \mathbf{y}\|^2\}\}, \tag{2.17}$$

where ∂F is the boundary of the open set F defined in (2.13). Furthermore, in order to obtain $u(\mathbf{x}, 0)$, we need to determine ϕ^* such that

$$\phi^* = \arg\min_{\phi \in \partial F} [\|\mathbf{x} - \phi\| + \|\mathbf{y} - \phi\|], \tag{2.18}$$

since the term $\|\mathbf{x}-\mathbf{y}\|^2$ does not depend on ϕ. Hence, in order to find ϕ^*, we need to find the length-minimizing path that starts from the coordinate $\mathbf{x}$, touches a point along the boundary of the set F, and then ends at the coordinate $\mathbf{y}$.

In the remainder of this section, we discuss our approach to the optimization problem (2.18), thus obtaining the value of $u(\mathbf{x}, 0)$ in (2.17). We focus on a two-dimensional process. Similar calculations can be performed for a higher dimensional process, and they will be discussed in Section 2.2.1.

In the two-dimensional case, $\mathbf{x}$ and $\mathbf{y}$ are 2×1 vectors, and the open set F is specified in the R^2 space. The vectors $\mathbf{x}$ and $\mathbf{y}$ are represented as $[x_1, x_2]^T$ and $[y_1, y_2]^T$, respectively. The boundary of the set F can be represented by a collection of hyperplanes in R^2. We shall denote them as $B_i, i = 1, \ldots, n$, where n is the number of linear boundaries and B_i is the i^{th} boundary represented $\{(z_1, z_2) \in R^2 \mid a_{i1}z_1 + a_{i2}z_2 = c_i\}$. In R^2, we will normally have two barriers, one for each component of the process. Hence, $n = 2$. We also assume that the points $\mathbf{x}$ and $\mathbf{y}$ belong to the interior of F. We now formulate a number of lemmas that will help us solve the optimization problem in (2.18).

Lemma 2.1.2 *Suppose that B is a straight line represented by $a_1z_1 + a_2z_2 = c$ and that the points $\mathbf{x} = [x_1, x_2]^T$ and $\mathbf{y} = [y_1, y_2]^T$ are located on one side of this line. Then the point $\mathbf{b}^*$ such that*

$$\mathbf{b}^* = \arg\min_{\epsilon \in B} [\|\mathbf{x} - \epsilon\| + \|\mathbf{y} - \epsilon\|] \tag{2.19}$$

can be obtained by the following procedure. We draw a straight line from $\mathbf{x}$ to $\mathbf{y}'$,

which is a mirrored point of $\mathbf{y}$ *reflected around the line* B*. Then, the intersecting point of this straight line and the line* B *is* $\mathbf{b}^*$*.*

Proof.

By the definition of $\mathbf{y}^{'}$, we have

$$\begin{aligned} \mathbf{b}^* &= \arg\min_{\epsilon \in B}[\|\mathbf{x}-\epsilon\| + \|\mathbf{y}-\epsilon\|] && (2.20) \\ &= \arg\min_{\epsilon \in B}[\|\mathbf{x}-\epsilon\| + \|\mathbf{y}^{'}-\epsilon\|]. && (2.21) \end{aligned}$$

The points $\mathbf{x}$ and $\mathbf{y}^{'}$ are on different sides of the line B, and $\|\mathbf{x}-\epsilon\|+\|\mathbf{y}^{'}-\epsilon\|$ is the distance of the path from $\mathbf{x}$ to $\mathbf{y}^{'}$ that goes through a point $\epsilon \in B$. The distance-minimizing path from $\mathbf{x}$ to $\mathbf{y}^{'}$ is a straight line between $\mathbf{x}$ and $\mathbf{y}^{'}$. Therefore, $\mathbf{b}^*$ is given by the intersection between the line B and the straight line from $\mathbf{x}$ to $\mathbf{y}^{'}$. □

We are now ready to prove the main theorem of this section.

Theorem 2.1.1 *Suppose that* W *is an open set in* R^2 *whose boundary can be represented by* n *lines,* $B_i, i = 1, \ldots, n$*. Each* B_i *is represented by a linear equation,* $a_{i1}z_1 + a_{i2}z_2 = c_i$*. Suppose that we have two points* $\mathbf{x}, \mathbf{y} \in W$ *so that* $\mathbf{x}$ *and* $\mathbf{y}$ *are located on one side of each* $B_i, i = 1, \ldots, n$*. For each line* B_i*, we define* $\mathbf{y}_i^{'}$ *by mirroring the point* $\mathbf{y}$ *on the line* B_i*. Then the following equivalence holds:*

$$\inf_{\phi \in \partial W}\{\|\mathbf{x}-\phi\| + \|\mathbf{y}-\phi\|\} = \min_{i \in [1,2,\ldots,n]}\{\|\mathbf{x}-\mathbf{y}_i^{'}\|\} \quad (2.22)$$

Proof.

This is a straightforward application of Lemma 2.1.2. For each line B_i, we obtain $\mathbf{b}_i^*$ such that $\mathbf{b}_i^* = \arg\min_{\epsilon \in B_i}[|\mathbf{x}-\epsilon|+|\mathbf{y}-\epsilon|]$. Also, note that $\partial W = \bigcup_{i=1}^{n} B_i$. Hence,

$$\inf_{\phi \in \partial W}\{\|\mathbf{x}-\phi\| + \|\mathbf{y}-\phi\|\} \tag{2.23}$$

$$= \min_{i \in \{1,2,\ldots,n\}}\{\|\mathbf{x}-\mathbf{b}_i^*\| + \|\mathbf{y}-\mathbf{b}_i^*\|\} \tag{2.24}$$

$$= \min_{i \in \{1,2,\ldots,n\}}\{\|\mathbf{x}-\mathbf{b}_i^*\| + \|\mathbf{y}_i^{'}-\mathbf{b}_i^*\|\} \tag{2.25}$$

$$= \min_{i \in \{1,2,\ldots,n\}}\{\|\mathbf{x}-\mathbf{y}_i^{'}\|\}. \tag{2.26}$$

The last equality follows from Lemma 2.1.2, because $\mathbf{b}_i^*$ is the intersecting point between the straight line from $\mathbf{x}$ to $\mathbf{y}_i^{'}$ and the line B_i. $\square$

Property of Large Deviation Estimate of $P(E_1 \cup E_2)$

By using results described in this section, we can obtain an estimate of $P(E_1 \cup E_2)$ where $P(E_1 \cup E_2)$ is the probability that at least one of two components cross its respective barrier. In this section, we show that this estimate based on Large Deviations Theory may not be an appropriate estimate to use, because it does not take into account the correlation structure of the Brownian Motion process. Moreover, the estimate of $P(E_1 \cup E_2)$ turns out to be the maximum of the barrier crossing probabilities of the first component of the stochastic process and that of the second component, i.e. $P(E_1 \cup E_2) = \max(P(E_1), P(E_2))$.

Suppose that we have a two-dimensional Brownian Bridge process with zero drift, as specified in (1.22). Without a loss of generality, we assume that this process has

Σ such that

$$\Sigma\Sigma^T = \begin{bmatrix} 1 & r \\ r & 1 \end{bmatrix}. \tag{2.27}$$

For the Brownian Bridge process with the value of variance to be other than 1, we can scale the variance to be 1 and also scale the corresponding barrier level and the terminal value of the corresponding component. Under the structural form of (2.27), the covariance, r, is the same as the correlation of the two components.

Suppose that the barrier levels for the first and the second component of the two dimensional process are constant and given by c_1 and c_2, respectively. In R^2, these barriers are represented by a vertical and a horizontal line. Mathematically, these barriers can be expressed as $z_1 = c_1$ and $z_2 = c_2$. Also, without loss of generality, we further assume $x_1 < c_1$, $x_2 < c_2$, $y_1 < c_1$, and $y_2 < c_2$.

In order to reduce the problem with a correlated process into an uncorrelated one, we need to perform a transformation of the variables. The transformation matrix K is given as

$$\begin{aligned} K &= ((\Sigma\Sigma^T)^{-1})^{1/2} && (2.28)\\ &= \left(\frac{1}{1-r^2}\begin{bmatrix} 1 & -r \\ -r & 1 \end{bmatrix}\right)^{1/2} && (2.29)\\ &= \frac{1}{\sqrt{1-r^2}}\begin{bmatrix} 1 & -r \\ -r & 1 \end{bmatrix}^{1/2} && (2.30)\\ &= \frac{1}{\sqrt{1-r^2}}\begin{bmatrix} \frac{\sqrt{1-r}}{2}+\frac{\sqrt{1+r}}{2} & \frac{\sqrt{1-r}}{2}-\frac{\sqrt{1+r}}{2} \\ \frac{\sqrt{1-r}}{2}-\frac{\sqrt{1+r}}{2} & \frac{\sqrt{1-r}}{2}+\frac{\sqrt{1+r}}{2} \end{bmatrix}. && (2.31) \end{aligned}$$

Note that K is a symmetric matrix and can be expressed as $K = \begin{bmatrix} k_1 & k_2 \\ k_2 & k_3 \end{bmatrix}$. K is a function of r.

Lemma 2.1.3 *If we transform the line $a_1 z_1 + a_2 z_2 = c$ by the symmetric transformation matrix K, then we obtain a new equation $a_1^{'} z_1 + a_2^{'} z_2 = c^{'}$, where $a_1^{'} = a_1 k_3 - a_2 k_2$, $a_2^{'} = a_2 k_1 - a_1 k_2$, and $c^{'} = c(k_1 k_3 - k_2^2)$.*

Proof: Shown in Appendix A.1.

In the original space, the barriers are expressed as $z_1 = c_1$ and $z_2 = c_2$, and we can use Lemma 2.1.3 to get the equations of barriers in the transformed space. These transformed equations correspond to the boundaries of the set F, and are given by

$$k_3 z_1 - k_2 z_2 = c_1(k_1 k_3 - k_2^2) \tag{2.32}$$

$$-k_2 z_1 + k_1 z_2 = c_2(k_1 k_3 - k_2^2). \tag{2.33}$$

Now we are ready to solve the optimization problem that is formulated in (2.15) and (2.16). The set of equations representing the boundaries of F are given by (2.32)-(2.33). We denote

$$\mathbf{v} = K\mathbf{x} \tag{2.34}$$

$$\mathbf{w} = K\mathbf{y}, \tag{2.35}$$

which are initial and terminal values of the transformed variables. Hence, by Theorem 1.2.3, we need to consider the problem of finding u given by

$$u(\mathbf{x}, 0) = \inf_{\phi \in \partial F} \frac{1}{2}\{(\|\mathbf{v} - \phi\| + \|\mathbf{w} - \phi\|)^2 - \|\mathbf{v} - \mathbf{w}\|^2\}. \tag{2.36}$$

Since ϕ^* that minimizes $\|\mathbf{v}-\phi\| - \|\mathbf{w}-\phi\|$ is equivalent to ϕ^* that minimizes $\frac{1}{2}\{(\|\mathbf{v}-\phi\| - \|\mathbf{w}-\phi\|)^2 - \|\mathbf{v}-\mathbf{w}\|^2\}$, we can obtain, by Theorem 2.1.1, the value of $u(\mathbf{v},0)$ by the following procedure. For each line i, $i=1,2$, that constitute the boundary of F, we compute

$$u_i(\mathbf{v},0) = \frac{1}{2}(\|\mathbf{v}-\mathbf{w}_i^{'}\|^2 - \|\mathbf{v}-\mathbf{w}\|^2), \tag{2.37}$$

where $\mathbf{w}_i^{'}$ is a mirrored point of $\mathbf{w}$ around the i^{th} boundary equation. Then we obtain $u(\mathbf{v},0)$ to be the minimum of all $u_i(\mathbf{v},0)$'s. The relationship between the value of $u(\mathbf{v},0)$ and the exit probability $P^{\epsilon}_{\mathbf{X},0}\{\tau \leq 1\}$ is given in (1.14). In order to compute $\mathbf{w}_i^{'}$, we make use of the following lemma.

Lemma 2.1.4 *The coordinates of* $\mathbf{w}^{'} = [w_1^{'}, w_2^{'}]^T$*, which is a mirrored point of* $\mathbf{w} = [w_1, w_2]^T$ *around the line* B*,* $a_1 z_1 + a_2 z_2 = c$*, is given as follows:*

$$w_1^{'} = -\frac{a_1^2 w_1 - a_2^2 w_1 + 2a_1 a_2 w_2 - 2a_1 c}{a_1^2 + a_2^2} \tag{2.38}$$

$$w_2^{'} = -\frac{-a_1^2 w_2 + a_2^2 w_2 + 2a_1 a_2 w_1 - 2a_2 c}{a_1^2 + a_2^2}. \tag{2.39}$$

Proof: Shown in Appendix A.2.

Lemma 2.1.4 gives us, in particular, the following coordinates of $\mathbf{w}_2^{'} = [w_1^{'}, w_2^{'}]$ with respect to the second boundary given by (2.33),

$$w_1^{'} = -\frac{k_2^2 w_1 - k_1^2 w_1 - 2k_2 k_1 w_2 + 2k_2 c_2 (k_1 k_3 - k_2^2)}{k_2^2 + k_1^2} \tag{2.40}$$

$$w_2^{'} = -\frac{-k_2^2 w_2 + k_1^2 w_2 - 2k_2 k_1 w_1 - 2k_1 c_2 (k_1 k_3 - k_2^2)}{k_2^2 + k_1^2}. \tag{2.41}$$

We need to evaluate $u_i(\mathbf{v}, 0)$'s for each respective barrier. In the case when $i = 2$, we can substitute (2.40)-(2.41) and (2.34)-(2.35) into (2.37), and express (2.37) in terms of original variables, x_1, x_2, y_1, and y_2. The expression for $u_2(\mathbf{x}, 0)$ can be simplified using the symbolic computation module of MATLAB^{TM}, and we obtain

$$u_2(\mathbf{v}, 0) = 2(-c_2 y_2 + c_2^2 + x_2 y_2 - c_2 x_2). \tag{2.42}$$

We can obtain a similar result for $u_1(\mathbf{v}, 0)$. We note that the expressions of $u_2(\mathbf{v}, 0)$ and $u_1(\mathbf{v}, 0)$ do not contain the covariance value of r. Hence, since $u(\mathbf{v}, 0)$ is the minimum of $u_1(\mathbf{v}, 0)$ and $u_2(\mathbf{v}, 0)$, it also does not depend on r. Consequently, the barrier crossing probability $P(E_1 \cup E_2)$ is not affected by covariance of the underlying process. Moreover, the expression we obtained for $u_2(\mathbf{v}, 0)$ in (2.42) is in fact the same as $u(\mathbf{x}, 0)$, which we obtain when we only look at the second component of the Brownian Motion with a barrier level at c_2. $u(\mathbf{x}, 0)$ for a one-dimensional process can be identified from (2.2) by using the relationship between $u(.)$ and the barrier crossing probability shown in (1.14). Hence, the marginal probability that one component of 2-dimensional Brownian Motion crosses its barrier level is the same as the barrier crossing probability of an one-dimensional Brownian Motion of the component.

Therefore, we have shown that the Large Deviations estimate of $P(E_1 \cup E_2)$ in the extension of Baldi's framework is just a maximum of $P(E_1)$ and $P(E_2)$. This finding is consistent with the asymptotic nature of Large Deviations Theory. However, a better estimate needs to be sought, because this method totally neglects the covariance of a 2- or higher-dimensional process. In the next section, we compute

$P(E_1 \cap E_2)$ directly rather than $P(E_1 \cup E_2)$ and show that this method incorporates the effect of the covariance r.

The method that we have discussed in this section will be referred to as "Baldi's Method" throughout the thesis. This approach is extendible to higher dimensions, where we want to compute $P(E_1 \cup E_2 \cup \ldots \cup E_n)$. In this case, the estimate of $P(E_1 \cup E_2 \cup \ldots \cup E_n)$ will be the maximum of $P(E_1)$, $P(E_2)$, ..., $P(E_n)$. In this section, we have computed the probability that the process exits the region D defined by a set of linear boundaries. In Appendix F, we illustrate that the estimate is indeed a sharp Large Deviations estimate, so that we can express

$$P^{\epsilon}_{\mathbf{X},0}\{\tau \leq 1\} = \exp(-\frac{u(\mathbf{x},0)}{\epsilon})(1 + o(\epsilon^m)) \tag{2.43}$$

for every $m > 0$. Here we provide intuitive justification that the estimate is a sharp Large Deviations estimate. In the Large Deviations Theory, when the process exits a region, it goes through the most likely path. Hence, the exit probability of the process is asymptotically the same as the probability that the process goes through the hyperplane that is most likely to be breached. Since the exit probability when a boundary is a hyperplane is given by a form of (2.43), we know that our estimate for $P(E_1 \cup E_2 \cup \ldots \cup E_n)$ is indeed a sharp Large Deviations estimate.

2.1.3 Approximation of $P(E_1 \cap E_2)$

In Section 2.1.2, we showed that the estimate for $P(E_1 \cup E_2)$ based on Baldi's method does not have desirable properties. In this section, we approximate $P(E_1 \cap$

E_2) directly. From $P(E_1 \cap E_2)$, we can easily obtain $P(E_1 \cup E_2)$ using (2.6), and we can completely characterize joint behavior of a two-dimensional process.

Whether we look at $P(E_1 \cap E_2)$ or $P(E_1 \cup E_2)$, the underlying process still remains a two-dimensional Brownian Bridge process with fixed values at times 0 and 1. Hence, regardless of which probability we want to estimate, by Lemma 1.2.1, the underlying process satisfies the Large Deviations Principle with the same rate function, or action functional. As previously shown in equation (2.10) of Section 2.1.2, the rate function for the correlated Brownian Motion process with fixed values at times 0 and 1 is given as follows:

$$J_{0,1}(\gamma) = \frac{1}{2}\int_0^1 \|K(\gamma^{'}(t) + \frac{\gamma(t) - \mathbf{y}}{1-t})\|^2 \mathrm{d}t, \tag{2.44}$$

where $\gamma(t) = [\gamma_1(t), \gamma_2(t)]^T$ and $\gamma(t) \in R^2$. Also note that, when we compute $P(E_1)$, we take the infimum of the above function (2.44) over the set

$$\begin{aligned}\Gamma_1 = \{&\text{absolutely continuous } \gamma(t) \in R^2, 0 < t < 1 | \gamma(0) = \mathbf{x}, \gamma(1) = \mathbf{y}, \\ &\gamma_1(t) = c_1 \text{ for some t}, 0 \leq t \leq 1\}.\end{aligned}$$

Similarly, for computing $P(E_2)$, we take the infimum of the above function over the set

$$\begin{aligned}\Gamma_2 = \{&\text{absolutely continuous } \gamma(t) \in R^2, 0 < t < 1 | \gamma(0) = \mathbf{x}, \gamma(1) = \mathbf{y}, \\ &\gamma_2(t) = c_2 \text{ for some t}, 0 \leq t \leq 1\}.\end{aligned}$$

Moreover, we define

$$\begin{aligned}\Gamma_{1,2} = \{&\text{absolutely continuous } \gamma(t) \in R^2, 0 < t < 1 \mid \gamma(0) = \mathbf{x}, \gamma(1) = \mathbf{y}, \\ &\gamma_1(t_1) = c_1 \text{ for some } t_1, 0 \leq t_1 \leq 1, \gamma_2(t_2) = c_2 \text{ for some } t_2, 0 \leq t_2 \leq 1\}.\end{aligned}$$

In other words, $\Gamma_{1,2}$ is the set of paths $\gamma(t), 0 \leq t \leq 1$, where both the first component γ_1 and the second component γ_2 of the process breach their corresponding barriers between time 0 and 1. Because $\Gamma_{1,2} = \Gamma_1 \cap \Gamma_2$, we know that $\Gamma_{1,2} \subseteq \mathcal{B}$, since $\mathcal{B}$ is a σ-algebra in our space.

Hence, by Lemma 1.2.1, $P(E_1 \cap E_2)$ satisfies the Large Deviations Principle with the rate function $J_{0,1}(\gamma)$ in (2.44), and $u(\mathbf{x}, 0)$ can be computed by taking infimum over the set $\Gamma_{1,2}$ as shown in the following expression:

$$u(\mathbf{x}, 0) = \inf_{\gamma \in \Gamma_{1,2}} J_{0,1}(\gamma). \tag{2.45}$$

To account for variance and covariance of the process, we apply a similar change of variables and transformation by the matrix K as in (2.10) - (2.12). Then, the expression (2.45) can be equivalently written as follows:

$$u(\mathbf{x}, 0) = \inf_{\eta \in H_{1,2}} J_{0,1}(\eta) \tag{2.46}$$

$$J_{0,1}(\eta) = \frac{1}{2} \int_0^1 \|\eta^{'}(t) + \frac{\eta(t) - w}{1 - t}\|^2 \mathrm{d}t, \tag{2.47}$$

where $\eta_t = K\gamma_t$, and $w = K\mathbf{y}$. Let B_1 be the line obtained from transforming the line $z_1 = c_1$ by the matrix K. Similarly, B_2 is obtained from transforming $z_2 = c_2$ by the matrix K. These transformations of the lines can be done using Lemma 2.1.3. Let F_1 be an open set defined by B_1, and F_2 is similarly defined. Then we have

$$\begin{aligned} H_{1,2} = \{&\text{absolutely continuous } \eta(t) \in R^2, 0 < t < 1 \mid \gamma(0) = K\mathbf{x}, \gamma(1) = K\mathbf{y}, \\ &\eta(t_1) \in F_1^C \text{ for some } t_1, 0 \leq t_1 \leq 1 \text{ and } \eta(t_2) \in F_2^C \text{ for some } t_2, 0 \leq t_2 \leq 1\}. \end{aligned}$$

We now solve the optimization problem in (2.46) and (2.47). For notational convenience, and with some abuse of notations, from here on we represent $K\mathbf{x}$ as $\mathbf{x}$, and w as $\mathbf{y}$. Denoting that t_1 and t_2 are the time that boundary B_1 and B_2 are breached respectively, we need to consider the following three cases:

(1) $t_1 < t_2$

(2) $t_1 > t_2$

(3) $t_1 = t_2$.

We first consider the case where $t_1 < t_2$, and we have the following proposition.

Proposition 2.1.2 *Let $\phi_1 \in B_1$ and $\phi_2 \in B_2$. Assuming that $t_1 < t_2$, $u(\mathbf{x}, 0)$ in (2.46) can be written as*

$$u(\mathbf{x}, 0) = \inf_{\phi_1 \in B_1, \phi_2 \in B_2} \frac{1}{2}\{(\|\mathbf{x} - \phi_1\| + \|\phi_1 - \phi_2\| + \|\mathbf{y} - \phi_2\|)^2 - \|\mathbf{x} - \mathbf{y}\|^2\}. \quad (2.48)$$

Proof.

We want to minimize $J_{0,1}(\eta)$ from (2.47) with respect to $\eta(t)$. Hence, by selecting $\eta(t)$ on the interval $(t_2, 1]$ in such a way that

$$\eta^{'}(t) = -\frac{\eta(t) - \mathbf{y}}{1 - t} \quad (2.49)$$

$$\eta(t_2) = \phi_2, \quad (2.50)$$

we obtain the integrand $\|\eta^{'}(t) + \frac{\eta(t)-\mathbf{y}}{1-t}\|^2$ to be zero on the interval $(t_2, 1]$, and the integral vanishes. The conditions (2.49) and (2.50) are satisfied by setting

$$\eta(t) = \phi_2 + \frac{t - t_2}{1 - t_2}(\mathbf{y} - \phi_2). \quad (2.51)$$

Hence, we need to minimize the action functional on $[0, t_2]$, and the integral can be broken into two pieces

$$J_{0,1}(\eta) = \frac{1}{2}\int_0^{t_1} \|\eta'(t) + \frac{\eta(t)-\mathbf{y}}{1-t}\|^2 \mathrm{d}t + \frac{1}{2}\int_{t_1}^{t_2} \|\eta'(t) + \frac{\eta(t)-\mathbf{y}}{1-t}\|^2 \mathrm{d}t. \tag{2.52}$$

We simplify the optimization problem in (2.46) in the following way:

$$\begin{aligned}
u(\mathbf{x},0) &= \inf_{\eta\in H_{1,2}} J_{0,1}(\eta) && (2.53)\\
&= \inf_{\eta\in H_{1,2}} \left\{ \frac{1}{2}\int_0^{t_1} \|\eta'(t) + \frac{\eta(t)-\mathbf{y}}{1-t}\|^2 \mathrm{d}t \right. \\
&\quad \left. + \frac{1}{2}\int_{t_1}^{t_2} \|\eta'(t) + \frac{\eta(t)-\mathbf{y}}{1-t}\|^2 \mathrm{d}t \right\} && (2.54)\\
&= \inf_{t_1,t_2,\phi_1\in B_1,\phi_2\in B_2} \left\{ \frac{1}{2}\{\frac{\|\mathbf{x}-\phi_1\|^2}{t_1} + \frac{\|\mathbf{y}-\phi_1\|^2}{1-t_1} - \|\mathbf{x}-\mathbf{y}\|^2\} \right. \\
&\quad \left. + \frac{1}{2}\{\frac{\|\phi_1-\phi_2\|^2}{t_2-t_1} + \frac{\|\mathbf{y}-\phi_2\|^2}{1-t_2} - \frac{\|\phi_1-\mathbf{y}\|^2}{1-t_1}\} \right\} && (2.55)\\
&= \inf_{t_1,t_2,\phi_1\in B_1,\phi_2\in B_2} \frac{1}{2} \left\{ \frac{\|\mathbf{x}-\phi_1\|^2}{t_1} + \frac{\|\phi_1-\phi_2\|^2}{t_2-t_1} \right. \\
&\quad \left. + \frac{\|\mathbf{y}-\phi_2\|^2}{1-t_2} + \|\mathbf{x}-\mathbf{y}\|^2 \right\}. && (2.56)
\end{aligned}$$

The expression (2.54) is obtained from (2.52). We evaluate each of the two integrals in (2.54) using Lemma 1.2.2 and obtain results in (2.55). We minimize (2.56) with respect to t_1 and t_2 by using Lagrange multipliers for given ϕ_1 and ϕ_2. As shown in Appendix A.3, the solutions, t_1^* and t_2^*, are given by

$$t_1^* = \frac{\|\mathbf{x}-\phi_1\|}{\|\mathbf{x}-\phi_1\| + \|\phi_1-\phi_2\| + \|\mathbf{y}-\phi_2\|} \tag{2.57}$$

$$t_2^* = \frac{\|\phi_1-\phi_2\| + \|\mathbf{x}-\phi_1\|}{\|\mathbf{x}-\phi_1\| + \|\phi_1-\phi_2\| + \|\mathbf{y}-\phi_2\|}. \tag{2.58}$$

By substituting t_1^* and t_2^* into (2.56), we obtain the following minimization problem

$$u(\mathbf{x},0) = \inf_{\phi_1\in B_1,\phi_2\in B_2} \frac{1}{2}\{(\|\mathbf{x}-\phi_1\| + \|\phi_1-\phi_2\| + \|\mathbf{y}-\phi_2\|)^2 - \|\mathbf{x}-\mathbf{y}\|^2\}. \qquad \square$$

By Proposition 2.1.2, we can evaluate $u(\mathbf{x}, 0)$ by finding ϕ_1 and ϕ_2 such that the sum of Euclidean distances between $\mathbf{x}$ and ϕ_1, ϕ_1 and ϕ_2, and ϕ_2 and $\mathbf{y}$ is minimized.

In the second case where $t_1 > t_2$, a similar result can be derived

$$u(\mathbf{x}, 0) = \inf_{\phi_1 \in B_1, \phi_2 \in B_2} \frac{1}{2}\{(\|\mathbf{x} - \phi_2\| + \|\phi_2 - \phi_1\| + \|\mathbf{y} - \phi_1\|)^2 - \|\mathbf{x} - \mathbf{y}\|^2\}. \quad (2.59)$$

In the last case where $t_1 = t_2$, let ϕ_{12} be the point where the first barrier and the second barrier intersect. In this case, the first barrier and the second barrier are touched simultaneously. Then, we have

$$u(\mathbf{x}, 0) = \frac{1}{2}\{(\|\mathbf{x} - \phi_{12}\| + \|\mathbf{y} - \phi_{12}\|)^2 - \|\mathbf{x} - \mathbf{y}\|^2\}. \quad (2.60)$$

We obtain $u(\mathbf{x}, 0)$ by taking the minimum of (2.48), (2.59), and (2.60).

Now we address the optimization problem, (2.48) which corresponds to the first case where $t_1 < t_2$. Since the last term of the objective function in (2.48) does not depend on parameters ϕ_1 and ϕ_2, and square is a monotonic function on positive numbers, we instead focus on the following corresponding problem:

$$\inf_{\phi_1 \in B_1, \phi_2 \in B_2} (\|\mathbf{x} - \phi_1\| + \|\phi_1 - \phi_2\| + \|\mathbf{y} - \phi_2\|). \quad (2.61)$$

Now we look at how we can evaluate (2.61) in a two-dimensional case. Suppose that in R^2 there are two barriers, B_1 and B_2, represented by $a_{11}z_1 + a_{12}z_2 = c_1$ and $a_{21}z_1 + a_{22}z_2 = c_2$, respectively. The points $\mathbf{x} = [x_1, x_2]^T$ and $\mathbf{y} = [y_1, y_2]^T$ are located on the same side of these lines. Also, let $\mathbf{p} = [p_1, p_2]^T$ be the intersection point of the lines B_1 and B_2, assuming that it exists. Moreover, we define $\mathbf{x}'_{B_1}$ to

be a mirrored point of $\mathbf{x}$ around the line B_1, and $\mathbf{y}'_{B_2}$ to be a mirrored point of $\mathbf{y}$ around the line B_2. The coordinates of these mirrored points can be obtained by Lemma 2.1.4. The equation of a line connecting $\mathbf{x}'_{B_1} = [x'_1, x'_2]^T$ and $\mathbf{y}'_{B_2} = [y'_1, y'_2]^T$ is expressed by $a_{r_1} z_1 + a_{r_2} z_2 = 1$, where $a_{r_1} = \left[\left(\frac{x'_2 - y'_2}{y'_1 - x'_1}\right) x'_1 + x'_2\right]^{-1} \left(\frac{x'_2 - y'_2}{y'_1 - x'_1}\right)$ and $a_{r_2} = \left[\left(\frac{x'_2 - y'_2}{y'_1 - x'_1}\right) x'_1 + x'_2\right]^{-1}$.

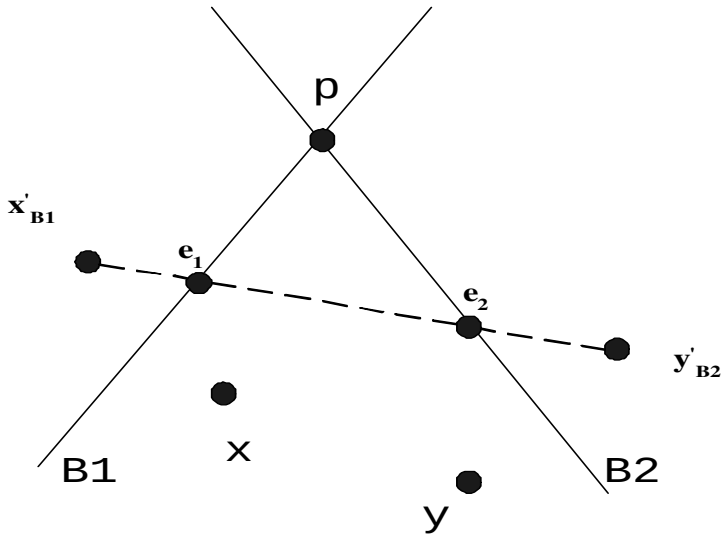

Figure 2.1: Illustration of the Shortest Path

Now in the case that $a_{r_1} p_1 + a_{r_2} p_2 \geq 1$, the line connecting $\mathbf{x}'_{B_1}$ and $\mathbf{y}'_{B_2}$ cross both barriers B_1 and B_2. In this case, we have

$$\min_{\phi_1 \in B_1, \phi_2 \in B_2} [\|\mathbf{x} - \phi_1\| + \|\phi_2 - \phi_1\| + \|\mathbf{y} - \phi_2\|] \tag{2.62}$$

$$= \min_{\phi_1 \in B_1, \phi_2 \in B_2} [\|\mathbf{x}'_{B_1} - \phi_1\| + \|\phi_2 - \phi_1\| + \|\mathbf{y}'_{B_2} - \phi_2\|] \tag{2.63}$$

$$= \|\mathbf{x}'_{B_1} - \mathbf{y}'_{B_2}\|, \tag{2.64}$$

and the path is graphically shown in Figure 2.1.

On the other hand, the case where $a_{r_1}p_1 + a_{r_2}p_2 < 1$ is the situation where the line connecting $\mathbf{x}'_{B_1}$ and $\mathbf{y}'_{B_2}$ does not cross both barriers B_1 and B_2. Then we have,

$$\min_{\phi_1 \in B_1, \phi_2 \in B_2} [\|\mathbf{x} - \phi_1\| + \|\phi_2 - \phi_1\| + \|\mathbf{y} - \phi_2\|] \tag{2.65}$$

$$= \begin{cases} \min_{\phi \in B_1}[\|\mathbf{x} - \phi\| + \|\mathbf{y} - \phi\|] & , \quad \text{if path x-}\phi^*\text{-y crosses line } B_2 \\ \min_{\phi \in B_2}[\|\mathbf{x} - \phi\| + \|\mathbf{y} - \phi\|] & , \quad \text{if path x-}\phi^*\text{-y crosses line } B_1 \\ \|\mathbf{x} - \mathbf{p}\| + \|\mathbf{y} - \mathbf{p}\| & , \quad \text{otherwise} \end{cases} \tag{2.66}$$

$$= \begin{cases} \|\mathbf{x}'_{B_1} - \mathbf{y}\| & , \quad \text{if path x-}\phi^*\text{-y crosses line } B_2 \\ \|\mathbf{x} - \mathbf{y}'_{B_2}\| & , \quad \text{if path x-}\phi^*\text{-y crosses line } B_1 \\ \|\mathbf{x} - \mathbf{p}\| + \|\mathbf{y} - \mathbf{p}\| & , \quad \text{otherwise} \end{cases} \tag{2.67}$$

In the above equation, if the shortest path from $\mathbf{x}$ to $\mathbf{y}$ that touches one barrier happens to cross the other barrier in the process, that particular path would be the shortest path from $\mathbf{x}$ and $\mathbf{y}$ such that touches both lines. This can be intuitively explained by graphical arguments. Otherwise, the shortest path is the path that touches the point $\mathbf{p}$, the intersection of the two lines. The complete proof of the results in (2.66) and (2.67) is given in Appendix C. Once we obtain $\min_{\phi_1 \in B_1, \phi_2 \in B_2}[\|\mathbf{x} - \phi_1\| + \|\phi_2 - \phi_1\| + \|\mathbf{y} - \phi_2\|]$, we can obtain $u(\mathbf{x}, 0)$ easily from the equation (2.48).

Now we can perform a similar calculation for the second case where $t_1 > t_2$. In this case, we use $\mathbf{x}'_{B_2}$ which is a reflection of $\mathbf{x}$ along the line B_2, and $\mathbf{y}'_{B_1}$ which is a reflection of $\mathbf{y}$ along the line B_1, because the second barrier is assumed to be hit first.

Also, in the third case where $t_1 = t_2$, we trivially see that

$$\begin{aligned} & \min_{\phi_1 \in B_1, \phi_2 \in B_2} [\|\mathbf{x} - \phi_1\| + \|\phi_2 - \phi_1\| + \|\mathbf{y} - \phi_2\|] \\ = \; & \|\mathbf{x} - \mathbf{p}\| + \|\mathbf{y} - \mathbf{p}\|. \end{aligned}$$

2.2 Exit Probabilities of Multidimensional Processes

2.2.1 Generalization to a Multidimensional Process

Let us assume that $(b_1, \ldots, b_d)$ are numbers such that $X_1(0) > b_1, \ldots, X_d(0) > b_d$ for a d-dimensional process. Then, we can define the following events:

$$E_1 = \{X_1(t) \leq b_1 \text{ for some t}, 0 \leq t \leq 1\} \tag{2.68}$$

$$E_2 = \{X_2(t) \leq b_2 \text{ for some t}, 0 \leq t \leq 1\} \tag{2.69}$$

$$\vdots \tag{2.70}$$

$$E_d = \{X_d(t) \leq b_d \text{ for some t}, 0 \leq t \leq 1\}. \tag{2.71}$$

Hence, E_i is the event where the i^{th} component of the process breaches its corresponding barrier, b_i.

The set relation from (2.6) in Section 2.1.1 can be generalized in the standard way:

$$\begin{aligned} & P(E_1 \cup E_2 \cup E_3 \cup \ldots \cup E_d) \\ = \; & \sum_i P(E_i) - \sum_{i \neq j} P(E_i \cap E_j) + \sum_{i \neq j \neq k} P(E_i \cap E_j \cap E_k) \\ - \; & \sum_{i \neq j \neq k \neq l} P(E_i \cap E_j \cap E_k \cap E_l) + \cdots, \end{aligned} \tag{2.72}$$

where the subscripts are all different.

Hence, in order to characterize the joint barrier crossing probability $P(E_1 \cup E_2 \cup E_3 \cup \ldots \cup E_d)$, we need to estimate joint probabilities of $P(E_i \cap E_j)$, $P(E_i \cap E_j \cap E_k)$, $\cdots$. In case where the underlying process follows the Brownian Bridge process with the interval size of ϵ, by Lemma 1.2.1 these probabilities satisfy the Large Deviations Principle with the same rate function as in (1.24).

In this section, we focus on the three-way joint probability, but our discussion can be generalized to arbitrarily high dimensions. We discuss two approaches. The first approach involves higher-order approximations, which require more computation. The second approach involves terms up to the second order. This approach has less computational burden but is also less accurate.

Higher-Order Approximations

When $d = 3$, we consider the following inclusion-exclusion principle,

$$\begin{aligned} P(E_1 \cup E_2 \cup E_3) &= P(E_1) + P(E_2) + P(E_3) - P(E_1 \cup E_2) \\ &- P(E_2 \cup E_3) - P(E_1 \cup E_3) \\ &+ P(E_1 \cap E_2 \cap E_3). \end{aligned} \tag{2.73}$$

Below we show how we can obtain an approximation of $P(E_1 \cap E_2 \cap E_3)$ by extending the concept presented in Section 2.1.3. We define $\Gamma_i, i = 1, 2, 3$, as in the Section

2.1.3, and we denote $\Gamma_{1,2,3} = \Gamma_1 \cap \Gamma_2 \cap \Gamma_3$. In other words,

$$\begin{aligned}\Gamma_{1,2,3} &= \{\text{absolutely continuous } \gamma(t) \in R^2, 0 < t < 1 | \gamma(0) = \mathbf{x}, \gamma(1) = \mathbf{y}, \\ &\quad \gamma_1(t_1) = c_1 \text{ for some } t_1, 0 \le t_1 \le 1, \\ &\quad \gamma_2(t_2) = c_2 \text{ for some } t_2, 0 \le t_2 \le 1, \\ &\quad \gamma_3(t_3) = c_3 \text{ for some } t_3, 0 \le t_3 \le 1\}.\end{aligned}$$

$\Gamma_{1,2,3}$ is the event where each component of the process breaches their corresponding barriers between time 0 and 1. Since $\Gamma_{1,2,3} \subseteq \mathcal{B}$, we can minimize the same action functional over the set $\Gamma_{1,2,3}$ as follows,

$$u(\mathbf{x}, 0) = \inf_{\eta \in \Gamma_{1,2,3}} J_{0,1}(\eta).$$

Suppose that $t_1 \le t_2 \le t_3$. By a similar transformation as in Section 2.1.3, we need to evaluate the following equivalent problem:

$$u(\mathbf{x}, 0) = \inf_{\eta \in H_{1,2,3}} J_{0,1}(\eta) \tag{2.74}$$

$$J_{0,1} = \frac{1}{2} \int_0^1 \|\eta^{'}(t) + \frac{\eta(t) - w}{1 - t}\|^2 \mathrm{d}t, \tag{2.75}$$

where all the variables are defined in similar manner as in Section 2.1.3. We also define B_i's in the same way. Now, with some abuse of notations, from here on we represent $K\mathbf{x}$ with $\mathbf{x}$, and w with $\mathbf{y}$. Then the above optimization problem can be reduced to the following problem:

$$\begin{aligned}u(\mathbf{x}, 0) &= \inf_{\phi_1 \in B_1, \phi_2 \in B_2, \phi_3 \in B_3} \frac{1}{2}\{(\|\mathbf{x} - \phi_1\| + \|\phi_1 - \phi_2\| + \|\phi_2 - \phi_3\| + \|\mathbf{y} - \phi_3\|)^2 \\ &\quad - \|\mathbf{x} - \mathbf{y}\|^2\},\end{aligned} \tag{2.76}$$

where ϕ_1 is the coordinate where the path $\eta(t)$ hits the first barrier B_1, and ϕ_2 and ϕ_3 are similarly defined for the second and the third barrier. This result implies that we can focus on solving the following optimization problem,

$$\inf_{\phi_1 \in B_1, \phi_2 \in B_2, \phi_3 \in B_3} \|\mathbf{x} - \phi_1\| + \|\phi_1 - \phi_2\| + \|\phi_2 - \phi_3\| + \|\mathbf{y} - \phi_3\|. \tag{2.77}$$

For higher-order joint probabilities involving four or more components, this method can be extended in a straight forward manner. For a general d-way interaction, the optimization problem that we need to address is

$$\inf_{\phi_1 \in B_1, \phi_2 \in B_2, \ldots, \phi_d \in B_d} \|\mathbf{x} - \phi_1\| + \|\phi_1 - \phi_2\| + \|\phi_2 - \phi_3\| + \ldots + \|\mathbf{y} - \phi_d\|, \tag{2.78}$$

where $\phi_1, \phi_2, \ldots, \phi_d$ are points on the hyperplanes $B_1, B_2, \ldots, B_d$, respectively. The only complication is that the optimization problem in (2.78) will involve more terms, and hence it will become more complicated.

We have assumed one particular sequence of ordering of $t_1, t_2, \ldots, t_d$, where $t_1 \leq t_2 \leq \ldots \leq t_d$. We also need to consider different sequences of $t_1, t_2, \ldots, t_d$, and there are $d!$ different sequences to consider. In order to obtain the true infimum of the action functional in (2.74), we compute the infimum under all the possible sequences of $t_1, t_2, \ldots, t_d$ and take the smallest number.

Solution to the Optimization Problem

Suppose that for $i = 1, \ldots, d$, ϕ_i is a vector of the form $[\phi_{i1}, \phi_{i2}, \ldots, \phi_{id}]^T$. Also, the hyperplanes $B_1, B_2, \ldots, B_d$ are represented by the linear equations $a_{i1}z_1 + a_{i2}z_2 +$

$\ldots + a_{id}z_d = c_i$. The problem in (2.78) can be formulated as a standard constrained minimization problem:

$$\inf_{\phi_1,\phi_2,\ldots,\phi_d} \|\mathbf{x} - \phi_1\| + \|\phi_1 - \phi_2\| + \|\phi_2 - \phi_3\| + \ldots + \|\mathbf{y} - \phi_d\| \tag{2.79}$$

with constraints

$$\begin{aligned} a_{11}\phi_{11} + a_{12}\phi_{12} + \ldots + a_{1d}\phi_{1d} &= c_1 \\ a_{21}\phi_{21} + a_{22}z_{22} + \ldots + a_{2d}z_{2d} &= c_2 \\ &\vdots \\ a_{d1}z_{d1} + a_{d2}z_{d2} + \ldots + a_{dd}z_{dd} &= c_d. \end{aligned} \tag{2.80}$$

Since ϕ_i's are d-dimensional vectors, the number of decision variables is d^2. We demonstrate that the objective function in (2.79) is indeed convex.

Lemma 2.2.1 *The objective function specified in (2.79) is convex.*

Proof. Let $\mathbf{s}$ be any point in R^d. Let $f(\mathbf{s})$ be the Euclidean norm of $\mathbf{s}$. First, we show that $f()$ is convex. Let $s_1, s_2 \in R^d$. By definition, we need to show that $\alpha f(s_1) + (1-\alpha)f(s_2) \geq f(\alpha s_1 + (1-\alpha)s_2)$, for $0 \leq \alpha \leq 1$.

$$\begin{aligned} f(\alpha s_1 + (1-\alpha)s_2) &= \|\alpha s_1 + (1-\alpha)s_2\| \\ &\leq \alpha\|s_1\| + (1-\alpha)\|s_2\| \\ &= \alpha f(s_1) + (1-\alpha)f(s_2) \end{aligned}$$

The objective function in (2.79) is expressed as a sum of many Euclidean norms. Since the sum of convex functions is also convex, the objective function in (2.79) is

a convex function of $(\mathbf{x}-\phi_1),(\phi_1-\phi_2),\ldots,(\mathbf{y}-\phi_d)$. By Theorem 5.7 of Rockafellar (1970), (2.79) is a convex function of $\phi_1,\ldots,\phi_d$, because $\phi_1,\ldots,\phi_d$ are linear transformations of $(\mathbf{x}-\phi_1),(\phi_1-\phi_2),\ldots,(\mathbf{y}-\phi_d)$. $\square$

From Lemma 2.2.1, we see that the optimization problem formulated in (2.79)-(2.80) is a convex optimization problem, which is a standard problem in the field of optimization. Convexity of the objective function guarantees convergence to the solution using an iterative numerical approach. In other words, the local minimum of this function is always a global minimum as well. Hence, in this thesis, we use a MATLAB optimization function "fmincon".

Using only Second Order Approximations

We have discussed how we can obtain approximations for $P(E_1\cap E_2\cap E_3)$, and more generally $P(E_1\cap E_2\cap\ldots\cap E_d)$. Alternatively, we can simply assume that for higher order terms $P(E_1\cap E_2\cap E_3)=0$ or $P(E_1\cap E_2\cap\ldots\cap E_d)=0$. This approximation is reasonable, because for a sufficiently short period of time the probability that all three or four barriers are breached will be small. This assumption may be violated, if all the components are highly correlated with one another and all the barriers are located very close to the initial or ending value of the underlying process.

If we assume for higher order interaction terms that $P(E_1\cap E_2\cap E_3)=0$ and $P(E_1\cap E_2\cap\ldots\cap E_d)=0$, then the computation of $P(E_1\cup E_2\cup E_3)$ or $P(E_1\cup E_2\cup\ldots\cup E_d)$ is simplified, because then we need to compute only the marginal barrier crossing probabilities and the two-way joint probabilities.

2.2.2 Generalizations to Other Situations

In Section 2.1, we focused on the situation where the underlying process was a two-dimensional Brownian Motion with zero drift and the barrier was constant over time. In this section, we relax some of these assumptions. First, we consider a Brownian Motion process with a non-zero drift. Then, we consider the situation where the barrier is changing linearly as a function of time.

Correlated Multivariate Brownian Motion with a non-zero Drift

In Section 2.1, we assumed that the drift term μ is zero. Here we investigate the situation where the underlying stochastic process follows a Brownian Motion process with a nonzero drift μ between the time s and $s+\epsilon$. Assuming fixed initial and terminal values of the interval to be $\mathbf{x}$ and $\mathbf{y}$, we demonstrate in Appendix B.2 that regardless of the value of μ the corresponding Brownian Bridge process is as follows:

$$d\mathbf{X}(t) = -\frac{\mathbf{X}(t)-\mathbf{y}}{1-t}dt + \sqrt{\epsilon}\Sigma d\mathbf{W}(t) \qquad \text{for} \qquad t \in [0,1) \tag{2.81}$$

with $\mathbf{X}(0) = \mathbf{x}$.

This process is exactly in the same form as the equation (2.3) in Section 2.1.1. Hence, the nonzero drift μ does not add any more complexity to the problem.

Time-Varying Barriers

In this section, we assume that the barrier level b is changing linearly as a function of time as follows,

$$b(t) = q \cdot (t - s) + b(s), \qquad t \in [s, s + \epsilon], \tag{2.82}$$

where q is a constant. Since in equations (1.19) and (1.21) we re-scale the time parameter t for the underlying process, we need to re-scale the time parameter in the representation (2.82). Hence, by changing the variable $t \to t/\epsilon$ and setting $s = 0$, we obtain the following representation of the barrier

$$b(t) = \epsilon q t + b(0), \qquad t \in [0, 1], \tag{2.83}$$

where the initial value $b(0)$ after re-scaling should be the same as the value of the variable $b(s)$. In order to present this idea clearly, we first focus on the 1-dimensional process with one barrier, then we discuss the correlated d-dimensional stochastic process with several barriers.

From (1.22), the drift term of the Brownian Bridge is $\frac{y-x}{1-t}$. where x and y are the fixed values of the Brownian Motion process at time 0 and time 1, respectively. Suppose that there is one barrier whose value changes over time according to a deterministic function $b(t) = \epsilon q t + b(0)$, for $0 \leq t \leq 1$. Computation of the probability that this Brownian Bridge hits the barrier under this setting is equivalent to that under the following setting:

- The Brownian Bridge has the drift term $\frac{(y-\epsilon q)-x}{1-t}$, which implies that the corresponding Brownian Motion process has fixed values of x and $(y - \epsilon q)$ at time 0 and 1, respectively.

- There is a time constant barrier $b = b(0)$.

This result is evident by using a geometric and graphical argument. The latter setting is obtained by rotating the former so that the linear barrier becomes a horizontal line. Also, the barrier and the expected value of the process $X(t)$ at time 0, $E[X(t)|X(0) = x]$, are $\epsilon qt + b(0)$ and $x + t(y - x)$, in the former setting, and $b(0)$ and $x + t((y - \epsilon q) - x)$, in the latter. Hence, the expected distances between the barrier and the value of the stochastic process at any time t are the same under these two settings, and the volatility remains the same as well. Hence, computations of the barrier crossing probability under these two settings yield the same result.

We can reformulate this problem by defining a new variable $v = y - \epsilon q$. Then the drift term of the Brownian Bridge can be written as $\frac{v-x}{1-t}$, with a time-constant barrier $b(0)$. After this change of a variable, the underlying stochastic process is a Brownian Bridge and the barrier is constant at $b(0)$, which is the formulation considered in Section 2.1.

We now consider a d-dimensional process with their corresponding barriers represented by b_i, $i = 1, \ldots, d$. We assume that $b_i, i = 1, \ldots, d$ are changing on $[0, 1]$ according to linear functions of time, represented by $b_i(t) = \epsilon q_i t + b_i(0)$. Originally, $\mathbf{y}$ is a $d \times 1$ vector of the terminal values of $\mathbf{X}$ at time 1. For the i^{th} component of this vector, y_i, we define a new variable $v_i = y_i - \epsilon q_i$. In a vector form, we have $\mathbf{v} = \mathbf{y} - \epsilon\mathbf{q}$, where $\mathbf{v} = [v_1, \ldots, v_d]^T$ and $\mathbf{q} = [q_1, \ldots, q_d]^T$. Hence, in order to remove the time variability of the i^{th} barrier, we replace y_i with v_i. We modify the drift

term of i^{th} component to be $\frac{v_i - x}{1-t}$ in the place of $\frac{y_i - x}{1-t}$. With this modification, we can consider a problem where the barriers are constant at the level of $b_i(0)$, and the underlying process is in the form of (2.3) in Section 2.1.1.

2.3 Numerical Examples of One-Interval Exit Probabilities

In this section, we provide some numerical examples of applications of the theoretical concepts introduced in Sections 2.1 and 2.2. For a two-dimensional Brownian Motion process, we approximate a barrier crossing probability for a small interval with fixed initial and terminal values.

For a two-dimensional Brownian Bridge process, we have a semi-analytic solution of the barrier-crossing probability given by He et al. (1998). We use this result as a benchmark to evaluate accuracy of our approximations.

In this numerical study, we use a variance-covariance matrix of the following form, with varying degrees of covariance represented by the number r:

$$VCV = \begin{bmatrix} 0.1 & r \\ r & 0.08 \end{bmatrix}. \tag{2.84}$$

Note that VCV corresponds to $\Sigma\Sigma^T$ using the earlier notations.

Table 2.1 shows the list of the covariance values, r, that will be used throughout this numerical study. It also gives the corresponding correlation ρ, which is computed from the usual formula, $\rho = \frac{r}{\sqrt{0.1}\sqrt{0.08}}$.

Table 2.1: Values of Covariance and Corresponding Correlation

Variance-Covariance	r	ρ
VCV1	0.075	0.83853
VCV2	0.05	0.55902
VCV3	0.035	0.39131
VCV4	0.025	0.27951
VCV5	0.005	0.055902
VCV6	0.001	0.01118
VCV7	-0.001	-0.01118
VCV8	-0.005	-0.055902
VCV9	-0.025	-0.27951
VCV10	-0.035	-0.39131
VCV11	-0.05	-0.55902
VCV12	-0.075	-0.83853
VCV13	0	0

We compute $P(E_1 \cup E_2)$, the probability that the underlying process hits one or both of the barriers in a 2-dimensional case. Firstly, in Section 2.3.1 we perform numerical calculations using the extension of Baldi's method as described in Section 2.1.2. Then, in Section 2.3.2 we do the calculations in the same setting using our proposed method as described in Section 2.1.3. We also explore additional numerical examples in order to gain better understanding of accuracy of our proposed method. In Section 2.3.3, we compute barrier crossing probabilities when the underlying process follows a 3-dimensional Brownian Motion. We let $\mathbf{x}$ and $\mathbf{y}$ be 2×1 vectors corresponding to the initial and terminal values of the Brownian Bridge. In addition, B is a 2×1 vector of corresponding barrier levels, and T denotes the length of the interval.

2.3.1 Calculations Using Extended Baldi's Approach

Table 2.2: Results of Baldi's approach

Variance-Covariance	Baldi's Approximation	True Value
VCV2	0.278	0.2861
VCV11	0.278	0.3072
VCV13	0.278	0.3002
$\mathbf{x} = [0.984, 0.978]^T$, $\mathbf{y} = [0.988, 0.981]^T$, $T = 0.003$, $B = [1, 1]^T$,		

In Table 2.2, we present "Baldi's approximation" obtained from Baldi's method discussed in Section 2.1.2, and "True Value", obtained from the closed-form solution given in He et al. (1998). As we vary the covariance between two components, we notice that Baldi's estimates remain the same. Moreover, Baldi's estimates are equal to the one-dimensional barrier crossing probability of the first component. These observations are consistent with our findings in Section 2.1.2. The true values are different under the three different covariance structures. The difference exists because the barrier crossing can occur when the underlying process goes through paths other than the most likely path for the event of the barrier crossing. Hence, we see in this example that Baldi's approach is not adequate.

Table 2.3: Results of Baldi's approach

Variance-Covariance	Baldi's Approximation	True Value
VCV2	0.1601	0.2066
VCV11	0.1601	0.2455
VCV13	0.1601	0.2340
$\mathbf{x} = [0.784, 0.778]^T$, $\mathbf{y} = [0.788, 0.781]^T$, $T = 0.5$, $B = [1, 1]^T$		

In Table 2.3, we use the same variance-covariance structures as in the Table 2.2. However, we increased the interval size to be much larger, from 0.003 to 0.5. We also moved $\mathbf{x}$ and $\mathbf{y}$ further from the barriers. As expected, Baldi's approximations are the same under different variance-covariance structure. However, these estimates differ more from the true probability, illustrating the inadequacy of these estimates.

Table 2.4: Results of Baldi's approach

Barriers	Variance-Covariance	Baldi's Approximation	True Value
$[1, 1.3]^T$	VCV2	0.278	0.278
	VCV11	0.278	0.278
	VCV13	0.278	0.278
$[1.01, 1.01]^T$	VCV2	0.0221	0.022318
	VCV11	0.0221	0.022512
	VCV13	0.0221	0.022503
$[0.99, 0.99]^T$	VCV2	0.9231	0.93237
	VCV11	0.9231	0.97716
	VCV13	0.9231	0.95438
$\mathbf{x} = [0.984, 0.978]^T$, $\mathbf{y} = [0.988, 0.981]^T$, $T = 0.003$			

In Table 2.4, we consider different locations of the barriers. We note that if one of the barriers is located far from the initial and terminal values of the process, then Baldi's estimates is similar to the true values. This is consistent with the nature of the Large Deviations approximations.

In Table 2.5, in the first trial, we set the starting point and the terminal point of the first component to be similar to those of the second component. In the subsequent trials, we make the starting point and the terminal point of the first component to be more different than those of the second dimension. As the relative location of

Table 2.5: Results of Baldi's approach

$\mathbf{x}$	$\mathbf{y}$	Var-Cov	Baldi's Approx.	True Value
$[0.984, 0.981]^T$	$[0.988, 0.985]^T$	VCV2	0.278	0.31134
		VCV11	0.278	0.36411
		VCV13	0.278	0.34519
$[0.984, 0.971]^T$	$[0.988, 0.969]^T$	VCV2	0.278	0.27808
		VCV11	0.278	0.27858
		VCV13	0.278	0.27844
$[0.984, 0.964]^T$	$[0.988, 0.961]^T$	VCV2	0.278	0.278037
		VCV11	0.278	0.278046
		VCV13	0.278	0.278043
$T = 0.003$, $B = [1, 1]^T$				

the second component is further away from the barrier, the true probability is less dependent on the covariance, because the effect of the second component becomes negligible. Hence, only in this situation, Baldi's approach may be appropriate to use.

Table 2.6: Results of Baldi's approach

Variance-Covariance	Baldi's Approximation	True Value
VCV2	0.6188	0.61891
VCV11	0.6188	0.62231
VCV13	0.6188	0.620505
$\mathbf{x} = [0.984, 0.978]^T$, $y = [0.988, 0.981]^T$, $T = 0.0005$, $B = [0.99, 0.99]^T$		

In Table 2.6, we reduce the interval size to be 0.0005. Here we do not see much improvement of accuracy compared to the situation where the interval size was 0.003. We still observe that Baldi's approximation does not depend on the covariance.

Overall we see that there are many explanations for the discrepancy between Baldi's estimates and the true values. First of all, Baldi's method is a first-order approximation. Secondly, the probability of the barrier crossing via the length-minimizing path γ does not completely dominate the barrier crossing probability via other routes. To address the shortcoming of Baldi's method, we proposed a new method in Section 2.1.3, and numerical results based on this approach are given in the next section.

2.3.2 Calculations Using the New Approach

The basic idea in this method is that we compute $P(E_1)$, $P(E_2)$, and $P(E_1 \cap E_2)$ separately, and from these values, we obtain the estimate of $P(E_1 \cup E_2)$. We obtain $P(E_1)$ and $P(E_2)$ from the analytic solution in (2.2). We obtain $P(E_1 \cap E_2)$ using the method described in Section 2.1.3, and $P(E_1 \cup E_2)$ from the inclusion-exclusion principle.

We use the same examples as in Section 2.3.1, so the proposed approach can be assessed in comparison to the Baldi's approach. Then we provide some more detailed numerical study in order to understand the characteristics of results based on our proposed approach.

Using the Same Example as in Section 2.3.1

In Table 2.7, $P(E_1 \cup E_2)$ are compared to the true value. We note that our estimates for $P(E_1 \cup E_2)$ vary, as we use different variance-covariance matrices. Hence, our

Table 2.7: Results of our approach

Variance-Covariance	$P(E_1)$	$P(E_2)$	$P(E_1 \cap E_2)$	$P(E_1 \cup E_2)$	True Value
VCV2	0.278	0.0307	0.0303	0.2784	0.2861
VCV11	0.278	0.0307	0.0010	0.3078	0.3072
VCV13	0.278	0.0307	0.0085	0.3002	0.3002
$\mathbf{x} = [0.984, 0.978]^T$, $\mathbf{y} = [0.988, 0.981]^T$, $T = 0.003$ $B = [1, 1]^T$					

estimates depend on correlations of underlying processes. Consequently, the accuracy of our estimates seems to be significantly better than that of Baldi's approach. When the correlation is 0, our estimate coincides with the true value.

Table 2.8: Results of our approach

Variance-Covariance	$P(E_1)$	$P(E_2)$	$P(E_1 \cap E_2)$	$P(E_1 \cup E_2)$	True Value
VCV2	0.1601	0.08795	0.06275	0.1854	0.2066
VCV11	0.1601	0.08795	0.00134	0.2468	0.2455
VCV13	0.1601	0.08795	0.01409	0.2340	0.2340
$\mathbf{x} = [0.784, 0.778]^T$, $\mathbf{y} = [0.788, 0.781]^T$, $T = 0.5$, $B = [1, 1]^T$					

Similarly, the accuracy of our proposed method is better under a different setting as shown in Table 2.8.

In Table 2.9, we consider different barrier levels. In the case with the barrier at $[1, 1.3]$, the barrier of the second component is far away from the initial value and the ending value of the second component. In this case, the probability of barrier crossing by the second component is almost negligible and consequently $P(E_1 \cap E_2)$ is zero as well. For the barrier $[0.99, 0.99]$ and the variance-covariance matrix given by VCV2 (positively correlated), we note that $P(E_2)$ is the same as $P(E_1 \cap E_2)$.

Table 2.9: Results of our approach

Barriers	Var-Cov	$P(E_1)$	$P(E_2)$	$P(E_1 \cap E_2)$	$P(E_1 \cup E_2)$	True Value
$[1, 1.3]^T$	VCV2	0.278	0	0	0.278	0.278
	VCV11	0.278	0	0	0.278	0.278
	VCV13	0.278	0	0	0.278	0.278
$[1.01, 1.01]^T$	VCV2	0.022074	0.000438	0.0003474	0.022165	0.022318
	VCV11	0.022074	0.000438	2.7383E-08	0.022512	0.022512
	VCV13	0.022074	0.000438	0.000009668	0.022503	0.022503
$(0.99, 0.99)^T$	VCV2	0.92312	0.40657	0.40657	0.92312	0.93237
	VCV11	0.92312	0.40657	0.30728	1	0.97716
	VCV13	0.92312	0.40657	0.37531	0.95438	0.95438
$\mathbf{x} = [0.984, 0.978]^T$, $\mathbf{y} = [0.988, 0.981]^T$, $T = 0.003$						

In this case, the probability of barrier hitting of the first component completely dominates that of the second component. The event that the second barrier is breached is a subset of the event that the first barrier is breached.

In Table 2.10, we fix the initial value and the end value of the first component as we vary those of the second component. We can see that our estimates change with covariance values.

In Table 2.11, we see that our proposed method estimates the barrier crossing probability reasonably well.

Detailed Numerical Study 1

Now we provide more in-depth numerical study in order to evaluate properties of our estimates. We examine four cases, and the results are shown in Tables D.1 - D.7 in Appendix D. We consider the following four cases of the initial point $\mathbf{x}$ and

Table 2.10: Results of our approach

Table 5							
x	**y**	Var-Cov	$P(E_1)$	$P(E_2)$	$P(E_1 \cap E_2)$	$P(E_1 \cup E_2)$	True Value
[0.984, 0.981]^T	[0.988, 0.985]^T	VCV2	0.278037	0.093014	0.08365	0.287407	0.31134
		VCV11	0.278037	0.093014	0.003868	0.367184	0.36411
		VCV13	0.278037	0.093014	0.02586	0.34519	0.34519
[0.984, 0.971]^T	[0.988, 0.969]^T	VCV2	0.278037	0.000558	0.0005577	0.278037	0.27808
		VCV11	0.278037	0.000558	8.532E-06	0.278586	0.27858
		VCV13	0.278037	0.000558	0.000155	0.27844	0.27844
[0.984, 0.964]^T	[0.988, 0.961]^T	VCV2	0.278037	8.29E-06	8.29E-6	0.278037	0.278037
		VCV11	0.278037	8.29E-06	6.30083E-8	0.278046	0.278046
		VCV13	0.278037	8.29E-06	2.30599E-6	0.278043	0.278043
$T = 0.003$, $B = [1, 1]^T$							

Table 2.11: Results of our approach

Variance-Covariance	$P(E_1)$	$P(E_2)$	$P(E_1 \cap E_2)$	$P(E_1 \cup E_2)$	True Value
VCV2	0.6188	0.004517	0.004517	0.6188	0.61891
VCV11	0.6188	0.004517	0.0008418	0.622458	0.62231
VCV13	0.6188	0.004517	0.0027948	0.620505	0.620505
$\mathbf{x} = [0.984, 0.978]^T$, $\mathbf{y} = [0.988, 0.981]^T$, $T = 0.0005$, $B = [0.99, 0.99]^T$					

the terminal point $\mathbf{y}$ for different combinations of a variance-covariance matrix and a time horizon, T.

- Case 1: $\mathbf{x} = [0.784, 0.778]^T$, $\mathbf{y} = [0.788, 0.781]^T$, $B = [1, 1]^T$
- Case 2: $\mathbf{x} = [0.884, 0.878]^T$, $\mathbf{y} = [0.688, 0.681]^T$, $B = [1, 1]^T$
- Case 3: $\mathbf{x} = [0.954, 0.948]^T$, $\mathbf{y} = [0.968, 0.951]^T$, $B = [1, 1]^T$
- Case 4: $\mathbf{x} = [0.654, 0.648]^T$, $\mathbf{y} = [0.668, 0.651]^T$, $B = [1, 1]^T$

The results are partially summarized in Figures 2.2 - 2.5, where we compare the results of our proposed method and Baldi's method to the benchmark values. B is the level of barriers, and T is the length of time interval. The tables in Appendix D display the probability that at least one component breaches its corresponding barrier. True values are computed based on He et al. (1998), and the values in the column "LDT" shows the results from our proposed approach as discussed in Section 2.1.3. In addition, we show the actual error and the percentage error amount. The values in the column "Baldi's" show the approximations based on Baldi's approach, which is described in Section 2.1.2.

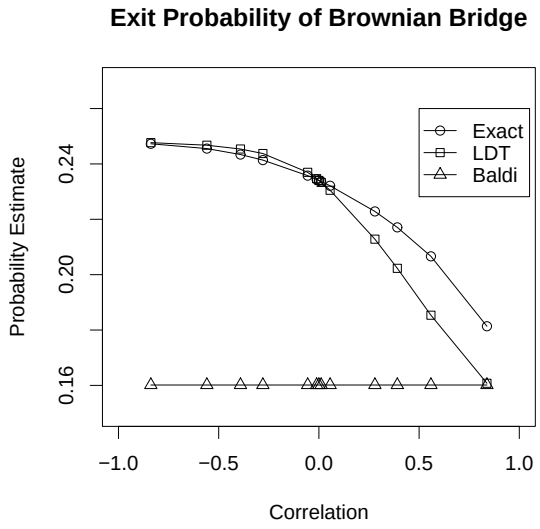

Figure 2.2: Estimates of Exit Probability for Case 1 with $T = 0.5$

The setting of Case 1 is the same as that in Table 2.8. We compute the barrier crossing probability for different variance-covariance matrices and different time interval lengths. Case 2 is designed such that $\mathbf{x}$ is brought closer to the barrier and

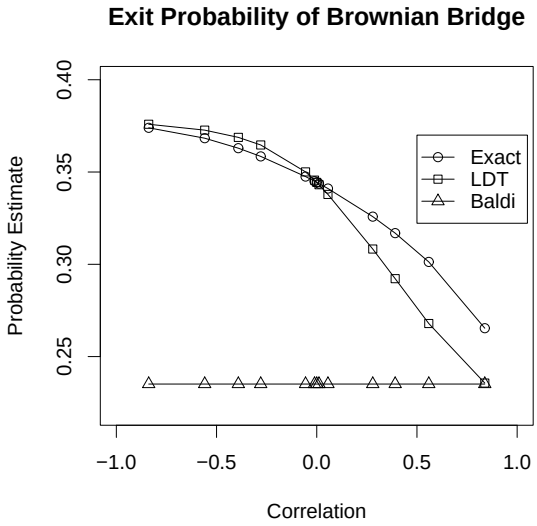

Figure 2.3: Estimates of Exit Probability for Case 2 with $T = 0.5$

$\mathbf{y}$ further from the barrier. Case 3 is the situation where $\mathbf{x}$ and $\mathbf{y}$ are located very close the barriers. In Case 4, $\mathbf{x}$ and $\mathbf{y}$ are very distant from the barrier.

Overall, our proposed method results in reasonable approximations of the true barrier crossing probabilities. We make several remarks from our results.

- Both absolute and percentage errors do not tend to increase much as T increases. Accuracy does not deteriorate very fast as a function of time. For the approximations with time interval $T = 1$, we still have reasonable approximations.

- When $\rho = 0$, our estimates coincide with the true value.

- In all four cases, our estimates are the worst at a high positive correlation. As we gradually change the correlation from high positive correlation toward

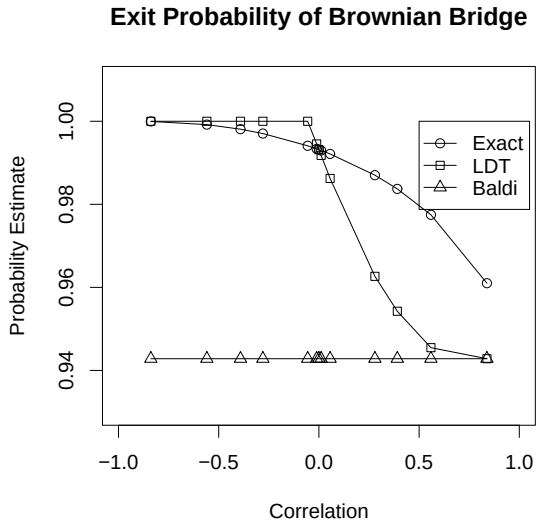

Figure 2.4: Estimates of Exit Probability for Case 3 with $T = 0.5$

high negative correlation, accuracy of our estimates tend to increase. Hence, our estimation works very well when the correlation is highly negative.

- Our estimates underestimate the true value when $\rho > 0$ and overestimate when $\rho < 0$.

- Our estimates in Case 1 and Case 2 show similar accuracy. This indicates that, as long as the probability of hitting barriers is within a similar range (neither too high nor too low), the accuracy is relatively similar.

- In Case 3, the probability of barrier crossing is very high and indeed very close to 1. In this case, the percentages errors are quite small. In some cases, our estimates turned out to be a number greater than 1, in which case we simply assign a value of 1 to the probability of barrier crossing.

- In Case 4, the probability of barrier crossing is very low. In this case, the

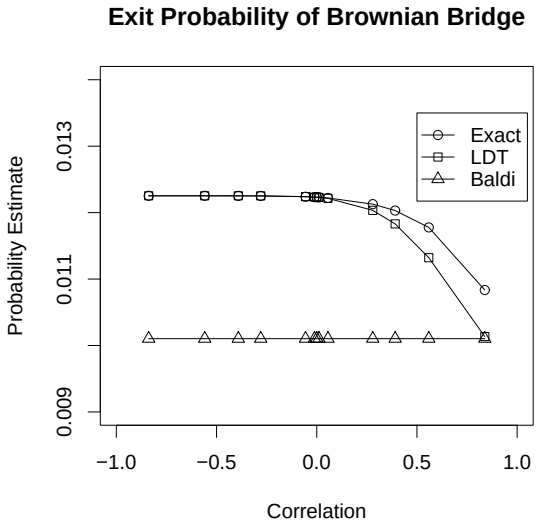

Figure 2.5: Estimates of Exit Probability for Case 4 with $T = 0.5$

percentage errors are fairly small. However, we note that as before the error increases for high positive correlation.

- We notice that Baldi's approach always underestimates the true probability because, due to its asymptotic nature, the estimate based on this approach turns out to be the same as the maximum of barrier crossing probability of the first component and that of the second. On the other hand, our approach considers the event that two barriers are breached, which is of the second-order. Hence, our estimates are always bigger than Baldi's and provide better approximations than Baldi's.

These observations show that our proposed method works reasonably well under various settings.

Detailed Numerical Study 2

In previous section, we attributed magnitude of error of our estimates to different factors. However, it is difficult to characterize the pattern, because the important factors such as instantaneous variance, length of time interval, and the location of initial and end points with respect to the barrier levels are all confounded. In this numerical study, we investigate the relationship between the probability of barrier crossing and the magnitude of the error of our proposed method. In particular, we evaluate the probability that both barriers are breached in the 2-dimensional case, and we consider different combinations of the initial value $\mathbf{x}$, the end value $\mathbf{y}$, and correlations ρ for the given interval:

$\mathbf{x} = [0.99, 0.99], [0.9, 0.9], [0.8, 0.8]$

$\mathbf{y} = [0.99, 0.99], [0.9, 0.9], [0.8, 0.8]$

$T = 0.0005, 0.001, 0.005, 0.01, 0.05, 0.1, 0.5, 1$

$\rho = -0.4, -0.1, 0, 0.1, 0.4$

Figure 2.6 establishes how the error magnitude of our proposed method is related to the barrier crossing probability. We note that the error is quite small when the probability of barrier crossing is either close to 1 or 0.

Figure 2.7 shows the relationship between the barrier crossing probability and the percentage error of our proposed method. We see that the percentage error is smallest when the barrier crossing probability is high, and that it gets larger as this probability decreases toward 0.

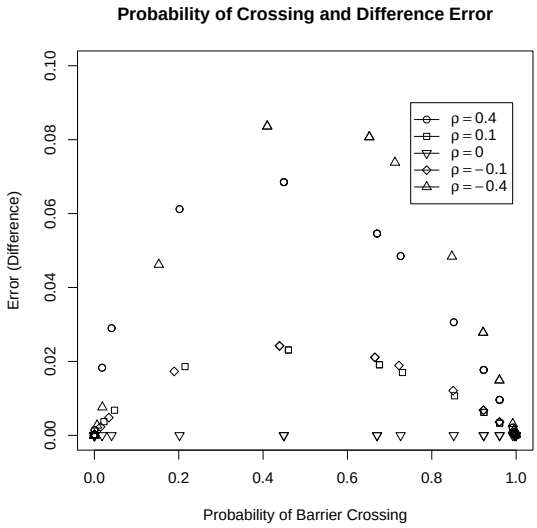

Figure 2.6: Relationship between Barrier Crossing Probability and Difference Error

From these numerical examples, we also note that generally the estimates are accurate when correlation is close to 0, and the error increases as the correlation deviates from zero in either direction.

2.3.3 Our Approach for the 3-Dimensional Case

In this section, we apply our proposed methodology from Section 2.1.3 to a 3-dimensional Brownian Motion process with fixed terminal values. Since this is a problem with dimension $d > 2$, it involves solving the optimization problem described in Section 2.2.1.

We consider a 3-dimensional Brownian Bridge process with the following information:

- The length of time interval T is 0.25.

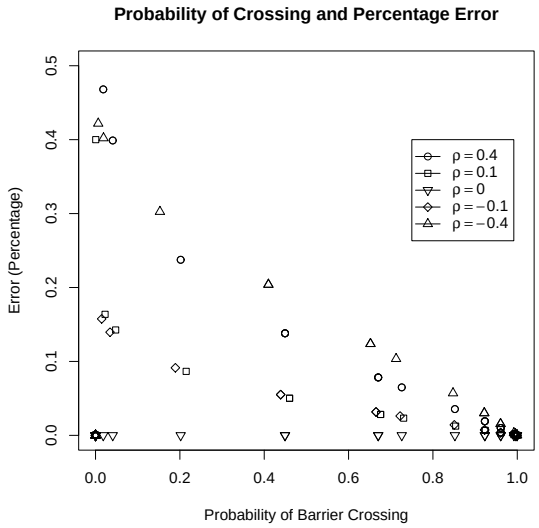

Figure 2.7: Relationship between Barrier Crossing Probability and Percentage Error

- The process has a fixed value $\mathbf{x} = [0.984, 0.978, 988]^T$ at the beginning of the interval and $\mathbf{y} = [0.988, 0.981, 0.98]^T$ at the end.
- The levels of barriers for these three components are $c = [1, 1, 1]^T$.
- The variance-covariance matrix for this correlated process is given to be

$$VCV = \begin{bmatrix} 0.1 & r & r \\ r & 0.08 & r \\ r & r & 0.1 \end{bmatrix} \tag{2.85}$$

  where r is the covariance.

In this numerical study, we compute the probability that all three components of this 3-dimensional Brownian Bridge cross their respective barriers for the time interval $T = 0.25$. The marginal 1-dimensional barrier crossing probabilities of each

component are 0.9847, 0.9591, and 0.9810, respectively. Hence, we know that the true value of the three-way joint barrier crossing probability with zero covariance should be $0.9847 \times 0.9591 \times 0.9810 = 0.9265$.

Table 2.12: Joint Exit Probabilities of 3-Dimensional Pinned Brownian Motion

Covariance	Simulation	Our Approach	Our Approach (tol)
0.075	0.934294 (0.003)	0.959062	0.9588
0.05	0.913941 (0.002)	0.957735	0.9548
0.035	0.912647 (0.003)	0.953284	0.9501
0.025	0.911059 (0.004)	0.948336	0.9469
0.005	0.912824 (0.003)	0.931937	0.9291
0.001	0.908647 (0.002)	0.927597	0.9245
0	0.905706 (0.003)	0.926479	0.9249
-0.001	0.906647 (0.003)	0.925353	0.9205
-0.005	0.905588 (0.004)	0.920741	0.9174
-0.025	0.905176 (0.002)	0.895547	0.8936
-0.035	0.906471 (0.003)	0.881685	0.8804

Table 2.12 presents our estimates with varying degrees of covariance. Under the column "Simulation", we present this joint exit probabilities computed from the Crude Monte Carlo approach with 1,300 subintervals and 17,000 runs of simulations. We do not know the exact value of the joint exit probability, but we know

that the Crude Monte Carlo method converges to the true value as we increase the number of subintervals and the number of simulations. Our "Simulation" value at zero correlation does not match our known result, indicating that the Crude Monte Carlo estimate still has a downward bias even with using 1,300 subintervals. The column "Our Approach" shows the results we obtain from our proposed method in Section 2.1.3. The column "Our Approach (Tol)" is the same as the previous column except that we have increased the tolerance level of the Matlab optimization function "fmincon" to be $0.15 \times T$, in order to reduce time for solving the optimization problem. From this table, we see that we do not lose much accuracy by increasing the tolerance level. The efficient ways of approximating the solution to this optimization problem are further discussed in detail in Section 3.1.3.

In our numerical study, we have explored our proposed methodology with different locations of the initial point, $\mathbf{x}$, and the ending point, $\mathbf{y}$. In terms of percentage error, our method works the best when the initial and the ending point are close to the barriers (i.e. when the probability of crossing barriers is high). As the probability of crossing all the barriers becomes smaller, the percentage error increases up to as high as 50-60 percent . However, in practice, this should not be a serious problem because in such cases the absolute error is very small. In summary, the proposed method works the best when the barrier crossing probability is high. The situation where the barrier crossing probability is high for the given interval is the case that matters the most when we compute the barrier crossing probability of a Brownian Motion process, as discussed in the next chapter.

Chapter 3

Simulation Methods of Exit Probabilities of a Multivariate Brownian Motion

In the previous chapter, we have discussed a method of computing the barrier crossing probability of a Brownian Bridge process in one fixed interval. In this chapter, we extend these concepts and propose an algorithm of computing a barrier crossing probability for a given time interval when the underlying process follows a correlated multivariate Brownian Motion process.

We first assume that the underlying process is 3-dimensional and describe an algorithm for computing the barrier crossing probability. This algorithm is easily extendible to higher dimensional processes. We consider a 3-dimensional Brownian

Motion $\mathbf{X}(t)$ of the following form

$$d\mathbf{X}(t) = Udt + \Sigma d\mathbf{W}(t), \tag{3.1}$$

with barrier levels $B = [b_1, b_2, b_3]^T$, where U is a 3×1 vector of drift terms, $\{\mathbf{W}(t)\}$ is a 3-dimensional standard Brownian Motion, and Σ is a 3×3 matrix corresponding to a square root of an instantaneous variance-covariance matrix.

In this chapter, we develop methods of efficiently computing a barrier crossing probability of a multivariate Brownian Motion. In Section 3.1, we extend the idea from Chapter 2 and propose an algorithm in a simulation framework for computing the probability that at least one component breach its respective barrier. In Section 3.2, we propose a more time-efficient version of the algorithm described in Section 3.1. In Section 3.3, we compare efficiency of the proposed method to that of existing methods. The remainder of this chapter deals with applications and extension of our proposed algorithm. We compute the distribution of number of components crossing barriers in Section 3.4 and price a credit basket derivative in Section 3.5.

3.1 An Effective Algorithm in a Simulation Framework

We present a general simulation framework for computing a barrier crossing probability of a multivariate Brownian Motion process. In particular, we focus on computing a probability that at least one component of the multivariate process

breaches its respective barrier within a given time horizon. We describe the simulation framework in Section 3.1.1. Then, in Section 3.1.2, we describe three different methods of simulating barrier crossing probability, namely *Crude Monte Carlo Method*, *Baldi's Method*, and *Our Proposed Method*. The optimization involved in *Our Proposed Method* imposes a huge computational burden. In Section 3.1.3, we discuss some methods for solving the optimization problem, which was described in Section 2.2.1. In Section 3.1.4, we present some numerical examples, and in Section 3.1.5, we illustrate a stylized example in the context of credit risk application.

3.1.1 General Simulation Framework

For the given time horizon T, we can select an arbitrary number of subintervals, M, for simulating the barrier crossing probabilities within this time horizon. First we suggest an algorithm for the case $M = 1$, and then show how this algorithm can be generalized to any number of subintervals, $M > 1$.

For $M = 1$, we can apply the following algorithm with N runs of simulation to evaluate the probability that at least one component breaches its corresponding barrier. The justification for using the following algorithm for computing a barrier crossing probability is given in Appendix E.

1. Let $Default\_Cnt = 0$ and suppose that $\mathbf{X}(0) = [x_1(0), x_2(0)x_3(0)]^T$, such that $x_1(0) > b_1$, $x_2(0) > b_2$, and $x_3(0) > b_3$.

2. Generate a value $\mathbf{X}(T) = [x_1(T), x_2(T), x_3(T)]^T$ according to the Brownian Motion process (3.1).

3. If $x_1(T) \leq b_1$, $x_2(T) \leq b_2$, or $x_3(T) \leq b_3$, then at least one barrier is breached, and we increment $Default\_Cnt = Default\_Cnt + 1$.

4. If $x_1(T) > b_1$, $x_2(T) > b_2$, and $x_3(T) > b_3$, then a barrier crossing does not occur at the simulated point T. We compute CP, which is the probability that the process $\mathbf{X}$ crosses the barrier B with fixed values $X(0) = [x_1(0), x_2(0), x_3(0)]^T$ and $X(T) = [x_1(T), x_2(T), x_3(T)]^T$. We increment $Default\_Cnt$ by CP. i.e. $Default\_Cnt = Default\_Cnt + CP$

5. we repeat Steps 2-4 N times.

6. The probability of barrier crossing by at least one component is obtained as $\frac{Default\_Cnt}{N}$.

The methods of calculating CP in the above algorithm are discussed in the next section. Now we consider the case $M > 1$. The above procedure will be slightly modified in Steps 2, 3 and 4.

$2^{'}$ Generate values $\mathbf{X}(i\epsilon) = [x_1(i\epsilon), x_2(i\epsilon), x_3(i\epsilon)]^T, i = 1, \ldots, M$ according to the Brownian Motion process (3.1), where ϵ is the size of each time step.

$3^{'}$ If there exists $i \in \{1, \ldots M\}$ such that $X_1(i\epsilon) \leq b_1$, $X_2(i\epsilon) \leq b_2$ or $X_3(i\epsilon) \leq b_3$, the barrier is breached by the simulated path. We increment $Default\_Cnt = Default\_Cnt + 1$.

$4^{'}$ If $\forall i \in \{1, \ldots M\}$, $x_1(i\epsilon) > b_1$, $x_2(i\epsilon) > b_2$, and $x_3(i\epsilon) > b_3$, the barriers are not breached at the end points of subintervals.. We compute $CP_i, i = 1, \ldots, M$,

where CP_i is the probability that the process $\mathbf{X}$ crosses the barrier B during the interval from $(i-1)\epsilon$ to $i\epsilon$ with fixed values of the process $X((i-1)\epsilon) = [x_1((i-1)\epsilon), x_2((i-1)\epsilon), x_3((i-1)\epsilon)]^T$ and $X(i\epsilon) = [x_1(i\epsilon), x_2(i\epsilon), x_3(i\epsilon)]$. The probability that $\{\mathbf{X}(t), 0 \leq t \leq M\epsilon\}$ crosses at least one barrier is given to be $1-\prod_{i=1}^{M}(1-CP_i)$. Hence, we increment $Default\_Cnt$ by $1-\prod_{i=1}^{M}(1-CP_i)$. i.e. $Default\_Cnt = Default\_Cnt + (1-\prod_{i=1}^{M}(1-CP_i))$. Note that $M\epsilon = T$, which is the specified time horizon.

In the above algorithm, CP is the probability that any of the component of the multidimensional process crosses its corresponding barrier. We have not yet specified how to formulate the values of CP in the single step case, or CP_i in the multi-step case. In the next section, we propose three different methods for simulating a barrier crossing probability. The only difference among these methods is the way we obtain CP or CP_i's.

3.1.2 Description of Simulation Methods

All three simulation methods are based on the same simulation scheme described in Section 3.1.1, except for the way we compute CP.

Simulation 1: Crude Monte Carlo (*CMC*)

In this case, we neglect the probability that the barrier may be breached between the discrete time intervals. In other words, we always assume $CP = 0$ in a single-step case, and $CP_i = 0$ in the multi-step case.

Simulation 2: Baldi's Method (*LDMC1*)

This is a method based on Section 2.1.2. Suppose that we define the event

$$E_k = \{\text{The } k^{th} \text{ component breaches its corresponding barrier.}\} \tag{3.2}$$

for $k = 1, 2, 3$. As discussed in Section 2.1.2, CP is computed in the following way,

$$CP = \max(P(E_1), P(E_2), P(E_3)) \tag{3.3}$$

in a single step case. Estimates of CP_i's are obtained in a similar way.

Simulation 3: Our Proposed Method (*LDMC2*)

CP is the probability that any of the components of the d dimension crosses its corresponding barrier. CP is computed based on the method from Section 2.1.3. Hence, using the notation of this section, $CP = P(E_1 \cup E_2 \cup E_2)$, when $d = 3$. We know that

$$\begin{aligned} P(E_1 \cup E_2 \cup E_3) &= P(E_1) + P(E_2) + P(E_3) - P(E_1 \cap E_2) \\ &- P(E_2 \cap E_3) - P(E_1 \cap E_3) \\ &+ P(E_1 \cap E_2 \cap E_3). \end{aligned} \tag{3.4}$$

In the above expression, the one-dimensional barrier crossing probabilities, $P(E_1)$, $P(E_2)$, and $P(E_3)$ are easily obtained from the closed-form expression in (2.2). Also, the pairwise exit probabilities such as $P(E_1 \cap E_2)$, $P(E_2 \cap E_3)$, and $P(E_1 \cap E_3)$ are obtained in the computationally efficient way, because we have the semi-analytic approach as described in Section 2.1.3. For $P(E_1 \cap E_2 \cap E_3)$, we have discussed how to obtain this probability in Section 2.2.1. However, this calculation is computationally expensive, since it involves solving a convex optimization problem that

requires many iterations of numerical procedures. Hence, in the subsequent section, we incorporate procedures that help to reduce computational burden of this procedure.

3.1.3 Approaches for Solving the Optimization Problem in Our Proposed Method

In Our Proposed Method(*LDMC2*), the evaluation of $P(E_1 \cap E_2 \cap E_3)$ takes a lot of time, because we need to solve the optimization problem described in Section 2.2.1. In order to reduce the number of these evaluations, we incorporate the ideas from Section 2.2.1. In many situations, $P(E_1 \cap E_2 \cap E_3)$ is very small, and hence it is reasonable to assume that this quantity is zero. We need to have some criteria to determine whether this probability is very small, and hence this term can be ignored. We consider quantities, $\min(P(E_1), P(E_2), P(E_3))$ and $\min(P(E_1 \cap E_2), P(E_2 \cap E_3), P(E_1 \cap E_3))$. If one of these quantities are very small, we can comfortably assume $P(E_1 \cap E_2 \cap E_3)$ to be zero. Hence, we can specify threshold values of α_1 and α_2 for $\min(P(E_1), P(E_2), P(E_3))$ and $\min(P(E_1 \cap E_2), P(E_2 \cap E_3), P(E_1 \cap E_3))$, respectively. If any of these quantities are below the threshold values, we can let $P(E_1 \cap E_2 \cap E_3) = 0$. Otherwise, we compute $P(E_1 \cap E_2 \cap E_3)$ using one of the approaches described below.

Approach I: Matlab-based Optimization

This method uses the original approach described in Section 2.2.1. From Lemma 2.2.1, we have shown that the objective function (2.79) is convex. Hence, the Matlab function "fmincon" gives the global minimum of this problem.

This approach gives us the most accurate result. However, the drawback of this method is that it takes too much time to perform this optimization task, because the function "fmincon" finds the solution using an iterative approach. Moreover, we need to consider all the possible orderings of $\phi_1, \phi_2, \ldots, \phi_d$. The number of times that we need to perform is $d!$, which is rather unmanageable in high dimensions.

Approach II: Algorithm Based On Local Optima

We describe a heuristic approach that gives us local minima. For the fixed sequence of $\phi_1, \phi_2, \ldots, \phi_d \in R^d$, we perform the following procedure.

1. Initialize the values of $\phi_1, \phi_2, \ldots, \phi_d$. For the ease of notations, we use ϕ_0, and ϕ_{d+1} to denote the fixed beginning value $\mathbf{x}$ and the terminal value $\mathbf{y}$ of the process, respectively.

2. For each i where $i = 1, \ldots, d$, we fix the values of ϕ_{i-1} and ϕ_{i+1}. Then, we find the point $\phi_i^* \in B_i$, such that the length of the path ϕ_{i-1}-ϕ_i^*-ϕ_{i+1} is minimized.

3. We update $\phi_i = \phi_i^*$.

4. We iterate Step 2 and 3 until certain convergence criteria are reached, or for the fixed number of iterations.

Given two points ϕ_{i-1} and ϕ_{i+1} for each $i = 1, \ldots, d$, this algorithm finds ϕ_i^* such that the length of the path from ϕ_{i-1} to ϕ_{i+1} that touches the hyperplane defined by the i^{th} constraint is minimized. This approach performs a piece-wise optimization, and hence it does not guarantee to yield global optima. However, it gives us the

values that are quite close to the global optima in all the cases that we considered. Also, in terms of time efficiency, this algorithm is much faster than Approach I.

Similar to Approach I, we also need to consider all the possible orderings of $\phi_1, \phi_2, \ldots, \phi_d$. However, the time taken to perform each optimization is much faster.

Approach III: Combination of Approach I and II

Approach I requires a lot of computation time to handle all the possible orderings of $\phi_1, \phi_2, \ldots, \phi_d$. Hence, for all the possible orderings, we perform Approach II in order to determine which ordering minimizes the objective function. Then, for the selected ordering, we can fine-tune the objective function by performing Approach I.

This approach works faster than Approach I, but slower than Approach II. On the other hand, the accuracy of this method is better than Approach II, but worse than Method I. This method may be a good compromise between Approach I and II.

3.1.4 Numerical Examples

Problem Set-up

We show numerical examples in order to assess accuracy and computation efficiency of the proposed method discussed in this section. In the following example, we focus on computing the probability that at least one component of the process hits its corresponding barrier.

We assume that the underlying process follows a 3-dimensional correlated Brownian Motion with parameters of each component as specified in Table 3.1.

Table 3.1: Parameters of Brownian Motions

Component	Initial Value	μ	σ^2
1	4.54	0.07	0.02
2	4.54	0.0325	0.035
3	4.54	0.015	0.03

Because of the properties of Brownian Motion, the effect of variance, time horizon, and distance to barrier are confounded. Therefore, we can just change one variable to determine the accuracy of our results under different situations. In our study, we fix the time horizon $T = 1$ and vary the distance to barrier by moving barrier levels. Table 3.2 specifies different barrier levels used under different trials of this study.

Table 3.2: Barrier Levels Used under Different Trials

	Component 1	Component 2	Component 3
Trial 1	4.40	4.28	4.29
Trial 2	4.45	4.39	4.38
Trial 3	4.47	4.42	4.43
Trial 4	4.51	4.48	4.47
Trial 5	4.49	4.48	4.42

For each trial, we vary correlation $\rho = -0.2, 0, 0.2, 0.8$, where ρ is a correlation between each pair of the components. We vary the number of subintervals M. We

let N be the number of simulation runs. We also vary thresholds of α_1 and α_2, which, as described in Section 3.1.3, determine whether to calculate the third order term. We employ following different methods for obtaining the barrier crossing probability for the given time horizon.

- Method 0 (M0): Our proposed method (*LDMC2*) with Optimization Approach 1 from Section 3.1.3 ($N = 80000$)
- Method 1 (M1): Our proposed method (*LDMC2*) with Optimization Approach 2 from Section 3.1.3 ($N = 80000$)
- Method 2 (M2): Our proposed method (*LDMC2*) with Optimization Approach 3 from Section 3.1.3 ($N = 80000$)
- Method 3 (M3): Crude Monte Carlo method (*CMC*) ($N = 80000$)

Results and Findings

First of all, we note that the simulation results do not differ much whether we use the method M0, M1 or M2. In Figure 3.1, we show the barrier crossing probability estimate for different values of ρ and M. All the graphs show that the estimates of M1 are very close to those of M0 and M2. These observations hold true not only in this trial, but also in other trials as well. Hence, we can use M1, which involves time-efficient approximating algorithm for optimization instead of the Matlab built-in optimization function. Generally, the method M1 works about 2 to 10 times faster than M2 and 2 to 50 times faster than M0.

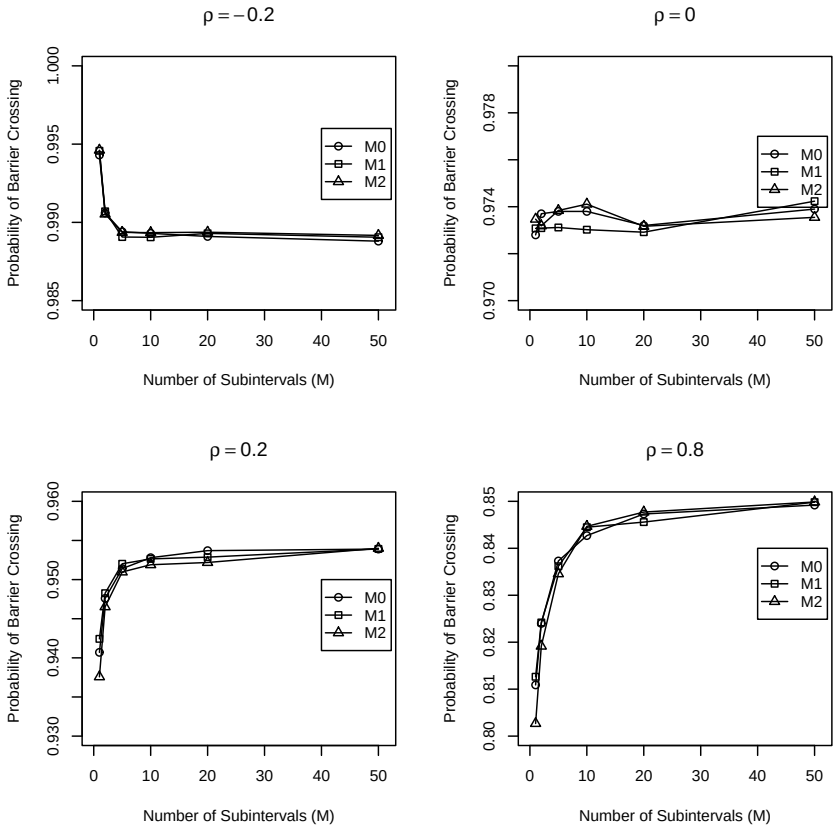

Figure 3.1: Comparison of Estimates from M0, M1, and M2 : Trial 4, with $\alpha_1 = 0.1$ and $\alpha_2 = 0.03$

Now we focus on the performance of M1 in comparison to other methods. Figure 3.2 and 3.3 show the estimates from M1 and M3 in the setting of Trial 4. The values of α_1 and α_2 are 0.1 and 0.03 for Case 1, 0.8 and 0.6 for Case 2, and 1 and 1 for Case 3, respectively. As described in Section 3.1.3, α_1 and α_2 determine how frequently we perform the computation of the third-order interaction term. In Case 3, the third-order interaction term is always completely ignored. In these figures, the graphs on the left hand side in Figures 3.2 and 3.3 display the estimates using

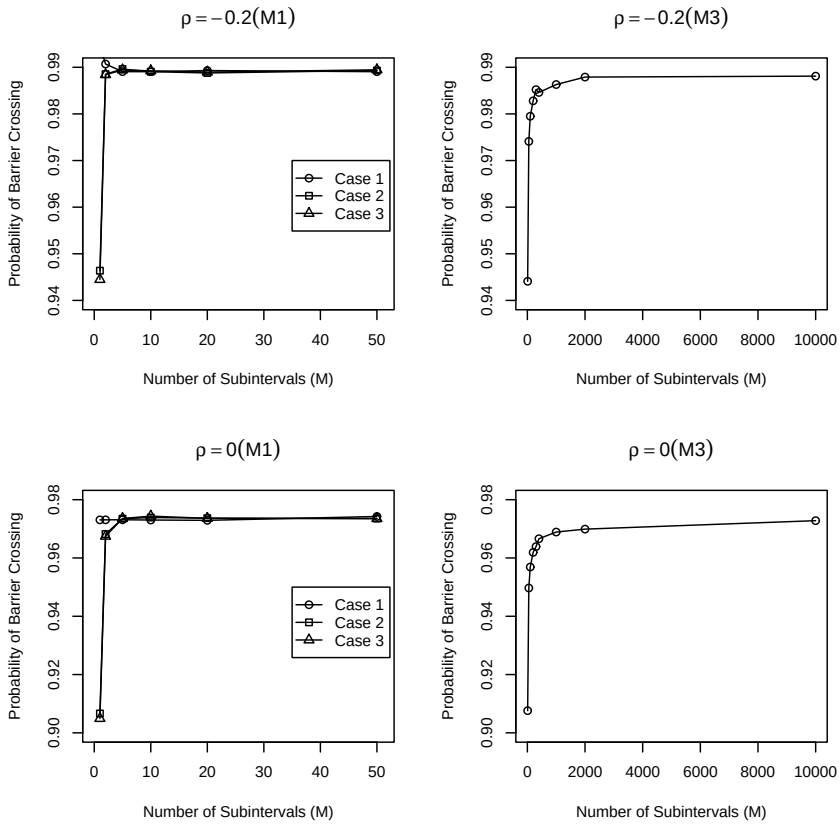

Figure 3.2: Comparison of Estimates from M1 and M3 : Trial 4 (Case 1: $\alpha_1 = 0.1, \alpha_2 = 0.03$, Case 2: $\alpha_1 = 0.8, \alpha_2 = 0.6$, Case 3: $\alpha_1 = 1, \alpha_2 = 1$) [Part 1]

M1 with various values of α_1 and α_2. The graphs on the right hand column show the results obtained from crude Monte Carlo simulations (M3). In both cases, we plot the values of estimates as a function of the number of subintervals (M). We do not know the true value of barrier crossing probability except for the case $\rho = 0$. However, we can safely assume the true value to be in a neighbourhood of the value where the curve resulted from M1 flattens and stabilizes at large values of M. Also, we know that the estimate from Crude Monte Carlo converges to the true value as

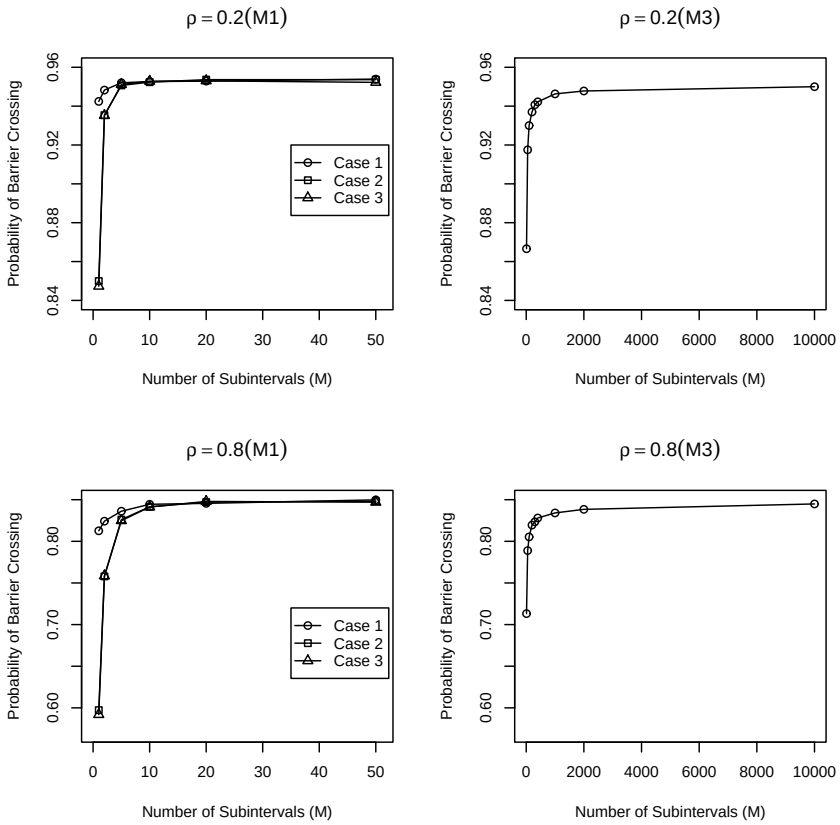

Figure 3.3: Comparison of Estimates from M1 and M3 : Trial 4 (Case 1: $\alpha_1 = 0.1, \alpha_2 = 0.03$, Case 2: $\alpha_1 = 0.8, \alpha_2 = 0.6$, Case 3: $\alpha_1 = 1, \alpha_2 = 1$) [Part 2]

$M \to \infty$. When $\rho = 0$, the true barrier crossing probability in this setting can be calculated explicitly and is 0.9736. Using the method M1, we obtain 0.9728 and 0.9733 with $M = 1$ and $M = 2$, respectively in the setting of Case 1. However, with M3 (Crude Monte Carlo), to achieve the same level of accuracy we need more than $M = 10,000$. Even when M is a very big number, such as 10,000, we do not completely remove the downward bias. We are not certain how many subintervals are needed in order to completely remove this downward bias.

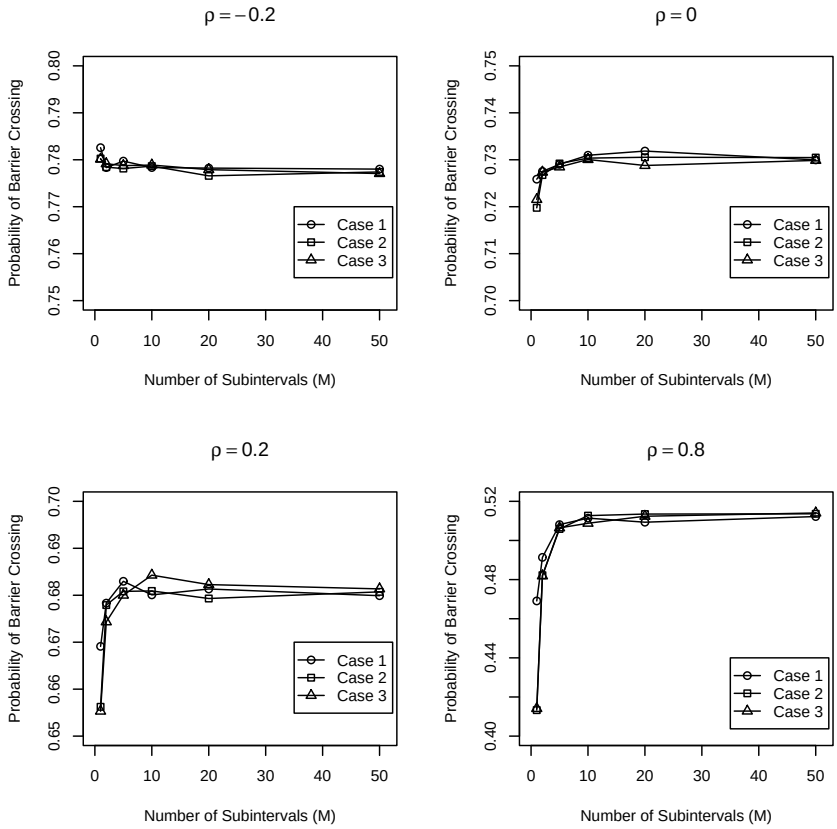

Figure 3.4: Estimates from M1 with various values of α_1 and α_2 : Trial 2 (Case 1: $\alpha_1 = 0.1, \alpha_2 = 0.03$, Case 2: $\alpha_1 = 0.8, \alpha_2 = 0.6$, Case 3: $\alpha_1 = 1, \alpha_2 = 1$)

Now we examine the effects of α_1 and α_2. For all values of the correlations, when we have low values of α_1 and α_2, our estimates of M1 are closer to the true value and converge faster as M increases. If we have small α's, then it takes more time to perform calculations, since it needs to evaluate the third-order term more frequently. This observation is true for other trials, as exemplified in Figures 3.4 and 3.5. However, we notice that as the barriers are situated further from the initial value, the third order term plays a less important role, and subsequently the effects

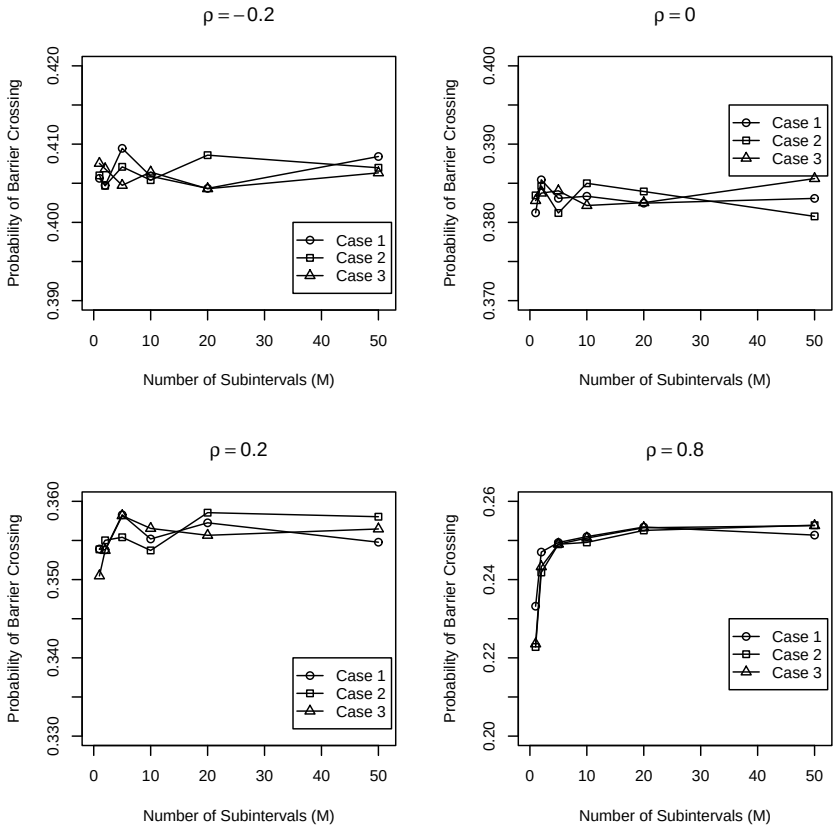

Figure 3.5: Estimates from M1 with various values of α_1 and α_2 : Trial 1 (Case 1: $\alpha_1 = 0.1, \alpha_2 = 0.03$, Case 2: $\alpha_1 = 0.8, \alpha_2 = 0.6$, Case 3: $\alpha_1 = 1, \alpha_2 = 1$)

of different values of α_1 and α_2 diminish.

We now assess how M1 performs under different correlation values. When $\rho = -0.2$ or 0, the estimate converges to the true value with $M = 1$ and $M = 2$, respectively in Case 1. When ρ is a positive value, we need a larger number of M as ρ increases. This finding is consistent with our earlier findings. When we look at the barrier crossing probability of an interval with fixed initial and ending values, the estimates of our proposed method are good when correlation is negative or close to 0. Hence,

we can determine the number of subintervals depending on correlation and the levels of α_1 and α_2. Also, when we determine the appropriate values of α_1 and α_2, we consider the distance to the barrier. The choices of α_1 and α_2 are less significant, because the sufficiently large value of M will ensure accuracy of the estimate, even with high values of α_1 and α_2.

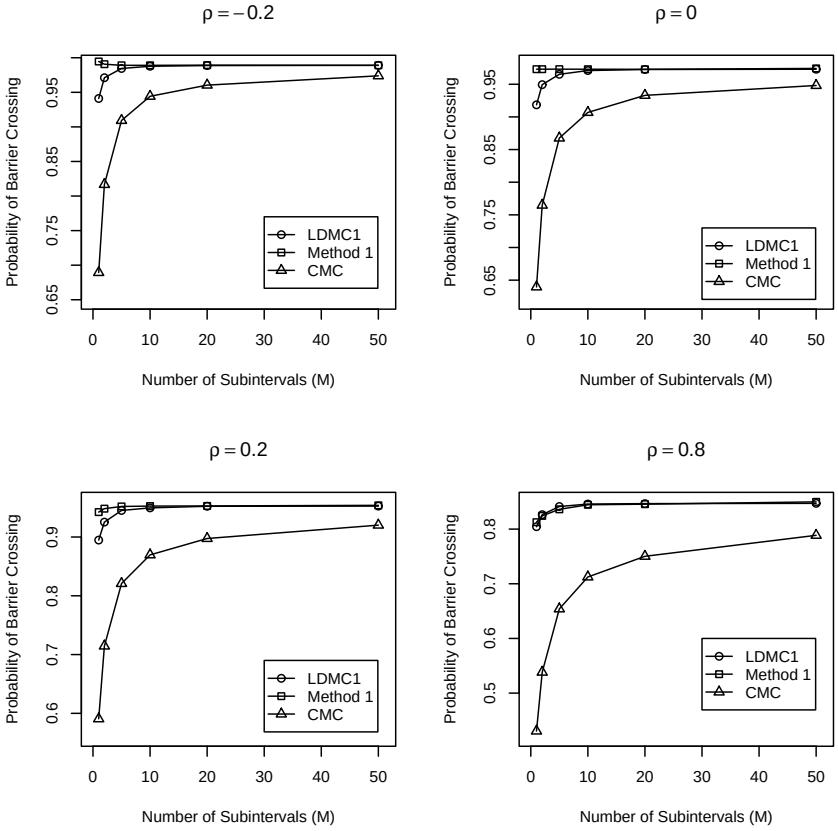

Figure 3.6: Comparison of Estimates of *LDMC1*, Method 1, and *CMC* : Trial 4

Figure 3.6 compares convergence of estimates under three different simulation approaches outlined in Section 3.1.2. As expected, our proposed approach, namely M1 (Case 1), exhibits the fastest convergence as a function of the number of subin-

tervals. This graph shows the results obtained under Trial 4. Similar results are obtained under different locations of barriers. Also, under more general correlation structure than the one where we assume the same pair-wise correlation values, we draw similar conclusions as well.

Table 3.3: Number of Subintervals Needed to Obtain Accurate Results (Trial 4)

	$\rho = -0.2$		$\rho = 0$		$\rho = 0.2$		$\rho = 0.8$	
Simulation Type	M	Time (sec)	M	Time (sec)	M	Time (sec)	M	Time (sec)
M1: Case 1	1	193.3	1	220.9	2	216.5	10	517.0
M1: Case 2	2	59.9	5	98.6	5	149.2	10	507.2
M1: Case 3	2	61.1	5	98.5	5	149.2	10	507.9
CMC	10,000	1375.4	10,000	1347	10,000	1383.3	10,000	1379.7
LDMC1	5	4.6	20	11.7	5	7.4	10	19.9

In Table 3.3, the column M shows the number of subintervals needed to achieve accurate estimates under different settings. Also, the column $Time$ is the time needed to obtain the estimate with the given number of M, and is measured in seconds. For the Crude Monte Carlo, we need a large number of subintervals to eliminate the bias. When we look at other trials with different distances to barriers, we also obtain similar results. Since the distance to barriers is confounded with all other variables of interests, such as T and σ, we can conclude that our findings in Table 3.3 generally hold true in most of the circumstances. Also, in terms of computational time, M1 (Case 1) performs at the faster speed compared to the Crude Monte Carlo method which achieves the same level of accuracy. M1 (Case 1) requires much fewer number of subintervals, and we can potentially increase

its speed by making the optimization more efficient. We can also utilize the low discrepancy sequences such as a Halton sequence in conjunction with M1, because M1 involves fewer number of dimensions.

When we compare the results of M1 (Case 1) to Baldi's method (*LDMC1*), M1 (Case 1) still converges at a smaller number of subintervals. However, the computational time is much smaller with *LDMC1*. Also, we note that *LDMC1* works very well at the presence of high correlation (i.e. $\rho = 0.8$). Hence, we need to devise an algorithm so that we can make M1 (Case 1) computationally more efficient. This issue is addressed in Section 3.2.

3.1.5 Credit Risk Example

Here we illustrate our proposed method using a practical example. Suppose that our portfolio consists of bonds issued by 3 different firms. We would like to determine the probability that at least one counterparty defaults within a horizon of 1 year. We adopt the structural approach as discussed in Section 1.3.4, and we use the stock prices as proxies for the values of the firms. We assume that these stock prices follow a 3-dimensional Geometric Brownian motions as follows:

$$d\mathbf{S}(t) = V\mathbf{S}(t)dt + diag[\mathbf{S}(t)]\Sigma dW(t), \tag{3.5}$$

with a default threshold level $C = [c_1, c_2, c_3]^T$. Here V is a 3×3 diagonal matrix, Σ is a 3×3 matrix, and $diag[\mathbf{S}(t)]$ is a 3×3 diagonal matrix with $\mathbf{S}(t)$ being the diagonal elements. Table 3.4 shows parameterizations of the Geometric Brownian Motion.

Table 3.4: Parameters of Geometric Brownian Motions for Stock Price Processes

Firm	Initial Price	Growth Rate	σ^2	Default threshold
1	100	0.08	0.02	90.9218
2	100	0.05	0.035	88.2347
3	100	0.03	0.03	87.3567

We apply a log-transformation to (3.5), and, by Ito's Lemma, we obtain the following stochastic differential equation:

$$d \ln \mathbf{S}(t) = U dt + \Sigma dW(t), \tag{3.6}$$

where $U = [\mu_1, \mu_2, \mu_3]^T$, $\mu_i = v_i - \frac{\sigma_i^2}{2}$, σ_i^2 is the i^{th} diagonal element of $\Sigma^T\Sigma$, and v_i is the i^{th} diagonal element of V. Hence, by setting $\mathbf{X} = \ln \mathbf{S}$ and $B = [b_1, b_2, b_3]^T = [\ln c_1 \ln c_2 \ln c_3]^T$, we have a stochastic process $\mathbf{X}(t)$ that follows a multivariate Brownian Motion of the following form,

$$d\mathbf{X}(t) = U dt + \Sigma dW(t), \tag{3.7}$$

with a new default threshold level $B = [b_1, b_2, b_3]^T$. In this example, the corresponding equivalent Brownian Motion process has parameters specified in Table 3.5. In this table, we also show the marginal default probability of each firm under the column "Default Probability".

From the default probabilities of individual firms, we see that these firms would have quite bad credit ratings. For the illustration purpose, we have set up the artificial portfolio with high probabilities of default, so that the joint probability is also not too small. The bonds issued by these counterparties would be classified

Table 3.5: Parameters of Brownian Motions for Underlying Stock Processes

Firm	Initial Value	μ	σ^2	Default threshold	Default Probability
1	4.60517	0.07	0.02	4.51	0.341969
2	4.60517	0.0325	0.035	4.48	0.445518
3	4.60517	0.015	0.03	4.47	0.406035

as junk bonds. We assume that the instantaneous correlation between any pair of these three processes is given to be 0.2. We apply the simulation method M1 described in Section 3.1.4 to compute the probability that at least one firm defaults within 1 year.

Table 3.6: Monte Carlo Simulation Result

No. of Time Steps	α_1	α_2	*CMC* Estimate	*LDMC2* Estimate
1	0.1	0.03	0.400463	0.721135
5	0.08	0.025	0.566688	0.735321
10	0.01	0.005	0.614625	0.73664
20	0.002	0.001	0.6492	0.7365
200	0.0002	0.0001	0.71056 (0.0005)	0.73843 (0.0003)

Table 3.6 summarizes our results of Monte Carlo simulation with $N = 80,000$. The values in parentheses are standard errors. In this table, "No. of Time Steps" is the number of subintervals, α_1 and α_2 are as defined in Section 3.1.3, *CMC* is the estimate based on M4, the Crude Monte Carlo method, and *LDMC2* is the estimate based on M1 as described in the previous section.

The estimates based on *LDMC2* give us consistent values regardless of the number of subintervals. On the other hand, we observe that the *CMC* estimates converge slowly to the consistent estimate as we increase the number of subintervals.

Table 3.7: Quasi-Monte Carlo Simulation Result

No. of Time Steps	α_1	α_2	*CQMC* Estimate	*LDMC2* Estimate
1	0.05	0.03	0.4003	0.723
2	0.04	0.02	0.4865	0.7326
5	0.015	0.01	0.5707	0.738
10	0.008	0.005	0.6222	0.7385
20	0.002	0.001	0.6627	0.7505

In this problem, in order to obtain faster convergence, we also generate random numbers using a low-discrepancy sequence. In particular, we used Halton's sequence to generate 10,000 runs. The estimates using the Quasi-Monte Carlo are summarized in Table 3.7. Crude Quasi-Monte Carlo (*CQMC*) estimates behaves similarly as in the Crude Monte Carlo case. *LDMC2* estimates are obtained using M1 in conjunction with the low discrepancy sequence. These estimates give us consistent values except for the case where the number of subintervals is 20. In this case, since we have 20 subintervals and 3 assets, the dimensionality of this simulation is $20 \times 3 = 60$. We know that the Quasi Monte Carlo method is not very good in high dimensions. Hence, the *LDMC2* estimate for the case with 20 subintervals is not very reliable, due to the high dimensionality.

3.2 An Improved Algorithm for Computing Barrier Crossing Probability

In the previous section, we have proposed an algorithm based on the Large Deviations Theory to compute the barrier crossing probability of a correlated multivariate Brownian Motion process. As we have seen in the numerical example, our proposed method, *LDMC2*, exhibits the fastest convergence rate as a function of the number of subintervals. With this simulation method, we need to take only 1 or 2 subintervals to obtain accurate approximations, whereas the other methods require a larger number of subintervals in order to reach convergence. However, it takes a lot of time to perform *LDMC2*, because this method involves solving a high dimensional optimization problem specified in Section 2.2.1. Hence, this method may be impractical. To overcome this inefficiency, in this section we suggest an algorithm which approximates *LDMC2*. In the first section, we describe the algorithm and the idea behind it, and then illustrate by numerical examples that this algorithm is much faster, and also as accurate as *LDMC2*. We refer to this algorithm as a Fast Large Deviations Monte Carlo (*FLDMC*) method, because it is a faster version of the simulation method based on the Large Deviations Theory.

3.2.1 Description of Algorithm

This method exploits the fact that we have an analytical representation of the probability that at least one barrier is breached during the given time horizon when the components of the process are uncorrelated. The algorithm is a two-stage

procedure. In the first stage, we run a small number of simulations to determine the ratio between the probability of barrier crossing under the given correlation structure and that under zero correlation. In the second stage, where we run the full set of simulations, we compute the barrier crossing probability under zero correlation and then use the estimated ratio in order to adjust for the correlation effects.

Step 1: Preliminary Runs

We perform the following procedures:

1. We generate a small number, for example $N = 200$, of values of the correlated Brownian Motion at the end of the first time interval.

2. For the i^{th} simulation run, we know the initial and the terminal values, $X^i(0) = \mathbf{x}$ and $X^i(\epsilon) = \mathbf{y}^i$, of the process. If $\mathbf{y}^i$ does not breach the barrier, we compute the probability CP^ρ that at least one component breaches its respective barrier. For this we use the Large Deviations method from Section 2.1.3. In addition, we can analytically obtain CP^0, which is the exit probability under zero correlation. Then, we find $Ratio^i = \frac{CP^\rho}{CP^0}$.

3. After generating N paths, let N' be the number of simulations where the end values did not breach the barrier. In this stage, we need to obtain the average ratio of the exit probability under the correlation structure ρ and under zero correlation. We set $RatioSum$ to be the sum of $Ratio^i$'s over the paths for which $\mathbf{y}^i$ did not breach the barrier. We can then obtain the desired average ratio by $Ratio = \frac{RatioSum}{N'}$. This ratio is used in the second stage.

Step 2 : Full Simulation

Now we perform a full set of simulation with a large number of runs, i.e. $N = 80,000$. The general simulation framework still remains the same as described in Section 3.1.1, but now we modify the way we calculate CP and CP_i's. We obtain $P(E_1 \cup E_2 \cup E_3)$ in the following way.

For a given subinterval we have an initial value and a terminal value for each simulated path. When the instantaneous correlation is 0, the probability that at least one component breaches its respective barrier can be calculated explicitly. For the 3-dimensional process, we denote this probability as $P^0(E_1 \cup E_2 \cup E_3)$. It can be expressed as

$$P^0(E_1 \cup E_2 \cup E_3) = \sum_{i=1}^{3} P(E_i) - \sum_{i \neq j} P(E_i)P(E_j) + P(E_1)P(E_2)P(E_3). \quad (3.8)$$

Since the marginal barrier crossing probability is given by formula (2.2), the computation of (3.8) is quite fast.

The quantity that we ultimately need to compute is $P^\rho(E_1 \cup E_2 \cup E_3)$, which is the exit probability under the specified correlation structure ρ. This can be approximated by adjusting $P^0(E_1 \cup E_2 \cup E_3)$ by the factor *Ratio* from Step 1 as follows,

$$P^\rho(E_1 \cup E_2 \cup E_3) \approx P^0(E_1 \cup E_2 \cup E_3) \times Ratio.$$

Once we obtain $P^\rho(E_1 \cup E_2 \cup E_3)$, the remaining parts follow in the same way as in *LDMC2*. When $M > 1$, the factor *Ratio* is calculated using the first subinterval as described in Stage 1. Then the same value of *Ratio* is applied to approximate values of the barrier crossing probabilities of other subintervals, namely $CP_i, i = 1, \ldots, M$.

This algorithm works well if the the ratio between the barrier crossing probability under the given correlation and that under zero correlation is more or less constant with respect to different time steps and different locations of initial and terminal values relative to the barrier levels. The numerical experiments that we have conducted affirm that this method greatly improves time efficiency while retaining accuracy of the estimates.

The method proposed in this section shares a similar idea with the control variate method in the sense that we make use of known results in order to improve computational efficiency. We present the method because it readily allows to compute the barrier crossing probability using a small number of subintervals. However, incorporating the control variate method in this framework is a good extension for future research.

3.2.2 Numerical Examples

We continue with the same example from Section 3.1.4 using *FLDMC*. We use Trial 4 with $N = 80,000$ for the illustration. We have seen that *LDMC2* is the best in terms of the convergence rate as a function of M, and that *LDMC1* is the best in terms of computational efficiency for the given M. By performing further numerical exercises, we claim that *FLDMC*, described in this section, is as good as *LDMC2* in convergence as a function of M, and as good as *LDMC1* in time efficiency for given M. Hence, we can arguably conclude that *FLDMC* is the best method to apply in this situation.

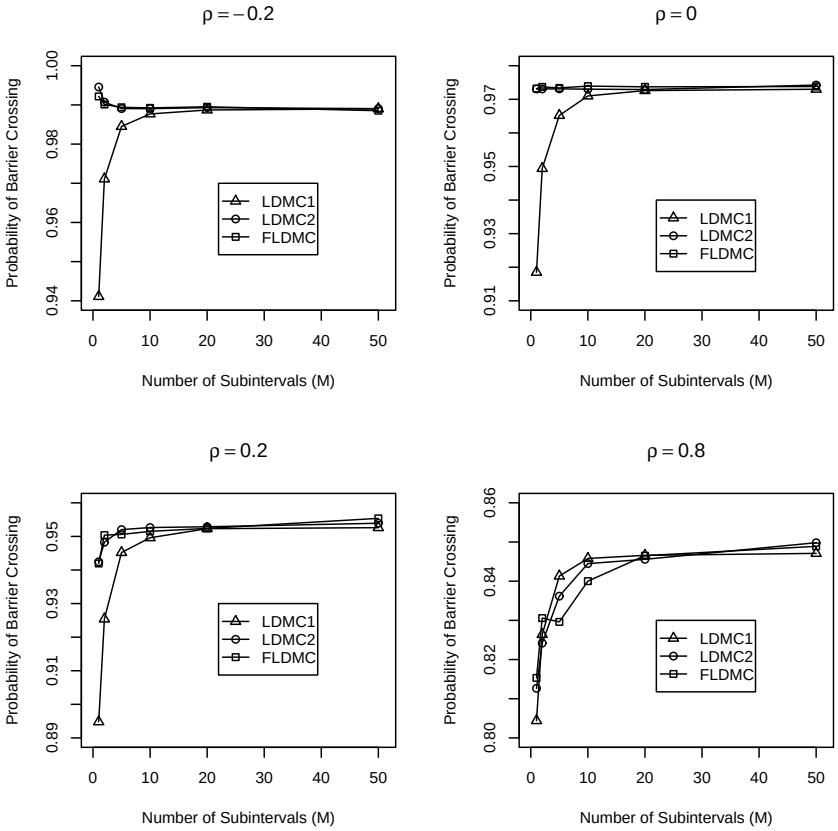

Figure 3.7: Comparison of Estimtes from Convergence rates of *LDMC1*, *LDMC2*, and *FLDMC*

Figure 3.7 shows the estimates of *LDMC1*, *LDMC2*, and *FLDMC* under different correlation assumptions as we vary the number of subintervals. Hence, we clearly see that the estimates of *FLDMC* are almost the same as those of *LDMC2* as desired. In terms of convergence rate as a function of the number of subintervals, *FLDMC* outperforms *LDMC1*, except in the case of high correlation, i.e. $\rho = 0.8$.

Now we compare the time efficiency of *FLDMC* and *LDMC1*. Figure 3.8 shows that *FLDMC* takes a similar amount of time as *LDMC1* for a given number of

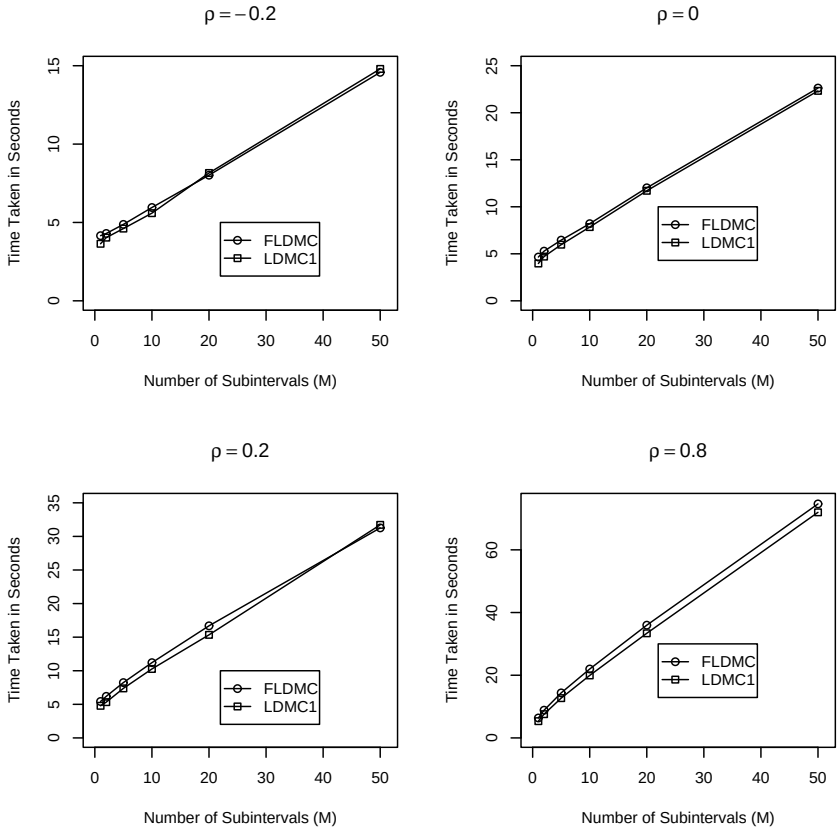

Figure 3.8: Comparison of Time Efficiency for *FLDMC* and *LDMC1*

subintervals.

From these observations, we conclude that *FLDMC* is the method of choice, because it is time efficient and exhibits the fastest convergence rate as a function of M. Even at high correlation $\rho = 0.8$, this method does not perform much worse than *LDMC1*. Consequently, we have confidence that this method works effectively and efficiently.

3.3 Existing Works on Multivariate Barrier Crossing Probability

In this section, we discuss the work of Shevchenko (2003), which also deals with a method of computing a multivariate barrier crossing probability. We briefly describe his methodology and explain why our proposed method can be considered to be more advantageous than Shevchenko's.

Shevchenko (2003) simulates the trajectories of the underlying process at discrete time intervals, and then computes the barrier crossing probability of Brownian Bridge for a given interval. In the earlier discussion, we have described a way of approximating barrier crossing probability based on the Large Deviations Theory. Shevchenko proposes to use upper and lower bounds based on Frechet Bounds. This result is stated in the following lemma.

Lemma 3.3.1 *(Frechet Bounds) Let $A_1, \ldots, A_k$ be the events such that $P(A_i) = a_i$, $i = 1, \ldots, k$. Then*

$$\max(0, \sum_{i=1}^{k} a_i - (k-1)) \leq P(A_1 \cap \ldots \cap A_k) \leq \min_{i=1,\ldots k} a_i. \tag{3.9}$$

Shevchenko proposes three estimators for joint barrier crossing probability of Brownian Bridge, denoted by P_U, P_L, and P_I. P_U and P_L correspond to the upper and the lower Frechet bounds given in Lemma 3.3.1. P_I is the joint barrier crossing probability assuming that underlying components are independent. Shevchenko argues that by appropriately computing the probability of barrier crossing of Brownian

Bridge for each time step of Monte Carlo simulation, we need to generate only a small number of discrete points in order to obtain the barrier crossing probability of a continuous process within reasonable accuracy.

We discuss how Shevchenko's methods are related to the methods discussed in the earlier sections of this chapter. We also demonstrate that his methods are no better than *FLDMC* discussed in Section 3.2. In addition, we discuss some shortcomings of Shevchenko's approach, which can be addressed using the method discussed in this thesis.

3.3.1 Relationship between Shevchenko's Method and Large Deviations Based Methods

We consider computing the probability that at least one of the components in the 3-dimensional continuous process breaches its respective barrier. The standard approaches in both Shevchenko and the Large Deviations based methods are that we generate paths of 3-dimensional underlying process in discrete time intervals and then use some method to approximate the probability of barrier crossing between the discrete time intervals.

Now we focus on the barrier crossing probability of a multivariate Brownian Bridge process. Let E_i be the event where the i^{th} component of the Brownian Bridge crosses its corresponding barrier. Since we are interested in the event that at least one component breaches its corresponding barrier, we are interested in the

probability

$$P(E_1 \cup E_2 \cup E_3) = \sum_i P(E_i) - \sum_{i<j} P(E_i \cap E_j) + P(E_1 \cap E_2 \cap E_3). \qquad (3.10)$$

As discussed in Section 2.1, the left hand side of (3.10) can be computed directly using the method as in *LDMC1*, or the expressions on the right hand side can be evaluated as in *LDMC2* or *FLDMC*.

In Shevchenko's method, the Frechet bounds are given for intersections of sets. Hence, the right hand side of (3.10) should be calculated. The marginal probabilities $P(E_i)$'s are computed easily, and the two-way probabilities $P(E_i \cap E_j)$'s are approximated by the semi-analytic result. Now the remaining term $P(E_1 \cap E_2 \cap E_3)$ is obtained by P_U, P_L, or P_I which are defined previously. These approximations reflect the possibility of barrier crossing during the discrete time interval.

Since in Shevchenko's method the marginal and the two-way probabilities need to be evaluated, this approach takes some more time compared to *LDMC1*. In the next section, we will show numerical examples to illustrate that the convergence to the true value as a function of M is fairly good, but not as good as *LDMC2* or *FLDMC*.

To obtain a better insight into the method by Shevchenko, suppose that we approximate the value of the two-way probability $P(E_i \cap E_j)$ by using the upper bound of Frechet bounds, that is $\min(P(E_i), P(E_j))$. Assume, without loss of generality,

$P(E_1) < P(E_2) < P(E_3)$. Then we have

$$\begin{aligned}
& P(E_1 \cup E_2 \cup E_3) \\
= & \sum_i P(E_i) - \sum_{i,j} P(E_i \cap E_j) + P(E_1 \cap E_2 \cap E_3) \\
\approx & P(E_1) + P(E_2) + P(E_3) - \min(P(E_1), P(E_2)) - \min(P(E_1), P(E_3)) \\
- & \min(P(E_2), P(E_3)) + \min(P(E_1), P(E_2), P(E_3)) \\
= & P(E_1) + P(E_2) + P(E_3) - P(E_1) - P(E_1) - P(E_2) + P(E_1) \\
= & P(E_3) \\
= & \max(P(E_1), P(E_2), P(E_3)).
\end{aligned}$$

Hence, if Frechet's upper bound is applied to compute two-way as well as three-way probabilities, this estimator reduces to be the same as *LDMC1*.

The estimator used in *LDMC1* can also be regarded as the Frechet lower bound for the union of several events, since the Frechet bounds are given as

$$\max(P(E_1), P(E_2), \ldots, P(E_n)) \leq P(E_1 \cup \ldots \cup E_n) \leq \min(1, \sum_{i=1}^{n} P(E_i)). \quad (3.11)$$

Future research can be addressed to finding tighter bounds for the probability of union of several sets.

3.3.2 Comparison of Computational Efficiency

We compute the probability that at least one component crosses its corresponding barrier with the same set-up as specified in Section 3.2.2. Figure 3.9 and 3.10 display the estimates of the barrier crossing probability and the time taken as a function

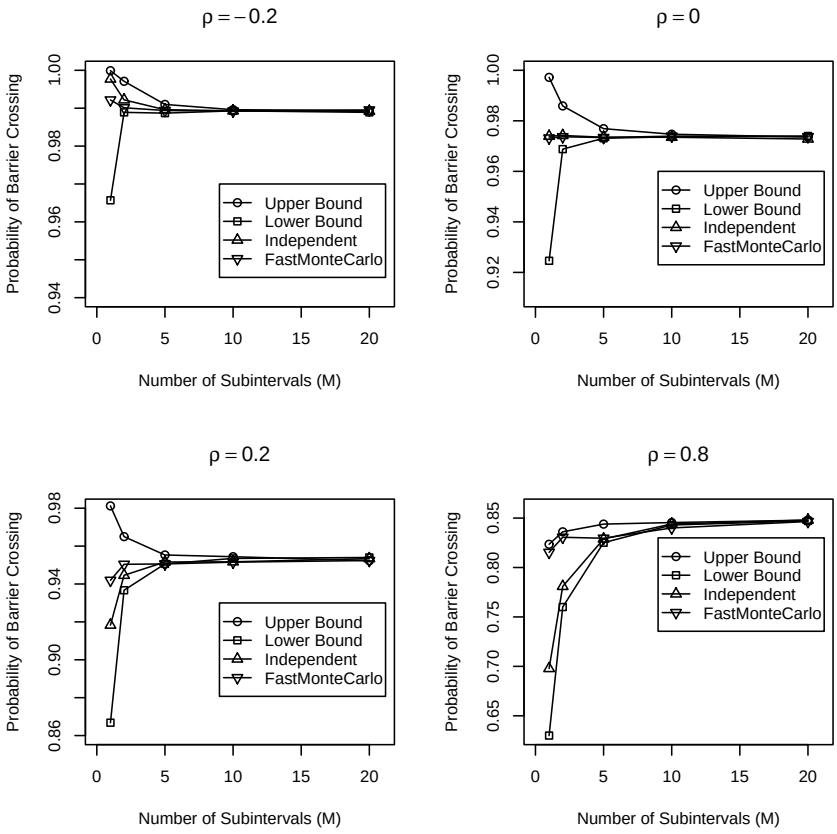

Figure 3.9: Comparison of Convergence Rates of P_U, P_L, P_I, and $FLDMC$

of the number of subintervals, M, respectively. The probability of barrier crossing during the discrete interval is computed by four different methods: P_U(Frechet upper bound from Lemma 3.3.1), P_L(Frechet lower bound), P_I(independence assumption), and $FLDMC$. Figure 3.9 shows that all the estimates are converging to the true value at a relatively small number of M. In particular, when we assume zero correlation ($\rho = 0$), $FLDMC$ performs as well as P_I. In all other situations, $FLDMC$ seems to converge to the true value faster than P_I. Moreover, $FLDMC$ outperforms P_U and P_L except for the highly positive correlation case ($\rho = 0.8$).

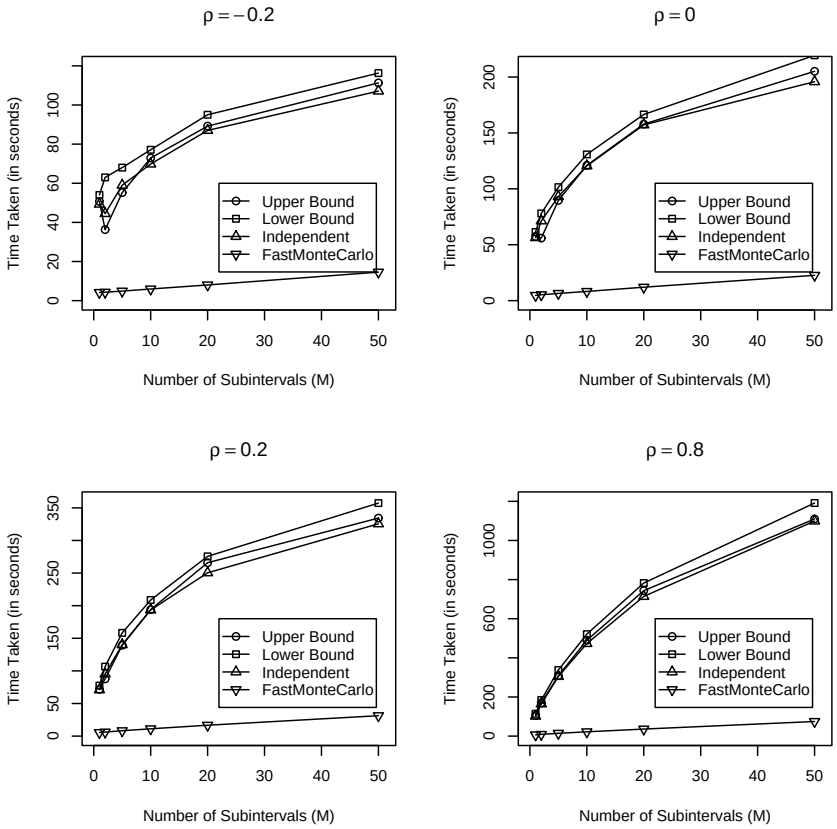

Figure 3.10: Time Taken to Obtain Estimates Using P_U, P_L, P_I, and *FLDMC*

Also, from Figure 3.10, we see that the estimates from *FLDMC* is the most time efficient because in Shevchenko's method we evaluate two-way probabilities using the results of He et al. (1998). Hence, we can conclude that the Monte Carlo simulation method combined with *FLDMC* is the most effective method unless the underlying components are uncorrelated or highly positively correlated.

3.3.3 Other Shortcomings of Shevchenko's Method

All the numerical examples we have studied so far deal with computing the probability that at least one of many components breaches its corresponding barrier. This problem can be solved by either Shevchenko's method or the Large Deviations based approach. Suppose that we consider related problems such as obtaining an accurate estimate of the distribution of the number of components breaching barriers or computing barrier crossing probabilities of a basket of Geometric Brownian Motions. Shevchenko's method can not give a straightforward extension to address these problems. On the other hand, the Large Deviations based method, *FLDMC* in particular, can be extended to address these issues, as will be shown in the following sections.

3.4 Distribution of the Number of Barrier Crossings

In the applications of multivariate barrier crossing probabilities in the context of finance and actuarial science, it is often not sufficient to know whether any of the components have breached a barrier. We often need to characterize the distribution of the number of components breaching barriers. For example, in credit risk, one would like to know the distribution of the number of companies defaulting in a given time horizon. In this section, we build upon our method based on the Large Deviations Theory, and we provide an algorithm for efficiently obtaining the distribution of the number of components breached. We primarily focus on the

situation where the underlying process is 3-dimensional. For higher dimensional processes, this approach can be extended, but some modifications of the algorithm are needed. We first present the algorithm, and then show some numerical examples to demonstrate efficiency of this method.

3.4.1 Description of Algorithm

In this section, we suppose that we have three components following a multivariate correlated Brownian Motion process. The objective is to obtain the distribution of the number of components breaching barriers in a given time horizon. The algorithm extends the general simulation framework presented in Section 3.1.1. The Large Deviations approach enables us to obtain not only the barrier crossing probability of one component but also the joint barrier crossing probabilities of two or more components for a given time interval. From these, for each time step of a given simulation path, we can characterize the probability of which components breach their respective barriers. Then, by performing a random draw, we can determine which event actually occurs for the given time interval of the given simulation path. Then, by going through each time step, we can find out how many components breach their respective barriers during the given time horizon. By generating simulation paths many times, we can approximate the proportion of the events that i components cross barriers, where $i = 0, 1, 2, 3$. Let N be the number of simulations, and M be the number of discrete time intervals. The algorithm consists of the following procedures.

Step 1:

- Simulate the underlying trajectory according to the specified multivariate Brownian Motion process

- For each trajectory, we have a vector of indicators, $W = [w_1, w_2, w_3]$, indicating whether each component breached its corresponding barrier or not. This vector is initialized to $W = [0, 0, 0]$.

- For each trajectory, we check the values of components at all M discrete points. If the i^{th} component value at any discrete time period has breached the barrier, then w_i is assigned to 1.

Step 2:

- We go through each time step from 1 to M. For each time step, we only look at components whose value of w_i is 0, and whose marginal probability of barrier crossing is greater than a pre-specified value, which we refer to as a $Cutoff$ value. The latter ensures that the components whose values are quite far from the barrier are excluded from the computation of barrier crossing probability for the sake of time efficiency. We denote the number of these components by k.

- From the previous calculation we obtain the value k, which can be 0, 1, 2, or 3. We denote the event where the i^{th} component breaches its barrier by E_i. We consider the following four cases.

  - **Case 1:** $k = 3$

    By using the Large Deviations based approach as discussed in Section

2.1.3, we can compute $P(E_1 \cap E_2 \cap E_3)$ and $P(E_i \cap E_j)$ for $i = 1, 2, 3,\ j = 1, 2, 3,\ i \neq j$. The marginal barrier crossing probabilities $P(E_i), i = 1, 2, 3$ can be easily obtained from the analytic formula. Now, using the elementary set theory, we obtain the estimates of the probabilities of all possible outcomes $P(E_1 \cap E_2 \cap E_3)$, $P(\bar{E}_1 \cap E_2 \cap E_3)$, $P(E_1 \cap \bar{E}_2 \cap E_3)$, $P(E_1 \cap E_2 \cap \bar{E}_3)$, $P(\bar{E}_1 \cap \bar{E}_2 \cap E_3)$, $P(E_1 \cap \bar{E}_2 \cap \bar{E}_3)$, $P(\bar{E}_1 \cap E_2 \cap \bar{E}_3)$, and $P(\bar{E}_1 \cap \bar{E}_2 \cap \bar{E}_3)$. Then using a random draw from a standard uniform distribution, we determine which of these 8 events occurred. From this, we determine which components have crossed the barriers, and we update the vector W, by switching the corresponding components of W to 1.

- **Case 2:** $k = 2$

  In this case, we compute $P(E_1 \cap E_2)$ using the semi-analytic solution based on the Large Deviations Theory, or the analytic solution by He et al. (1998). Then we obtain the estimates of $P(E_1 \cap E_2)$, $P(\bar{E}_1 \cap E_2)$, $P(E_1 \cap \bar{E}_2)$, and $P(\bar{E}_1 \cap \bar{E}_2)$. Using a random draw, we determine which of these events occurred. Then we update the vector W accordingly.

- **Case 3:** $k = 1$

  Since $P(E_1)$ can be easily computed by the closed-form formula, we generate a uniform random number to determine whether the component breached the barrier. Then we update W accordingly.

- **Case 4:** $k = 0$

  The vector W remains unchanged.

Step 3:

Once we go through all the discrete time steps for the given trajectory, we determine the number of components that breached the barriers by looking at the number of 1's in the vector W.

Step 4:

We repeat Steps 1 to Step 3 N times, and we obtain the proportion of frequency of 0, 1, 2, and 3 components crossing the barriers. This proportion is our estimate of the distribution of the number of components that crossed their corresponding barriers.

In this algorithm, we simulate paths according to the underlying process, and we also simulate which components breach their respective barriers for each time period according to the probabilities we estimate using the Large Deviation Theory. Since the Large Deviations Theory provides us with a reasonable tool to understand barrier crossing events during a time interval, the result of this algorithm should converge to the true value at a relatively small value of M.

3.4.2 Numerical Examples

In this section, we provide numerical examples to illustrate that our algorithm in Section 3.4.1 provides estimates of the distribution of the number of barrier crossing accurately and efficiently. We take the same example from Section 3.1.4. The location of the barrier is set according to Trial 4 in Section 3.1.4, and the number of simulation N is equal to 80,000.

Table 3.8: Estimates of Distribution of the Number of Defaults : Part I

Our Method	$\rho = -0.2$					$\rho = 0$				
	Number of Barrier Crossings					Number of Barrier Crossings				
M	0	1	2	3	Time	0	1	2	3	Time
1	0.0059	0.1727	0.539	0.2824	354.625	0.0266	0.1868	0.4425	0.3442	261.344
2	0.0095	0.1749	0.5227	0.2929	191.891	0.0266	0.1866	0.443	0.3438	176.031
5	0.0113	0.1756	0.5152	0.298	94.687	0.0282	0.1893	0.4446	0.3379	99.266
10	0.0113	0.1798	0.5121	0.2968	95.422	0.0257	0.1894	0.4461	0.3389	94.921
20	0.0114	0.1792	0.5127	0.2967	141.765	0.027	0.1899	0.4446	0.3385	138.797
	(0.0001)	(0.0002)	(0.0003)	(0.0002)		(0.0002)	(0.0002)	(0.0003)	(0.0002)	
Crude Monte Carlo	$\rho = -0.2$					$\rho = 0$				
	Number of Barrier Crossings					Number of Barrier Crossings				
M	0	1	2	3	Time	0	1	2	3	Time
1,000	0.0134	0.1944	0.5177	0.2745	151.8	0.031	0.2058	0.4424	0.3208	151.8
3,000	0.012	0.1899	0.5135	0.2846	475.7	0.0296	0.1995	0.4426	0.3283	475.9
5,000	0.0119	0.1845	0.5174	0.2862	793.2	0.0283	0.1976	0.442	0.3322	792.2
7,000	0.0119	0.1834	0.5145	0.2901	1109.6	0.028	0.1944	0.4419	0.3357	1109.3
10,000	0.0119	0.1834	0.5145	0.2901	1109.6	0.028	0.1944	0.4419	0.3357	1109.3
20,000	0.0111	0.18	0.5152	0.2937	3153.7	0.027	0.191	0.4452	0.3369	3156.5
	(0.0001)	(0.0002)	(0.0002)	(0.0002)		(0.0002)	(0.0002)	(0.0003)	(0.0002)	

Table 3.9: Estimates of Distribution of the Number of Defaults : Part II

Our Method	$\rho = 0.2$					$\rho = 0.8$				
	Number of Barrier Crossings					Number of Barrier Crossings				
M	0	1	2	3	Time	0	1	2	3	Time
1	0.0575	0.1897	0.3463	0.4065	354.625	0.1862	0.1013	0.1337	0.5787	261.344
2	0.0513	0.1871	0.369	0.3926	191.891	0.1634	0.115	0.1703	0.5513	176.031
5	0.0495	0.1888	0.3784	0.3833	94.687	0.1541	0.1186	0.185	0.5422	99.266
10	0.0467	0.192	0.3797	0.3816	95.422	0.1547	0.1295	0.179	0.5369	94.921
20	0.0475	0.191	0.3773	0.3842	141.765	0.1537	0.1356	0.1757	0.535	138.797
	(0.0002)	(0.0002)	(0.0003)	(0.0002)		(0.0002)	(0.0002)	(0.0003)	(0.0002)	
Crude Monte Carlo	$\rho = 0.2$					$\rho = 0.8$				
	Number of Barrier Crossings					Number of Barrier Crossings				
M	0	1	2	3	Time	0	1	2	3	Time
1,000	0.0542	0.203	0.381	0.3618	151.8	0.1637	0.1418	0.1771	0.5174	151.8
3,000	0.0509	0.1988	0.3796	0.3707	475.7	0.1577	0.1381	0.1745	0.5298	475.9
5,000	0.0502	0.1963	0.3785	0.375	793.2	0.1561	0.1383	0.1757	0.5299	792.2
7,000	0.0494	0.1969	0.3744	0.3793	1109.6	0.1553	0.1369	0.1752	0.5326	1109.3
10,000	0.0477	0.1939	0.3792	0.3792	1580.1	0.1564	0.1364	0.1756	0.5316	1579.6
20,000	0.0489	0.1923	0.3781	0.3807	3153.7	0.1569	0.1369	0.1742	0.532	3156.5
	(0.0001)	(0.0002)	(0.0002)	(0.0002)		(0.0002)	(0.0002)	(0.0003)	(0.0003)	

Table 3.10: True Values of the Distribution with $\rho = 0$

Number of Barrier Crossings	Probability
0	0.02636
1	0.18797
2	0.44234
3	0.34334

Tables 3.8 and 3.9 show the results of the simulations to approximate the number of components breaching the barriers. The values in parentheses are standard errors. We use the algorithm formulated in Section 3.4.1, and we refer to this algorithm as "Our Method". As before, we compare efficiency of "Our Method" to that of Crude Monte Carlo method. M denotes the number of subintervals used. The values, 0, 1, 2, and 3, in the column heading correspond to the number of components crossing barrier. We vary correlation ρ among the components to take values of -0.2, 0, 0.2, and 0.8. In addition, the column "Time" shows the time taken in seconds to perform this computation. For "Our Method", we use the $CutOff$ value of 0.02.

When the correlation of the underlying components is 0, we can obtain the true values of this distribution and they are given in Table 3.10. Since the true values of this distribution are unknown in non-zero correlation cases, we assume that the values of the estimates that stabilize at the sufficiently high number of subintervals, M, can be taken as true values. By examining the convergence of the estimates as a function of M, "Our Method" gives sufficiently accurate results when $M = 5$, and "Crude Monte Carlo" performs well with $M = 7000$. We show the estimates of "Our Method" under different values of M in order to demonstrate that the

convergence occurs at a small value of M. Hence, "Our Method" allows us to obtain the estimates of the distribution with much fewer number of subintervals compared to the Crude Monte Carlo method. Also, we note that the time required to perform "Our Method" with $M = 5$ is much less compared to that for "Crude Monte Carlo" with $M = 7000$, as observed from these tables.

We notice that the computational time for "Our Method" does not monotonically increase with the number of subintervals M. As we increase M, a lot of defaults are captured by the simulated values at discrete time points. Hence, we do not need perform as much for the computation of barrier crossing probability between the discrete times, which are computationally intensive.

"Our Method" performs well when we have negative or small positive correlation among the components, and gets slightly worse at a high correlation. On the other hand, Crude Monte Carlo converges at a faster rate when there is a high positive correlation. In addition, we have repeated this exercise with different location of barriers. The closer the barriers are located to the initial values of the underlying process, the more advantageous "Our Method" is over "Crude Monte Carlo".

"Our Method" effectively reduces dimensionality of this simulation because it allows us to use fewer number of subintervals. With this reduction, one can also consider to employ a more efficient simulation method such as a quasi-Monte Carlo method. We believe also that the computational procedure for determining which components may default between discrete times can be improved significantly. Hence, there is a lot of opportunity that this method can be implemented in a computationally

more efficient way.

3.5 Application: Pricing a Credit Basket Derivative

In this section, we apply the method developed in this thesis to pricing a credit derivative. In particular, we examine a credit default swap (CDS) with the reference entity consisting of three risky bonds and the assumption of no default by the CDS issuer. In this example, we consider the first-to-default swap, where the payment is triggered by the first default during a specified time horizon. The protection buyer pays a certain amount of fixed premium, s, periodically to a protection seller. In the credit event of the first default among the reference entities, the protection buyer receives a fixed amount of money R from the protection seller. Below we provide the description of the product in detail:

- The financial contract matures in a fixed time, T years.
- Premiums s are paid on a quarterly basis. The payments are made at the end of each quarterly period.
- In the case of a credit event (first-to-default), all the payments of the premiums are stopped without paying the accrued interest. The protection seller pays the protection buyer a fixed amount of money, R, at the time of the credit event.
- We assume no default by the protection seller.

3.5.1 Determination of Swap Rate

In Hull and White (2001), a fair premium s is calculated by equating the expected present value of all future cash flows of premium payments to the expected present value of the payout in the case of the credit event. The authors give the following simplified formula for s:

$$s = \frac{\int_0^T R \cdot \theta(t) \cdot \nu(t) dt}{\int_0^T \theta(t) \cdot u(t) dt + \pi u(T)}, \tag{3.12}$$

where $\theta(t) \cdot \Delta t$ is the probability of default by reference entity between times t and $t + \Delta t$ with no earlier default, $u(t)$ is the present value of quarterly payments at the rate of \$1 per year on the CDS payment dates between time zero and time t, and $\nu(t)$ is the present value of \$1 received at time t. Also, π is the probability of no default by any component of the reference basket during the life of the credit default swap.

The determination of s involves evaluating the integrals in the numerator and the denominator of (3.12). We note that both integrands are dependent upon the distribution of default time τ by any component of the reference basket. We extend the simulation methods discussed in the previous sections to determine in which time interval the default occurs for a given simulated trajectory of the underlying process. Then we approximate the exact timing of the default. Below we outline an algorithm that evaluate these integrals efficiently.

Evaluation of Integrals by Simulation

In the case when the components of the portfolio are assumed independent, we can generate the default time of each component by using the distribution of the hitting

time for a Brownian Motion. The minimum of default times of these components will give a simulated value of the exact first-to-default time. Hence, the evaluation of the integrals in (3.12) are straightforward.

Now we consider procedures for evaluating integrals in (3.12) when the underlying components are dependent.

1. We take the endpoints of subintervals corresponding to the quarterly CDS premium payment dates.

2. With the assumption of a correlated Multivariate Brownian Motion, we simulate the trajectories of the underlying process at the specified endpoints of subintervals.

3. For each subinterval, we determine occurrence of a credit event (first-to-default). If the terminal value of any component at the i^{th} subinterval has crossed the barrier, then we know for certain that the credit event occurred between $(i-1)^{th}$ and i^{th} points. If not, then we compute the probability of occurrence of the credit event, that is the probability that any one component of the process may have crossed the barrier during this subinterval given the terminal value. This probability can be estimated using *LDMC1* or *LDMC2* from Section 3.1, or *FLDMC* from Section 3.2. Once we obtain this probability, actual occurrence of the credit event is determined by a Bernoulli trial.

4. If we determine that a credit event has occurred in the i^{th} subinterval, we can estimate the default time τ by using the following procedure.

For dependent components of the portfolio an exact simulation of the default time is more difficult. In this case, we have to resort to Monte Carlo simulation of trajectories of a Brownian Bridge process. The number of steps will depend on the required accuracy of the generated first-to-default time.

Since in Step 3 we obtain Large Deviations estimates of default probabilities, the following approximation of the default time can also be considered. Among the three entities of the reference basket, suppose that the p^{th} entity has the highest marginal probability of default. Let X_0^p and X_1^p are the values of the p^{th} component of the underlying process at time $(i-1)b$ and ib, respectively, and b is the size of the subinterval. According to the Large Deviations Theory, the event of the barrier crossing occurs via the most likely path of the underlying process. Hence, as entity that defaults, we accept the one that has the highest probability. As discussed in Section 2.1.2, we need to consider the length minimizing path that starts from X_0^p to X_1^p that touches the barrier B_p where B_p is the default threshold of the p^{th} component. The corresponding elapsed time τ_p when this minimizing path touches its barrier B_p is given by

$$\tau_p = \frac{|X_0^p - B_p|}{|X_0^p - B_p| + |X_1^p - B_p|}.$$

Then, we estimate the default time τ by

$$\tau = (i-1)b + \tau_p b.$$

This procedure does not simulate default times from the exact distribution but is less computationally demanding than the previous one, and for small time steps it should lead to reasonably accurate approximations of the integrals

in (3.12), because our approximation method is consistent with the Large Deviations Theory.

5. For the given trajectory with the corresponding default time τ, we can evaluate the integrands of the numerator and denominator of (3.12). Then, by repeating Steps 2, 3, and 4, we evaluate these integrals. The probability of no default π is obtained by monitoring the proportion of trajectories which have no occurrences of the credit event during the time horizon T.

3.5.2 How Our Proposed Approach Differs from the Existing Approaches

The existing literature such as Li (1999) also discusses methods of modelling the correlation of default events in pricing credit basket derivatives. In these papers, the marginal distribution of the time of default is modelled and then an arbitrary copula function is imposed to construct dependency among default times of several counterparties. Laurent and Gregory (2005) use factor copulas in order to derive an analytic solution of CDS prices. A caveat of this approach is that the valuation of a credit derivative is dependent upon the choice of copula. Will (2003) provides some numerical examples showing that the prices of the credit basket derivative are impacted by the various copula choices.

In our suggested method of pricing CDS, instead of directly imposing arbitrary dependency assumption on the marginal default times of several counterparties, we establish dependency among the default times through an instantaneous variance-

covariance matrix of the underlying process. Hence, the dependency is specified from first principles and is more intuitive. In practice, these variance-covariance matrices are easier to estimate and test than copulas.

Since we can readily incorporate the simulation framework discussed in this thesis, we accurately simulate the default behavior of reference entities using a few discrete points in a time-efficient way, as shown in the next section.

3.5.3 Numerical Examples

Here we apply the methods *FLDMC*, *LDMC2*, and *CMC* to price a first-to-default credit default swap. In particular, the reference entity consists of 3 credit risky bonds issued by three distinct counterparties. The credit worthiness of these counterparties are modelled by a multivariate correlated Brownian Motion process whose parameterizations of the marginal processes are specified in Table 3.11.

Table 3.11: Parameterizations of the Brownian Motions for the Underlying Process

Firm	Initial Value	μ	σ^2	Default threshold
1	4.54	0.07	0.02	4.30
2	4.54	0.0325	0.035	4.27
3	4.54	0.03	0.015	4.28

We vary the instantaneous correlation ρ between these components, and we calculate the fair premium s of the credit default swap as described in the beginning of Section 3.5.1, with $T = 3$ and $R = 100$. Since the maturity of the CDS is 3

years with quarterly premium payments, we take subinterval points corresponding to premium payment dates, resulting in the number of subintervals to be 12 ($M = 12$) for the simulation methods *LDMC2* and *FLDMC*. We perform 80,000 runs of simulations ($N = 80,000$). The threshold values of α_1 and α_2, which are used in the computation of barrier crossing probability within a subinterval, are set to be 0.1 and 0.03, respectively. In the method *CMC*, we take many subintervals (M being a large number), and assume that the probability of default occurrence between the endpoints of subintervals is 0.

Table 3.12: Simulation Result for the Premium Value s of Credit Default Swap

	$\rho = -0.2$		$\rho = 0$		$\rho = 0.2$		$\rho = 0.8$	
Simulation Type	s	Time	s	Time	s	Time	s	Time
FLDMC	8.47 (0.01)	68	7.74 (0.02)	69	7.01 (0.01)	71	4.78 (0.02)	78
LDMC2	8.47 (0.01)	1128	7.70 (0.01)	1188	6.99 (0.02)	1379	4.66 (0.02)	1657
CMC ($M = 1200$)	8.19	516	7.46	529	6.74	525	4.57	549
CMC ($M = 8400$)	8.38	3563	7.55	3606	6.89	3646	4.68	3816
CMC ($M = 12000$)	8.43	5057	7.71	5128	6.91	5194	4.67	5432
CMC ($M = 24000$)	8.45 (0.02)	9307	7.71 (0.03)	9444	6.96 (0.03)	9564	4.71 (0.02)	9962

Table 3.12 summarizes the results obtained by different simulation methods with varying assumptions of the instantaneous correlation ρ. The column s shows the fair premium s, and the column $Time$ shows the amount of time taken for simulation, and the values in parentheses are standard errors. The estimates of *FLDMC* and *LDMC2* are very similar in value, but their computational times differ greatly. This observation reaffirms our earlier statement that *FLDMC* is to a great extent

more time efficient than *LDMC2*, without losing accuracy. As a way of verifying correctness of our estimates, we used the method *CMC* with very fine subintervals where M denotes the number of subintervals. The estimates from *CMC* should converge to the true value as we take finer partitions of subintervals. We observe that the *CMC* estimates with many subintervals converge to those of *FLDMC* and *LDMC2*. We also report standard errors of *CMC* estimates in parentheses for the case with $M = 24,000$. This indicates that our proposed simulation algorithms provide accurate results of the CDS prices. In particular, the method *FLDMC* is an accurate and time efficient technique of obtaining the CDS prices.

Chapter 4

Exit Probabilities of a Multivariate Brownian Motion with Curved Boundaries

In Chapters 2 and 3, we examined the problem of finding a probability that components of a multivariate Brownian Motion breach their respective barriers. In this case, the boundaries consist of a set of hyperplanes in R^d, where d is dimensionality of the process. In this chapter, we address a more general situation where we have curved boundaries instead of linear boundaries. This situation arises when we compute a barrier crossing probability of a sum of several Geometric Brownian Motions.

When the underlying process is one dimensional Geometric Brownian Motion, we have an analytic formula for a barrier crossing probability. Also, there are analytic valuation formulas for a barrier option with a single barrier and also with double

exponential barriers as given by Kolkiewicz (2002). However, the barrier crossing probability of a sum of several Geometric Brownian Motions is not known, and we propose an efficient method of computing this quantity in this chapter. In the context of finance, the sum of Geometric Brownian Motions can represent the process followed by a portfolio of stocks or futures.

We formulate the problem in a mathematical representation as follows. Suppose that $\mathbf{S} = [S_1, \ldots, S_d]^T$ follows a multivariate Geometric Brownian Motion process,

$$d\mathbf{S}(t) = U\mathbf{S}(t)dt + diag[\mathbf{S}(t)]\Sigma d\mathbf{W}(t), \tag{4.1}$$

where $\mathbf{W} = [W_1, \ldots, W_d]^T$ is a vector of independent Brownian Motions, U is a $d \times d$ diagonal matrix with diagonal values of $u_1, \ldots, u_d$, and Σ is a $d \times d$ matrix corresponding to a square root of an instantaneous variance-covariance matrix. Also, $diag[\mathbf{S}(t)]$ is a $d \times d$ diagonal matrix with components of $\mathbf{S}(t)$ being the diagonal elements. The initial value of $\mathbf{S}$ is denoted as $\mathbf{s}_0 = [s_{01}, \ldots, s_{0d}]^T$.

We define a stochastic process

$$Q(t) = S_1(t) + \ldots + S_d(t) \tag{4.2}$$

and denote by c a certain threshold value such that $Q(0) > c$. In this chapter, we discuss methods of computing $P(Q(t) \leq c, \text{ for some } t, 0 \leq t \leq T)$, which corresponds to the probability that the stochastic process $Q(t)$ breaches the threshold value c within the time horizon of T.

The probability distribution of a sum of Geometric Brownian Motions is not known. Practitioners typically approximate the sum of Geometric Brownian Motions by a

one-dimensional Geometric Brownian Motion process using moments matching, but this approximation is not very accurate. For computing the probability that the sum breaches a barrier, Monte Carlo simulation techniques can be used. However, as we have discussed earlier in this thesis, this method would require the use of many subintervals in order to remove bias in the estimates.

Thulin (2006) and Dionne et al. (2006) provide a comprehensive overview of the existing literature on a basket option pricing, which is related to the problem presented in this chapter. Most published works in this area such as Brigo et al. (2004) and Milevsky and Posner (1998) utilize a moment matching technique to approximate sums of lognormal distributions as some known distributions in order to price an European basket option or an Asian option. However, this technique is not suitable in computing a barrier crossing probability because the moment matching focuses only on a marginal distribution and not on an entire process. We have not been able to find any work in the existing literature that address the issue of computing a barrier crossing probability of the sum of Geometric Brownian Motions. This problem is non-trivial because it involves characterization of the underlying process correctly as well as computing its barrier crossing probability in continuous time.

In this chapter, we propose an approach based on Large Deviations Theory, so that we can approximate the barrier crossing probabilities using Monte Carlo simulation with a small number of subintervals. Earlier in this thesis, we addressed the problem of computing the probability that at least one component breaches its respective barrier. Here we extend this idea further to answer the question of computing the

barrier crossing probability of a sum of Geometric Brownian Motions.

This chapter is organized as follows. In Section 4.1, we compute the barrier crossing probability of a basket with fixed initial and terminal values. In Section 4.2, we show how the results from Section 4.1 can be incorporated into a simulation framework to compute barrier crossing probabilities of a sum of Geometric Brownian Motions with and without jumps added. In Section 4.3, we present numerical examples. Finally, in Section 4.4, we show that the method we develop in this chapter can be used to find an optimal portfolio that maximizes an economic agent's path-dependent utility function.

4.1 Barrier Crossing Probability of a Sum of Geometric Brownian Motions with Fixed Initial and Terminal Values

In order to address the main problem of this chapter, we consider different methods of characterizations of the process Q defined in (4.2) when the initial and terminal points are fixed. One naive approach is to freeze the coefficients and treat the process as a 1-dimensional Brownian Motion process. However, as reported in Baldi and Caramellino (2002), this crude approximation falls apart quickly as the interval size increases. In their paper, they compute the barrier crossing probability when the underlying process follows a general one-dimensional diffusion process. In order to apply the Large Deviations Theory, the authors use a series of transformations and prove the following lemma. We re-state Proposition 3.2 from Baldi and

Caramellino (2002) below.

Lemma 4.1.1 *Let U^ε solve the SDE*

$$dU_t^\varepsilon = \varepsilon\tilde{b}(U_t^\varepsilon)dt + \sqrt{\varepsilon}dB_t \tag{4.3}$$

$$U_s^\epsilon = u \tag{4.4}$$

where $s < t$, and let us set

$$W_{u,s}^\varepsilon(t) = u + \sqrt{\varepsilon}(B_t - B_s). \tag{4.5}$$

We consider the probability laws

$P_{u,s}^{\eta,\varepsilon}$ *: the law of $W_{u,s}^\varepsilon$ pinned by $W_{u,s}^\varepsilon(1) = \eta$*

$Q_{u,s}^{\eta,\varepsilon}$ *: the law of $U_{u,s}^\varepsilon$ pinned by $U_{u,s}^\varepsilon(1) = \eta$.*

Suppose that $\tilde{b}$ is a bounded and continuously differentiable function on R with bounded derivatives. If $A \in \mathcal{F}$ is an event, possibly depending on ϵ, then we have

$$Q_{u,s}^{\eta,\epsilon}(A) \sim P_{u,s}^{\eta,\epsilon}(A) \tag{4.6}$$

uniformly for (u, η) in a compact subset of R^2, where $p_\epsilon \sim q_\epsilon$ means $p_\epsilon/q_\epsilon \to 1$ as $\epsilon \to 0$.

Proof. The proof is given in Baldi and Caramellino (2002). □

In order to compute the barrier crossing probability of a sum of Geometric Brownian Motions instead of one dimensional general diffusion process, we follow a similar line of reasoning as Baldi and Caramellino (2002). We start with a correlated multivariate Geometric Brownian Motion process, and apply a series of transformations

in order to obtain a corresponding uncorrelated Brownian Motions with unit variances. Then we obtain the boundary of the region in R^d that corresponds to the barrier crossing (i.e. $Q(t) \leq c$) in the transformed space. Large Deviations Theory allows us to compute the exit probability of a multivariate Brownian Motion from this region. In particular, when the boundary of this region is a hyperplane, the exit probability can be easily obtained using methods discussed in Chapter 2. Hence, we need to show that the boundary of the region corresponding to the barrier crossing can be replaced by a hyperplane so that Large Deviations Theory can be readily applied to approximate the exit probability of the process.

4.1.1 Transformation

We consider the following standard transformation. Suppose that we have a stochastic differential equation,

$$dS(t) = \mu S(t)dt + S(t)\sigma dW(t) \tag{4.7}$$

with the fixed initial point s_0 and end point s_1. We denote the barrier level by c. We omit the time subscript t for notational convenience.

Let $Y(t) = F(S(t))$ where

$$\begin{aligned} F(s) &= \int_x^s \frac{1}{r\sigma} dr \\ &= \frac{1}{\sigma} \ln \frac{s}{x} \end{aligned} \tag{4.8}$$

and x is a constant such that $x \leq s$. Then, we obtain

$$\begin{aligned} \frac{\partial F}{\partial s} &= \frac{1}{s\sigma} \\ \frac{\partial^2 F}{\partial s^2} &= -\frac{1}{s^2\sigma} \\ \frac{\partial F}{\partial t} &= 0. \end{aligned}$$

By applying Ito's lemma, we obtain

$$dY(t) = \tilde{b}dt + dW(t) \tag{4.9}$$

with initial point $y_0 = F(s_0)$, ending point $y_1 = F(s_1)$, and the barrier $F(c)$. Here $\tilde{b}$ is a constant given by

$$\tilde{b} = \frac{\mu}{\sigma} - \frac{\sigma}{2}. \tag{4.10}$$

4.1.2 Sum of Two Geometric Brownian Motions

Let S_1 and S_2 follow correlated Geometric Brownian Motion processes,

$$dS_i(t) = \mu_i S_i(t)dt + S_i(t)\sigma_i dW_i(t) \tag{4.11}$$

for $i = 1, 2$, with the initial value of $\mathbf{S}(0) = \mathbf{s}_0 = [s_{01}, s_{02}]^T$ and the fixed terminal value of $\mathbf{S}(T) = \mathbf{s}_1 = [s_{11}, s_{12}]^T$, where T denotes the time horizon. We assume $E(dW_1 dW_2) = \rho dt$. For the process

$$Q(t) = S_1(t) + S_2(t), \tag{4.12}$$

we are interested in computing the probability that it breaches a barrier level c, where $Q(0) > c$. For notational simplicity, we omit the time subscript t of the process from now on.

For each of S_1 and S_2, we apply the transformation similar to (4.8),

$$F_i(s) = \int_{s_{0i}}^{s} \frac{1}{r\sigma_i} dr, \tag{4.13}$$

and we get

$$Y_1 = F_1(S_1)$$

$$Y_2 = F_2(S_2).$$

By rearranging the transformation $Y_i = F(S_i)$, we have

$$S_i \;\; = \;\; s_{0i} e^{\sigma Y_i}. \tag{4.14}$$

Equation (4.14) establishes the relationship between the original variable S_i and the transformed variable Y_i, for $i = 1, 2$.

From (4.9), we know that

$$dY_i = \tilde{b}_i dt + dW_i, \quad i = 1, 2, \tag{4.15}$$

with the initial point

$$\mathbf{y}_0 = [y_{01}, y_{02}]^T = [F_1(s_{01}), F_2(s_{02})]^T = [\frac{1}{\sigma_1} \ln \frac{s_{01}}{s_{01}}, \frac{1}{\sigma_2} \ln \frac{s_{02}}{s_{02}}]^T = [0, 0]^T,$$

and the ending point $\mathbf{y}_1 = [y_{11}, y_{12}]^T = [F_1(s_{11}), F_2(s_{12})]^T = [\frac{1}{\sigma_1} \ln \frac{s_{11}}{s_{01}}, \frac{1}{\sigma_2} \ln \frac{s_{12}}{s_{02}}]^T$. This transformation allows us to obtain processes with unit variances.

Assume for a moment that dW_1 and dW_2 are independent. We would like to find the boundary for the 2-dimensional process $\{Y_1, Y_2\}$ such that it corresponds to the process $Q = S_1 + S_2$ crossing a constant level c.

In order to do this, we first start with the boundary expressed in untransformed original variables,

$$\{(s_1, s_2) : s_1 + s_2 = c\}. \tag{4.16}$$

By substituting (4.14) into (4.16), we perform following algebraic manipulations

$$\begin{aligned} s_{01}e^{\sigma_1 y_1} + s_{02}e^{\sigma_2 y_2} &= c \\ s_{02}e^{\sigma_2 y_2} &= c - s_{01}e^{\sigma_1 y_1} \\ e^{\sigma_2 y_2} &= \frac{c}{s_{02}} - \frac{s_{01}}{s_{02}}e^{\sigma_1 y_1} \\ \sigma_2 y_2 &= \ln(\frac{c}{x_{02}} - \frac{s_{01}}{s_{02}}e^{\sigma_1 y_1}) \\ y_2 &= \frac{1}{\sigma_2}\ln(\frac{c}{s_{02}} - \frac{s_{01}}{s_{02}}e^{\sigma_1 y_1}). \end{aligned} \tag{4.17}$$

The expression in (4.17) determines the shape of the boundary in R^2 for the transformed variables Y_1 and Y_2.

Now we assume that the instantaneous correlation between dW_1 and dW_2 is ρ. Then the process (4.15) can be equivalently written as

$$d\mathbf{Y} = \tilde{b}dt + \Sigma d\tilde{\mathbf{W}} \tag{4.18}$$

where $\mathbf{Y}$ and $\tilde{\mathbf{W}}$ are 2×1 dimensional vectors, the components of $d\tilde{\mathbf{W}} = [d\tilde{W}_1, d\tilde{W}_2]^T$ are independent, and Σ is a 2×2 matrix, which is obtained by the Cholesky decomposition

$$\Sigma = \begin{bmatrix} 1 & 0 \\ \rho & \sqrt{1-\rho^2} \end{bmatrix} \tag{4.19}$$

so that

$$\Sigma^T\Sigma = \begin{bmatrix} 1 & \rho \\ \rho & 1 \end{bmatrix}. \tag{4.20}$$

Also, we have

$$\Sigma^{-1} = \begin{bmatrix} 1 & 0 \\ -\frac{\rho}{\sqrt{1-\rho^2}} & \frac{1}{\sqrt{1-\rho^2}} \end{bmatrix}. \tag{4.21}$$

In order to eliminate correlation between variables, we define a new variable $\mathbf{Z}$ from $\mathbf{Y}$ by the following transformation

$$\mathbf{Z} = G(\mathbf{Y}) = \Sigma^{-1}\mathbf{Y}. \tag{4.22}$$

By applying the multivariate version of Ito's Lemma, we obtain

$$d\mathbf{Z} = \tilde{\tilde{b}}dt + d\tilde{\mathbf{W}} \tag{4.23}$$

where $\mathbf{Z}$ has fixed initial value $\mathbf{z}_0 = [z_{01}z_{02}]^T = G(\mathbf{y}_0) = [0,0]^T$ and the fixed terminal value $\mathbf{z}_1 = [z_{11}z_{12}]^T = G(\mathbf{y}_1)$. Here $\tilde{\tilde{b}} = [\tilde{\tilde{b}_1}, \tilde{\tilde{b}_2}]$ is a vector of constants given as

$$\begin{aligned} \tilde{\tilde{b_1}} &= \tilde{b_1} \\ \tilde{\tilde{b_2}} &= -\frac{\rho}{\sqrt{1-\rho^2}}\tilde{b_1} + \frac{1}{\sqrt{1-\rho^2}}\tilde{b_2}. \end{aligned}$$

Now we need to express the corresponding boundary $S_1 + S_2 = c$ in terms of the newly transformed variables, Z_1 and Z_2. Since the transformation was

$$\mathbf{Z} = \Sigma^{-1}\mathbf{Y} \tag{4.24}$$

or

$$\begin{bmatrix} 1 & 0 \\ \rho & \sqrt{1-\rho^2} \end{bmatrix} \begin{bmatrix} z_1 \\ z_2 \end{bmatrix} = \begin{bmatrix} y_1 \\ y_2 \end{bmatrix},$$

we have

$$y_1 = z_1 \tag{4.25}$$

$$y_2 = \rho z_1 + \sqrt{1-\rho^2} z_2. \tag{4.26}$$

We can substitute (4.25) and (4.26) into (4.17) to obtain an expression for the boundary in terms of Z_1 and Z_2 as follows

$$\begin{aligned} y_2 &= \frac{1}{\sigma_2} \ln\left(\frac{c}{x_{02}} - \frac{s_{01}}{s_{02}} e^{\sigma_1 y_1}\right) \\ \rho z_1 + \sqrt{1-\rho^2} z_2 &= \frac{1}{\sigma_2} \ln\left(\frac{c}{s_{02}} - \frac{s_{01}}{s_{02}} e^{\sigma_1 z_1}\right) \\ \sqrt{1-\rho^2} z_2 &= \frac{1}{\sigma_2} \ln\left(\frac{c}{s_{02}} - \frac{s_{01}}{s_{02}} e^{\sigma_1 z_1}\right) - \rho z_1 \\ z_2 &= \frac{1}{\sqrt{1-\rho^2}} \left\{\frac{1}{\sigma_2} \ln\left(\frac{c}{s_{02}} - \frac{s_{01}}{s_{02}} e^{\sigma_1 z_1}\right) - \rho z_1\right\}. \end{aligned} \tag{4.27}$$

The expression in (4.17) determines the shape of the boundary corresponding to the barrier in the independent case, and the expression (4.27) for the correlated case. In the correlated case, let $D \in R^2$ be the region corresponding the values of $\{Z_1, Z_2\}$ for which the barrier is not breached. The problem is reduced to a problem of finding an exit probability that the 2-dimensional underlying process $\{Z_1, Z_2\}$ with unit variance and zero correlation exits the region D whose boundary is defined by (4.27).

4.1.3 Extension to a Sum of d Geometric Brownian Motions

Now we consider a sum of d correlated Geometric Brownian Motions with an instantaneous correlation matrix H. The process of the sum is represented by

$$Q = S_1 + S_2 + \ldots + S_d. \tag{4.28}$$

Our objective is to compute the probability that the process Q crosses a threshold value c, $Q(0) > c$, during the given time interval. Below we extend our discussion from Section 4.1.2 to address this issue.

We express the boundary that corresponds to the event $S_1 + \ldots + S_d = c$ using transformed variables $Y_1, \ldots, Y_d$. The equation

$$s_1 + s_2 + \ldots + s_d = c$$

or

$$s_{01}e^{\sigma_1 y_1} + s_{02}e^{\sigma_2 y_2} + \ldots + s_{0d}e^{\sigma_d y_d} = c$$

is equivalent to

$$\begin{aligned}
s_{0d}e^{\sigma_d y_d} &= c - s_{01}e^{\sigma_1 y_1} - s_{02}e^{\sigma_2 y_2} - \ldots - s_{0(d-1)}e^{\sigma_{d-1} y_{d-1}} \\
e^{\sigma_d y_d} &= \frac{c}{s_{0d}} - \frac{s_{01}}{s_{0d}}e^{\sigma_1 y_1} - \frac{s_{02}}{s_{0d}}e^{\sigma_2 y_2} - \ldots - \frac{s_{0(d-1)}}{s_{0d}}e^{\sigma_{d-1} y_{d-1}} \\
\sigma_d y_d &= \ln\left(\frac{c}{s_{0d}} - \frac{s_{01}}{s_{0d}}e^{\sigma_1 y_1} - \frac{s_{02}}{s_{0d}}e^{\sigma_2 y_2} - \ldots - \frac{s_{0(d-1)}}{s_{0d}}e^{\sigma_{d-1} y_{d-1}}\right) \\
y_d &= \frac{1}{\sigma_d}\ln\left(\frac{c}{s_{0d}} - \frac{s_{01}}{s_{0d}}e^{\sigma_1 y_1} - \frac{s_{02}}{s_{0d}}e^{\sigma_2 y_2} - \ldots - \frac{s_{0(d-1)}}{s_{0d}}e^{\sigma_{d-1} y_{d-1}}\right) . \quad (4.29)
\end{aligned}$$

Suppose that the correlation matrix H is given as follows,

$$H = \begin{bmatrix} 1 & \rho_{12} & \cdots & \rho_{1d} \\ \rho_{12} & 1 & \cdots & \rho_{2d} \\ \vdots & \vdots & \ddots & \vdots \\ \rho_{1d} & \rho_{2d} & \cdots & 1 \end{bmatrix}.$$

Note that H is also a variance-covariance matrix for the transformed variables, $Y_1, \ldots, Y_d$, because we perform a transformation such that $Y_1, \ldots, Y_d$ have unit

variances. Let $\tilde{\Sigma}$ be a $d \times d$ lower triangular matrix from Cholesky's decomposition of H, i.e. $H = \tilde{\Sigma}\tilde{\Sigma}^T$. We denote

$$\tilde{\Sigma} = \begin{bmatrix} q_{11} & 0 & \cdots & \cdots & 0 \\ q_{21} & q_{22} & 0 & \cdots & 0 \\ \vdots & \vdots & \ddots & \ddots & \vdots \\ q_{d1} & q_{d2} & \cdots & \cdots & q_{dd} \end{bmatrix}, \tilde{\Sigma}^{-1} = \begin{bmatrix} \varrho_{11} & 0 & \cdots & \cdots & 0 \\ \varrho_{21} & \varrho_{22} & 0 & \cdots & 0 \\ \vdots & \vdots & \ddots & \ddots & \vdots \\ \varrho_{d1} & \varrho_{d2} & \cdots & \cdots & \varrho_{dd} \end{bmatrix}.$$

The existence of $\tilde{\Sigma}$ is ensured by the positive semi-definiteness of H.

We transform the variable $\mathbf{Y}$ by $\tilde{\Sigma}^{-1}$ to obtain an uncorrelated process $\mathbf{Z}$ as follows,

$$\mathbf{Z} = \tilde{\Sigma}^{-1}\mathbf{Y}$$

or

$$\tilde{\Sigma}\mathbf{Z} = \mathbf{Y}, \tag{4.30}$$

and, by Ito's lemma, we obtain

$$d\mathbf{Z} = \tilde{\tilde{b}}dt + d\tilde{\mathbf{W}}, \tag{4.31}$$

where we use the same notations as in the previous section and $\tilde{\tilde{b}} = [\tilde{\tilde{b}}_1, \ldots, \tilde{\tilde{b}}_d]^T$ are given by

$$\begin{aligned} \tilde{\tilde{b}}_1 &= \varrho_{11}\tilde{b}_1 \\ \tilde{\tilde{b}}_2 &= \varrho_{21}\tilde{b}_1 + \varrho_{22}\tilde{b}_2 \\ &\vdots \\ \tilde{\tilde{b}}_d &= \varrho_{d1}\tilde{b}_1 + \varrho_{d2}\tilde{b}_2 + \ldots + \varrho_{dd}\tilde{b}_d. \end{aligned}$$

We note that $\tilde{\mathbf{W}}$ is a vector of d independent standard Brownian Motions. We know from Section 2.2.2 that the constant drift terms can be ignored when the

terminal value of the process is fixed. Since $\tilde{\tilde{b}}$ is a vector of constant values, the process (4.31) with the fixed initial and terminal values of $\mathbf{z}_0$ and $\mathbf{z}_1$ is equivalent to a d-dimensional standard Brownian Motion with pinned initial and terminal values of $\mathbf{z}_0$ and $\mathbf{z}_1$.

By re-writing (4.30) for each component of $\mathbf{Y}$, we get

$$\begin{aligned} y_1 &= q_{11}z_1 \qquad (4.32)\\ y_2 &= q_{21}z_1 + q_{22}z_2 \\ &\vdots \\ y_d &= q_{d1}z_1 + q_{d2}z_2 + \cdots + q_{dd}z_d. \qquad (4.33) \end{aligned}$$

Substituting (4.32) - (4.33) into (4.29), the boundary in R^d in terms of the original variables corresponding to $s_1 + \ldots + s_d = c$, can be expressed in terms of $Z_1, \ldots, Z_d$ in the following way:

$$\begin{aligned} & q_{d1}z_1 + q_{d2}z_2 + \cdots + q_{dd}z_d \\ = \;& \frac{1}{\sigma_d}\ln\left(\frac{c}{s_{0d}} - \frac{s_{01}}{s_{0d}}e^{\sigma_1 y_1} - \frac{s_{02}}{s_{0d}}e^{\sigma_2 y_2} - \ldots - \frac{s_{0(d-1)}}{s_{0d}}e^{\sigma_{d-1}y_{d-1}}\right) \end{aligned}$$

$$\begin{aligned} & q_{dd}z_d \\ = \;& \frac{1}{\sigma_d}\ln\left(\frac{c}{s_{0d}} - \frac{s_{01}}{s_{0d}}e^{\sigma_1(q_{11}z_1)} - \frac{s_{02}}{s_{0d}}e^{\sigma_2(q_{21}z_1+q_{22}z_2)} - \ldots - \frac{s_{0(d-1)}}{s_{0d}}e^{\sigma_{d-1}(q_{d1}z_1+q_{d2}z_2+\cdots+q_{d(d-1)}z_{d-1})}\right) \\ - \;& q_{d1}z_1 - q_{d2}z_2 - \cdots - q_{d(d-1)}z_{d-1} \end{aligned}$$

which gives

$$
\begin{aligned}
z_d \;&= \frac{1}{q_{dd}}\{\frac{1}{\sigma_d} \\
&\ln\left(\frac{c}{s_{0d}} - \frac{s_{01}}{s_{0d}}e^{\sigma_1(q_{11}z_1)} - \frac{s_{02}}{s_{0d}}e^{\sigma_2(q_{21}z_1+q_{22}z_2)} - \ldots - \frac{s_{0(d-1)}}{s_{0d}}e^{\sigma_{d-1}(q_{d1}z_1+q_{d2}z_2+\cdots+q_{d(d-1)}z_{d-1})}\right) \\
&-q_{d1}z_1 - q_{d2}z_2 - \cdots - q_{d(d-1)}z_{d-1}\}. \qquad (4.34)
\end{aligned}
$$

The expression (4.34) defines the boundary for the transformed variables $Z_1, \ldots, Z_d$ that follow a multivariate Brownian Bridge with unit variances and zero correlations. The initial and terminal values are fixed and equal to $\mathbf{z}_0$ and $\mathbf{z}_1$, respectively. The vectors $\mathbf{z}_0$ and $\mathbf{z}_1$ can be obtained in the same way as described in Section 4.1.2. We let D be the region corresponding to the barrier defined by (4.34). In the next two sections, we address the problem of computing the probability that the process $\mathbf{Z}$ with the fixed initial and terminal values of $\mathbf{z}_0 \in D$ and $\mathbf{z}_1 \in D$ exits the region D.

4.1.4 Linear Approximation of the Boundary

As discussed in the previous section, our problem is reduced to computing an exit probability from the region D that has a curved boundary. In this section, we show that for the purpose of computing an exit probability, the curved boundary of D can be replaced with a hyperplane in R^d. From Theorem 1.2.2, we see that we can easily compute an exit probability of a d-dimensional process when a boundary is a hyperplane. The series of propositions presented in this section provide justifications for replacing the curved boundary by a hyperplane, so that Large Deviations Theory for a process can be readily applied to compute the exit probability.

We need to consider two cases: (1) D is convex and (2) D^C is convex. We show in the next section that the fact whether the barrier is below or above the initial value determines the case (1) or (2).

In this section, we need the concept of a *supporting hyperplane*. A *supporting hyperplane* to a convex set V is a hyperplane which is the boundary of a *supporting half-space* to V, where a *supporting half-space* to V is a closed half-space which contains V and has a point of V in its boundary (Rockafellar (1970)).

We now consider following propositions.

Proposition 4.1.1 *Suppose V is a convex closed set. Assume also that x and y are points such that $x, y \notin V$. Let z^* be the unique point in V such that*

$$z^* = \arg\min\{z \in V \mid ||x - z|| + ||z - y||\}. \tag{4.35}$$

Let $L(V, z^*)$ be a set of supporting hyperplanes of V at z^*. Then, there exists a unique $l(z^*) \in L(V, z^*)$ such that

$$z^* = \arg\min\{w \in l(z^*) \mid ||x - w|| + ||w - y||\}. \tag{4.36}$$

Define, for any $r \geq 0$,

$$S(r) = \{w \mid ||x - w|| + ||w - y|| \leq r\}. \tag{4.37}$$

For any point w on the boundary of $S(r)$, let $L(S(r), w)$ be the set of supporting hyperplanes of $S(r)$ at w. The following lemma shows that the boundary of $S(r)$ is smooth.

Lemma 4.1.2 *The following statements are true for any $r \geq 0$.*

(i) $S(r)$ is convex.

(ii) If w is a point on the boundary of $S(r)$, then there is a unique supporting hyperplane of $S(r)$ at w.

Proof. The boundary of $S(r)$ can be represented by the set of points represented by

$$\{w \mid ||x - w|| + ||w - y|| = r\}. \tag{4.38}$$

Recall that an ellipse is the locus of points on a plane where the sum of the distances from any point on the curve to two fixed points is constant. Also, an ellipsoid is a a higher dimensional analogue of an ellipse. Hence, the surface given by (4.38) is an ellipsoid. From this, it follows that both (i) and (ii) are true. □

We now give a proof of Proposition 4.1.1.

Proof of Proposition 4.1.1: The existence of z^* follows from the closure of V and the continuity of the distance functions. For z^*, define

$$r^* \quad = \quad ||x - z^*|| + ||z^* - y||. \tag{4.39}$$

By the definition of $S(r)$, z^* is a boundary point of $S(r^*)$. Let l^* be the supporting hyperplane of $S(r^*)$ at z^*. It is unique by Lemma 4.1.2 (ii). By the definition of the supporting hyperplane, it follows that

$$z^* \quad = \quad \arg\min\{z \in l^* \mid ||x - z|| + ||z - y||\}. \tag{4.40}$$

i.e., z^* is the point on the hyperplane l^* that minimizes the sum of distances from x and y. Note that z^* is unique since l^* is unique. Thus, it remains to show that l^* is a supporting hyperplane of V.

Any hyperplane results in two open non-intersecting half-spaces. Let A and B be these half-spaces resulting from l^*. Let $\bar{A}$ and $\bar{B}$ be the closed half spaces from the closures of A and B, respectively. Without loss of generality, suppose $S(r^*)$ is contained in $\bar{A}$.

Suppose there exists $e \in A \cap V$. Consider the line segment $\overline{ez^*}$ between e and z^*. From $e \in A$ and the fact that the hyperplane l^* does not intersect with A (by the definition of A), it follows that the line segment $\overline{ez^*}$ is not contained in l^*. Thus, it follows that the line segment $\overline{ez^*}$ intersects with the interior of $S(r^*)$. Let u be the point on $\overline{ez^*}$ such that u is an interior point of $S(r^*)$. Thus,

$$||x - u|| + ||u - y|| < r^* = ||x - z^*|| + ||z^* - y||. \tag{4.41}$$

Recall that both e and z^* belong to V. Thus, by the convexity of V, we obtain that u is also in V. However, this contradicts the choice of z^* and hence $A \cap V = \emptyset$.

Therefore, l^* is a supporting hyperplane of V, and hence Proposition 4.1.1 is true. □

Now consider the case $x, y \in V$.

Proposition 4.1.2 *Suppose V is a convex closed set with a twice-differentiable boundary. Suppose x and y are points such that $x, y \in V$. Let z^* be any point on*

the boundary of V, ∂V, such that

$$z^* \quad = \quad \arg\min\{z \in \partial V \mid ||x - z|| + ||z - y||\}. \tag{4.42}$$

Let $L(V, z)$ be the set of supporting hyperplanes of V at z. Then the following statements are true.

(a) There exists a unique $l(z^*) \in L(V, z^*)$ such that

$$z^* \quad = \quad \arg\min\{w \in l(z^*) \mid ||x - w|| + ||w - y||\}. \tag{4.43}$$

(b) If the value of x is fixed and y is simulated from a continuous distribution, the probability that z^* is non-unique is 0.

Proof of Proposition 4.1.2 (a):

For a given z^*, $l(z^*) \in L(V, z^*)$ is unique because the boundary of V is twice-differentiable. Since V is convex, it follows from the definition of the supporting hyperplane

$$z^* \quad = \quad \arg\min\{w \in l(z^*) \mid ||x - w|| + ||w - y||\}. \quad \square$$

Proof of Proposition 4.1.2 (b):

We consider the shortest path that starts at x, touches a point on ∂V, and ends at y. We need to show that the probability of the shortest path being non-unique is 0.

Suppose that one of the shortest paths that touches ∂V is denoted by x-v^*-y where $v^* \in \partial V$ and the length of this path is r^*. We define an ellipsoid $S(y, r^*)$ in R^d

$$S(y, r^*) = \{w \mid ||x - w|| + ||w - y|| \leq r^*\}.$$

Note that $S(y, r^*)$ is completely contained in V, and there is at least one point on ∂V that is in contact with the surface of $S(y, r^*)$. We see that the path x-v^*-y is the unique shortest path only if the point of contact between ∂V and the surface of $S(y, r^*)$ is unique. Let $U(x)$, $U(x) \subseteq V$, be the set of all y's such that the point of contact between ∂V and the surface of $S(y, r^*)$ is not unique. Below we denote by $B_\delta(y)$ a ball around y with a radius of δ, $B_\delta(y) = \{x : ||y - x|| \leq \delta\}$.

Lemma 4.1.3 *Suppose that $y^{'} \in U(x)$. Then, there does not exist $\delta > 0$ such that $B_\delta(y^{'}) \subseteq U(x)$.*

Proof. Since $y^{'} \in U(x)$, the shortest path from x to $y^{'}$ that touches ∂V is not unique. Let x-v^*-$y^{'}$ be one of these paths with length r^*, where $v^* \in \partial V$. Now consider a point $y^{''} \in V$ on the line segment $\overline{v^* y^{'}}$ such that the length of the path x-v^*-$y^{''}$ is $r^* - \delta$ where δ is a small number.

Note that x-v^*-$y^{''}$ is the shortest path from x to $y^{''}$ that touches ∂V with length of $r^* - \delta$. We see that $v^* \in S(y^{''}, r^* - \delta)$. We now show that the ellipsoid $S(y^{''}, r^* - \delta)$ is completely contained in $S(y^{'}, r^*)$, with the only point of contact at v^*. This will imply that there is a point $y^{''} \in B_\delta(y^{'})$ that does not belong to $U(x)$.

Assume that we have a point $z \in S(y^{''}, r^* - \delta)$, $z \neq v^*$, such that it is located on the boundary or outside of $S(y^{'}, r^*)$. Then the length of x-z-$y^{''}$ is less or equal to $r^* - \delta$ because $z \in S(y^{''}, r^* - \delta)$. If by $dist(.)$ we denote length of a path, then this fact can be stated as

$$dist(xzy^{''}) \leq r^* - \delta. \tag{4.44}$$

We now separately examine the case when z is outside of $S(y^{'}, r^{*})$ and the case when z is on the boundary. When z is outside of $S(y^{'}, r^{*})$, we have

$$dist(xzy^{'}) > r^{*}. \tag{4.45}$$

Considering the path x-z-$y^{'}$, we have

$$\begin{aligned} dist(xzy^{'}) &\leq dist(xzy^{''}y^{'}) && (4.46)\\ &= dist(xzy^{''}) + dist(y^{''}y^{'}) && (4.47)\\ &\leq r^{*} - \delta + \delta && (4.48)\\ &= r^{*}, && (4.49) \end{aligned}$$

where we obtain (4.48) by substituting (4.44) into (4.47). We see that (4.46)-(4.49) contradict (4.45).

Similarly, when z is on the boundary of $S(y^{'}, r^{*})$, we have

$$dist(xzy^{'}) = r^{*}. \tag{4.50}$$

Considering the path x-z-$y^{'}$, we have

$$\begin{aligned} dist(xzy^{'}) &= dist(xv^{*}y^{'}) && (4.51)\\ &= dist(xv^{*}y^{''}y^{'}) && (4.52)\\ &\leq dist(xzy^{''}y^{'}) && (4.53)\\ &= dist(xz) + dist(zy^{''}y^{'}) && (4.54)\\ &< dist(xz) + dist(zy^{'}) && (4.55)\\ &= dist(xzy^{'}) && (4.56)\\ &= r^{*}, && (4.57) \end{aligned}$$

where we have equality in (4.51) because both z and v^* are on the boundary of $S(y^{'}, r^*)$, and we have inequality between (4.54) and (4.55) since z-$y^{''}$-$y^{'}$ is not a straight line due to $z \neq v^*$. The equality between (4.56) and (4.57) holds by (4.50). We see that (4.51)-(4.57) contradict (4.50).

By contradiction, the ellipsoid $S(y^{''}, r^* - \delta)$ is completely contained in $S(y^{'}, r^*)$ with the only point of contact at v^*. Since $S(y^{'}, r^*)$ is completely contained in V with v^* being one of the points of the contact, $S(y^{''}, r^* - \delta)$ is contained in V with the only point of contact at v^*.

Hence, for every $y^{'}$ and every $\delta > 0$, we can find a point $y^{''} \in B_\delta(y^{'})$ such that $y^{''} \notin U(x)$. $\square$

We introduce another lemma. By $\lambda(A)$ we denote a Lebesgue measure of a set $A \subseteq R^d$.

Lemma 4.1.4 *Suppose that for each point $g \in G \subseteq V$ there is a line $L(g)$ connecting g and a boundary of V, and all the points in $L(g)$ except g do not belong to G. Then $\lambda(G) = 0$.*

Proof.

Let G_1 be the set of points in the collection of lines generated by all points in G

$$G_1 = \{w \mid w \in L(g) \text{ for all } g \in G\}.$$

Let $L^{'}(g)$ denote the set of points in $L(g)$ with the point g removed. Also, we denote by G_2 the following subset of G_1

$$G_2 = \{w \mid w \in L^{'}(g) \text{ for all } g \in G\}.$$

By the fact that all the points in $L(g)$ except for the point g do not belong to G, it follows that no $L^{'}(g_1)$ for $g_1 \in G$ is entirely contained in another $L^{'}(g_2)$ for $g_2 \in G$ if $g_1 \neq g_2$. Also, we see that for any $g \in G$ we have $g \notin G_2$, and the corresponding line segments of $L(g)$ and $L^{'}(g)$ are added to the set G_1 and G_2, respectively. Hence, whether the line is with the point g or without will not affect the Lebesgue measure of the set. This shows that

$$\lambda(G_1) = \lambda(G_2). \tag{4.58}$$

Since G and G_2 are disjoint and $G_1 = G_2 \cup G$, it follows that

$$\lambda(G_1) = \lambda(G_2) + \lambda(G). \tag{4.59}$$

By combining (4.58) with (4.59), we get $\lambda(G) = 0$. $\square$

From Lemma 4.1.3, we see that there does not exist any ball in R^d that belongs to $U(x)$. Moreover, for each $y^{'} \in U(x)$, there is a line L connecting $y^{'}$ and a boundary of V, and all the points in L except $y^{'}$ do not belong to $U(x)$. From Lemma 4.1.4, these facts imply that the set $U(x)$ has a probability mass of zero, since the terminal value $y \in V$ is drawn from a continuous distribution. Therefore, the event that the shortest path is not unique has a probability of zero. This completes the proof for Proposition 4.1.2 (b). $\square$

We note that z^* in Proposition 4.1.2 may not be unique. This depends on the curvature of V and the locations of x and y. The fact that there may be more than one minimizing path implies that the exit probability calculated using the Large Deviations Theory must be suitably modified (Baldi (1995)). In the context of our simulation framework, when we compute the shortest path, the initial value

x is fixed and the terminal value y is simulated from a continuous multivariate distribution. Hence, by Proposition 4.1.2 (b), the event that z^* is not unique has a probability of zero.

Propositions 4.1.1 and 4.1.2 are applicable in the cases when D^C is convex and when D is convex, respectively. These propositions show that the point, say z^*, on the boundary of D that minimizes the distance from $x, y \in D$ to ∂D has the property that if you create a tangent hyperplane at this point then the minimum distance from the two end-points, x and y, to this hyperplane is achieved at exactly the same point z^*.

Using the above stated results and some properties of the Large Deviations approach, we can now show that the curved boundary of D can be replaced by a hyperplane. Whether D is convex or D^C is convex, the shortest path that touches a point in the boundary of D, z^*, is the same as the shortest path that touches the hyperplane that is a tangent of D at z^*. Let E denote the half-space defined by this tangent hyperplane. According to Baldi (1995), the theory of Large Deviations states that when the most likely path γ is unique, the exit probability of the process $\{\mathbf{Z}(t), t \geq 0\}$, $P^{\epsilon}\{\tau \leq T\}$, is asymptotically the same as $P^{\epsilon}\{\tau \leq T, \mathbf{Z} \in B_{\delta}(\gamma))\}$, where $B_{\delta}(\gamma)$ denotes the neighbourhood (a tube) of radius δ of γ, and τ is the first time the barrier is breached. The main result of this section can be summarized in the following way.

Let D be a region such that either D is convex or D^C is convex. For the underlying

process $\mathbf{Z}(t)$, we have

$$
\begin{aligned}
& P\{\mathbf{Z}(t) \notin D \text{ for some } t \in [t_0, t_0+\epsilon]\} && (4.60)\\
\approx\ & P\{\mathbf{Z}(t) \notin D \text{ for some } t \in [t_0, t_0+\epsilon], \mathbf{Z} \in B_\delta(\gamma)\} && (4.61)\\
\approx\ & P\{\mathbf{Z}(t) \notin E \text{ for some } t \in [t_0, t_0+\epsilon], \mathbf{Z} \in B_\delta(\gamma)\} && (4.62)\\
\approx\ & P\{\mathbf{Z}(t) \notin E \text{ for some } t \in [t_0, t_0+\epsilon]\}, && (4.63)
\end{aligned}
$$

where the approximation is valid as $\epsilon \to 0$ The quantity in (4.61) can be approximated by (4.62) because, by Propositions 4.1.1 and 4.1.2, the shortest paths γ are the same in both cases. Hence, the exit probability, $P\{\mathbf{Z}(t) \notin D \text{ for some } t \in [t_0, t_0+\epsilon]\}$ can be approximated by $P\{\mathbf{Z}(t) \notin E \text{ for some } t \in [t_0, t_0+\epsilon]\}$. From this, we see that the exit probability for the process $\mathbf{Z}(t)$ can be approximated by assuming that the boundary of D is replaced by a supporting hyperplane of D at $z^* \in \partial D$ that the minimizing path goes through.

4.1.5 Large Deviations Approach to Computing the Exit Probability of One Time Interval

Recall that D is the region corresponding to non-breaching of the barrier, whose boundary is defined by (4.27) in the case of a sum of two correlated Geometric Brownian Motions, or by (4.34), for a sum of d correlated Brownian Motion processes. In this section, we discuss properties of this region D, and then show a method of computing the exit probability from this region using the Large Deviations Theory.

We consider the region

$$\begin{aligned} V &= \{(z_1,\ldots,z_d) \mid z_d \le \frac{1}{q_{dd}}\{\frac{1}{\sigma_d} \\ &\quad \ln\left(\frac{c}{s_{0d}} - \frac{s_{01}}{s_{0d}}e^{\sigma_1(q_{11}z_1)} - \frac{s_{02}}{s_{0d}}e^{\sigma_2(q_{21}z_1+q_{22}z_2)} - \ldots - \frac{s_{0(d-1)}}{s_{0d}}e^{\sigma_{d-1}(q_{d1}z_1+q_{d2}z_2+\cdots+q_{d(d-1)}z_{d-1})}\right) \\ &- q_{d1}z_1 - q_{d2}z_2 - \cdots - q_{d(d-1)}z_{d-1}\}\}. \end{aligned} \tag{4.64}$$

We first show that V is convex and discuss how D is related to V. In particular, we show that D is the same as either V or the complement of V depending on whether the barrier is an upper or a lower barrier. The boundary of V is the same as the boundary of D, which is defined by (4.34),

$$\begin{aligned} z_d &= G(z_1,\ldots,z_{d-1}) \\ &= \frac{1}{q_{dd}}\{\frac{1}{\sigma_d} \\ &\quad \ln\left(\frac{c}{s_{0d}} - \frac{s_{01}}{s_{0d}}e^{\sigma_1(q_{11}z_1)} - \frac{s_{02}}{s_{0d}}e^{\sigma_2(q_{21}z_1+q_{22}z_2)} - \ldots - \frac{s_{0(d-1)}}{s_{0d}}e^{\sigma_{d-1}(q_{d1}z_1+q_{d2}z_2+\cdots+q_{d(d-1)}z_{d-1})}\right) \\ &- q_{d1}z_1 - q_{d2}z_2 - \cdots - q_{d(d-1)}z_{d-1}\}. \end{aligned} \tag{4.65}$$

We let

$$\begin{aligned} & H(z_1,\ldots,z_d) \\ = \; & \frac{1}{\sigma_d}\ln\left(\frac{c}{s_{0d}} - \frac{s_{01}}{s_{0d}}e^{\sigma_1(q_{11}z_1)} - \frac{s_{02}}{s_{0d}}e^{\sigma_2(q_{21}z_1+q_{22}z_2)} - \ldots - \frac{s_{0(d-1)}}{s_{0d}}e^{\sigma_{d-1}(q_{d1}z_1+q_{d2}z_2+\cdots+q_{d(d-1)}z_{d-1})}\right) \\ - \; & q_{d1}z_1 - q_{d2}z_2 - \cdots - q_{d(d-1)}z_{d-1} - q_{dd}z_d. \end{aligned} \tag{4.66}$$

Then the boundary of D, as shown in (4.65), can be expressed as

$$H(z_1,\ldots,z_d) = 0, \tag{4.67}$$

and V can be re-written as

$$V = \{(z_1,\ldots,z_d) \mid H(z_1,\ldots,z_d) \ge 0\}. \tag{4.68}$$

We note that the exponential function e^x is convex, and consider

$$f(\mathbf{x}) = f(x_1, \ldots, x_d) = e^{a_1 x_1 + \ldots + a_d x_d}, \tag{4.69}$$

where $a_1, \ldots, a_d$ are constants. With $\mathbf{v} = [v_1, \ldots, v_d]$, $\mathbf{w} = [w_1, \ldots, w_d]$, $g = a_1 v_1 + \ldots + a_d v_d$, and $h = a_1 h_1 + \ldots + a_d h_d$, we have

$$\begin{aligned}
& f(\alpha\mathbf{v} + (1-\alpha)\mathbf{w}) \\
= \; & e^{a_1(\alpha v_1 + (1-\alpha)w_1) + \ldots + a_d(\alpha v_d + (1-\alpha)w_d)} \\
= \; & e^{\alpha(a_1 v_1 + \ldots + a_d v_d) + (1-\alpha)(a_1 w_1 + \ldots + a_d w_d)} \\
= \; & e^{\alpha g + (1-\alpha)h} \\
\leq \; & \alpha e^g + (1-\alpha)e^h \\
= \; & \alpha e^{a_1 v_1 + \ldots + a_d v_d} + (1-\alpha)e^{a_1 h_1 + \ldots + a_d h_d} \\
= \; & \alpha f(\mathbf{v}) + (1-\alpha))f(\mathbf{w}).
\end{aligned}$$

Hence, $f(.)$ from (4.69) is convex. This implies that each of $\frac{s_{01}}{s_{0d}} e^{\sigma_1(q_{11}z_1)}$, $\frac{s_{02}}{s_{0d}} e^{\sigma_2(q_{21}z_1 + q_{22}z_2)}$, $\ldots$, $\frac{s_{0(d-1)}}{s_{0d}} e^{\sigma_{d-1}(q_{d1}z_1 + q_{d2}z_2 + \cdots + q_{d(d-1)}z_{d-1})}$ from (4.66) are convex with respect to z_i's. Since Theorem 5.2 of Rockafellar (1970) states that a sum of convex functions is convex and all the coefficients $\frac{s_{0i}}{s_{0d}}$, $i = 1, \ldots, d-1$, are positive, then

$$\left(\frac{s_{01}}{s_{0d}} e^{\sigma_1(q_{11}z_1)} + \frac{s_{02}}{s_{0d}} e^{\sigma_2(q_{21}z_1 + q_{22}z_2)} + \ldots + \frac{s_{0(d-1)}}{s_{0d}} e^{\sigma_{d-1}(q_{d1}z_1 + q_{d2}z_2 + \cdots + q_{d(d-1)}z_{d-1})} \right)$$

is convex as well. A *concave* function is a function whose negative is convex. Hence, the above result implies that

$$\left(\frac{c}{s_{0d}} - \frac{s_{01}}{s_{0d}} e^{\sigma_1(q_{11}z_1)} - \frac{s_{02}}{s_{0d}} e^{\sigma_2(q_{21}z_1 + q_{22}z_2)} - \ldots - \frac{s_{0(d-1)}}{s_{0d}} e^{\sigma_{d-1}(q_{d1}z_1 + q_{d2}z_2 + \cdots + q_{d(d-1)}z_{d-1})} \right)$$

is concave. Now we introduce two lemmas.

Lemma 4.1.5 *Let f be a concave function from R^d to $(-\infty, +\infty]$ and φ be a concave function from R to $(-\infty, +\infty]$ which is non-decreasing. Then $h(x) = \varphi(f(x))$ is concave on R^d.*

Proof. For x and y in R^d and $0 < \lambda < 1$, we have

$$f((1-\lambda)x + \lambda y) \geq (1-\lambda)f(x) + \lambda f(y). \tag{4.70}$$

By applying φ to both sides of this inequality, we get

$$h((1-\lambda)x + \lambda y) \geq \varphi((1-\lambda)f(x) + \lambda f(y)) \geq (1-\lambda)h(x) + \lambda h(y).$$

Thus h is concave. □

The following lemma is taken from Rockafellar (1970).

Lemma 4.1.6 *For any convex function f and any $\alpha \in [-\infty, +\infty]$, the level sets $\{x|f(x) < \alpha\}$ and $\{x|f(x) \leq \alpha\}$ are convex.*

Since ln(.) is a concave function, by Lemma 4.1.5 function $H(z_1, \ldots, z_d)$ defined in (4.66) is concave. The fact that $-H(z_1, \ldots, z_d)$ is convex and Lemma 4.1.6 imply that the set $\{(z_1, \ldots, z_d) \mid -H(z_1, \ldots, z_d) \leq 0\}$ is a convex set. Therefore,

$$V = \{(z_1, \ldots, z_d) \mid H(z_1, \ldots, z_d) \geq 0\} \tag{4.71}$$

is a convex set.

These results allow us to determine under what circumstances the region D is convex. We note that the initial values of components $(s_{01}, s_{02}, \ldots, s_{0d})$ correspond

to $(z_1, z_2, \ldots, z_d) = (0, 0, \ldots, 0)$ after going through the transformations described in Sections 4.1.2 and 4.1.3. Hence, when the sum of the initial values $s_{01}, \ldots, s_{0d}$ is smaller than the barrier level c, the point $(0, \ldots, 0)$ is in the region V. Therefore, D, which is a region corresponding to the non-breaching of the barrier, is the same as V, and our previous discussion implies that D is convex. Conversely, when the sum of the initial values $s_{01}, \ldots, s_{0d}$ is greater than the barrier level c, then the initial point $(0, \ldots, 0)$ is not in V. In this case, the region corresponding to non-breaching of the barrier, D, is the complement of V, and hence D^C is convex.

We now show how we can approximate the probability that the underlying process $\mathbf{Z}$ exits the region defined by D, $D \subseteq R^d$, using the Large Deviations Theory. Since $\mathbf{Z}$ follows the multivariate Brownian Bridge with unit variances and zero correlations, we first compute the following quantity,

$$u(\mathbf{z}_0, 0) = \inf_{\phi \in \partial D} \{\frac{1}{2}\{(\|\mathbf{z}_0 - \phi\| + \|\mathbf{z}_1 - \phi\|)^2 - \|\mathbf{z}_0 - \mathbf{z}_1\|^2\}\}, \tag{4.72}$$

where $\phi = [\phi_1, \ldots, \phi_d]^T$. Clearly, the optimal value of ϕ can be obtained from the following,

$$\inf_{\phi \in \partial D} (\|\mathbf{z}_0 - \phi\| + \|\mathbf{z}_1 - \phi\|). \tag{4.73}$$

Once again, we need to find the shortest path that starts from $\mathbf{z}_0$, touches a point along the boundary of D, which is given by (4.34), and goes back to $\mathbf{z}_1$. In particular, when $d = 2$, the objective function in (4.73) can be expressed as

$$h(\phi_1, \phi_2) = \sqrt{(z_{01} - \phi_1)^2 + (z_{02} - \phi_2)^2} + \sqrt{(z_{11} - \phi_1)^2 + (z_{12} - \phi_2)^2}. \tag{4.74}$$

We can reduce the number of arguments by substituting for ϕ_2 the expression $\phi_2 = \frac{1}{\sqrt{1-\rho^2}}\{\frac{1}{\sigma_2} \ln(\frac{c}{s_{02}} - \frac{s_{01}}{s_{02}} e^{\sigma_1 \phi_1}) - \rho \phi_1\}$ as given in (4.27). Even for this simplified

function, we were not able to obtain obtain the minimum point of $h(\phi_1)$ analytically. However, by Lemma 2.2.1, the objective function in (4.72) is convex. Therefore, numerical procedures utilizing Matlab function "fminbnd" can be used to obtain the global minimum value.

Suppose that $\mathbf{z}^*$ is the point on ∂D that the shortest path goes through. From (4.60) - (4.63), it follows that in both cases where D is convex or D^C is convex the curved boundary of D can be replaced with the supporting hyperplane E at $\mathbf{z}^*$. Therefore, by Propositions 4.1.1 and 4.1.2, the shortest path that touches E still goes through $\mathbf{z}^*$. For computing the exit probability we can now use Theorem 1.2.2. Application of this result in general is difficult as the quantities A and B that appear there are very expensive to compute. However, these quantities vanish when the boundary is a hyperplane. Since in our problem we can replace the boundary of D by a hyperplane, then, by Theorem 1.2.2 and our discussion in Section 1.2.4, the barrier crossing probability can be approximated as follows:

$$P^{\epsilon}_{\mathbf{X},0}\{\tau \leq 1\} = \exp(-\frac{u(\mathbf{z}_0, 0)}{\epsilon})(1 + o(\epsilon^m)) \tag{4.75}$$

for every $m > 0$, where ϵ is length of the time interval.

4.2 Simulation Method of Exit Probabilities

In this section, we discuss numerical methods for computing the probability that $Q = S_1 + \ldots + S_d$ breaches the level c, which can be above or below the sum of initial values $s_{0i}, i = 1, \ldots, d$. In the last section, we have developed a method

based on Large Deviations Theory to approximate the barrier crossing probability of Q during one time interval, when the initial and terminal values of components of Q are known. We now propose a simulation framework that allows us to compute the exit probability of Q for a given time horizon T, assuming that the underlying components $S_1, \ldots, S_d$ follow a correlated multivariate Geometric Brownian Motion.

The simulation framework is similar to what we introduced in Section 3.1.1. We first generate values of the underlying processes at discrete time intervals for a specified time horizon. If the process Q breaches the barrier at any of the discrete points, then the simulated path is considered to have crossed the barrier. Otherwise, for each subinterval with fixed initial and terminal values, we need to approximate the probability that the sum of the components have crossed the barrier. We do this using the method based on the Large Deviations Theory described in the previous section. In this way we generate simulated paths many times to approximate the barrier crossing probability.

The described method for computing the barrier crossing probability of a basket of risky securities can be applied to a process in either a risk-neutral or real measure, and it can be easily extended to the case where the components of the portfolio are assumed to follow a jump-diffusion process instead of a Geometric Brownian Motion. From our earlier discussion, we know how to estimate the barrier crossing probabilities for a diffusion process. By selecting endpoints of the subintervals to be times when jumps occur, we only need to address the computation of barrier crossing probabilities for diffusion processes for which we can apply the Large Devi-

ation Theory. In a typical application in finance, the number of jumps are relatively small, and hence we can expect that the number of subintervals will be comparable to the values that we used in our numerical experiments. This suggests that in such applications we should not see any additional accumulation of the computational error. A large intensity of jumps warrants additional studies, which we plan to conduct in a future.

We consider a multivariate jump diffusion model discussed by Kou (2002) and Kou and Wang (2004). For this model, the underlying process of the i^{th} component of the basket is assumed to follow

$$dS_i = \mu S_i dt + S_i \sigma dW_i + S_i d(\sum_{k=1}^{N(t)} (V_k - 1)), \tag{4.76}$$

where $\{N(t)\}$ is a Poisson process with rate λ, and V_k, $k = 1, 2, \ldots$, is a sequence of independent and identically distributed random variables such that $Y_k = \log V_k$ has a double exponential distribution with the density

$$f_Y(y) = p\eta_1 e^{-\eta_1 y} 1_{\{y \geq 0\}} + q\eta_2 e^{\eta_2 y} 1_{\{y<0\}},\ \eta_1 > 1,\ \eta_2 > 0. \tag{4.77}$$

In this model, the jumps are affecting all the components of the basket simultaneously as a common shock with the same magnitude. Below we briefly describe an algorithm to compute the barrier crossing probability of a basket whose components follow a joint jump-diffusion process:

1. Using the assumption of Poisson jumps, generate the inter-arrival times till the time horizon T. Then generate the jumps' magnitudes. The jumps occur simultaneously to all the components of the basket. Let $t_1, t_2, \ldots$ denote the times that the jumps occur.

2. Generate the simulated path of $S_1, \ldots S_d$ between the times of jumps by using a multivariate Geometric Brownian Motion.

3. From Steps 1 and 2, obtain the values of the trajectories of $S_1, \ldots, S_d$ at discrete times $t_1, t_2, \ldots$. If any of these values have breached the specified barrier, then the simulated path is considered to have crossed the barrier. Otherwise, for each time interval between discrete time points, the initial and the terminal values of the components of the basket are known. Using the method described in Section 4.1, we can determine the probability that the basket value crosses the barrier c during the given subinterval, because the process between the discrete interval points is a diffusion process.

4. Repeat Steps 1-3 many times to obtain the estimate of the barrier crossing probability of Q.

The jump-diffusion model used in this section is fairly simplistic but this framework can be extended to handle more general jump-diffusion models. This will be subjects of future research.

4.3 Numerical Examples

In this section, we present numerical examples to illustrate the proposed approximation method for computing barrier crossing probability of a basket of stocks. The components of the basket are assumed to follow a multivariate Geometric Brownian Motion process and a Jump-Diffusion process, and the results are presented in Section 4.3.1 and 4.3.2, respectively.

4.3.1 Sum of Geometric Brownian Motions

Here we present examples of computing the probability of barrier crossing for a sum of several Geometric Brownian Motions. We use the method presented in Sections 4.1-4.2, to which we refer as "LDT method". We compare results obtained from this method with the results from a Crude Monte Carlo method.

We consider a three-dimensional Geometric Brownian Motion process with the parameters as specified in Table 4.1. The instantaneous correlation among these processes is given by ρ, whose values are varied in our study.

Table 4.1: Parameters of Geometric Brownian Motions for Stock Price Processes

GBM	Initial Value	Growth Rate	σ^2
S_1	52	0.05	0.25
S_2	23	0.05	0.20
S_3	49	0.05	0.3

The process for the i^{th} component of the basket is denoted by $S_i(t), i = 1, 2, 3$. We define the basket process as $Q(t) = S_1(t) + S_2(t) + S_3(t)$. For a specific barrier level, c, we compute the probability that the basket process breaches the level before the time horizon $T = 1$. We also investigate different values of barrier levels c.

Tables 4.2, 4.3, and 4.4 report estimates of barrier crossing probabilities using the LDT method and the Crude Monte Carlo method when the barrier level is $c = 121.5, 115$, and 106, respectively. The values in parentheses are standard devi-

ations of the Crude Monte Carlo estimates. We also varied values of instantaneous correlation ρ. In these tables, M denotes the number of subintervals used.

Table 4.2: Estimates of Barrier Crossing Probabilities with Barrier $c = 121.5$

LDT Method with Quasi-Monte Carlo ($N = 10,000$)								
	$\rho = -0.2$		$\rho = 0$		$\rho = 0.2$		$\rho = 0.8$	
M	Estimates	Time (s)	Estimates	Time (s)	Estimates	Time (s)	Estimates	Time (s)
1	0.852	185	0.8819	181	0.8991	173	0.9259	168
2	0.8482	128	0.88	122	0.8982	125	0.9273	117
5	0.8442	501	0.8777	471	0.8963	463	0.9269	426.2
10	0.8419	786	0.877	722	0.8949	694	0.926	625
Crude Monte Carlo ($N = 50,000$)								
	$\rho = -0.2$		$\rho = 0$		$\rho = 0.2$		$\rho = 0.8$	
M	Estimates	Time (s)	Estimates	Time (s)	Estimates	Time (s)	Estimates	Time (s)
1000	0.8203 (0.0017)	259	0.857 (0.0012)	259	0.8798 (0.0017)	260	0.9135 (0.0001)	260
5000	0.8314 (0.0013)	1243	0.8668 (0.0007)	1244	0.8876 (0.0010	1244	0.9196 (0.0001)	1245
7000	0.8355 (0.0002)	1744	0.866 (0.0001)	1743	0.8862 (0.0011)	1743	0.9189 (0.0010)	1745
15000	0.8352 (0.0007)	3886	0.8706 (0.0018)	3856	0.891 (0.0007)	3812	0.9223 (0.0010)	3812
30000	0.8372 (0.0014)	7949	0.8723 (0.0012)	7925	0.8936 (0.0017)	7978	0.9222 (0.0019)	8066

Since we can use a small number of time intervals for the LDT method, we can combine this method with Quasi-Monte Carlo simulation, which works well in problems of low dimensionality and requires a lesser number of simulation trajectories for convergence. Hence, we use only 10,000 simulation runs, whereas for the Crude Monte Carlo method we use 50,000 simulation runs.

As the results in Tables 4.2, 4.3, and 4.4 demonstrate, the estimates from the LDT

Table 4.3: Estimates of Barrier Crossing Probabilities with Barrier $c = 115$

LDT Method with Quasi-Monte Carlo ($N = 10,000$)								
	$\rho = -0.2$		$\rho = 0$		$\rho = 0.2$		$\rho = 0.8$	
M	Estimates	Time (s)	Estimates	Time (s)	Estimates	Time (s)	Estimates	Time (s)
1	0.4874	212	0.5767	200	0.6323	197	0.7243	190
2	0.4806	330	0.5718	312	0.6294	304	0.7262	256
5	0.4835	370	0.5734	337	0.6296	352	0.7268	538
10	0.4858	1273	0.5811	1160	0.6302	1116	0.7304	942
Crude Monte Carlo ($N = 50,000$)								
	$\rho = -0.2$		$\rho = 0$		$\rho = 0.2$		$\rho = 0.8$	
M	Estimates	Time (s)	Estimates	Time (s)	Estimates	Time (s)	Estimates	Time (s)
1000	0.4778 (0.0019)	259	0.559 (0.0016)	260	0.625 (0.0015)	260	0.723 (0.0019)	260
5000	0.4778 (0.0002)	1240	0.5701 (0.0005)	1241	0.6299 (0.0007)	1242	0.7311 (0.0002)	1243
7000	0.48 (0.0001)	1736	0.5738 (0.0001)	1737	0.6344 (0.0001)	1738	0.7276 (0.0029)	1739
15000	0.4792 (0.0010)	3891	0.5767 (0.0010)	3895	0.6315 (0.0014)	3902	0.7336 (0.0016)	3904
30000	0.4813 (0.0016)	7839	0.5762 (0.0030)	7823	0.6338 (0.0028)	7803	0.7338 (0.0011)	7908

method with relatively small number of subintervals (5 or 10) are very close to the asymptotic values obtained by the Crude Monte Carlo method. The differences between the LDT estimates with $M = 10$ and the Crude Monte Carlo estimates with $M = 30,000$ are at most 0.005. We can attribute this discrepancy to the discretization error of the Crude Monte method and to the approximation error of the LDT method.

We can see that the computation time using the LDT method seems to be much shorter than that for Crude Monte Carlo. This can be explained by the fact that the

Table 4.4: Estimates of Barrier Crossing Probabilities with Barrier $c = 106$

LDT Method with Quasi-Monte Carlo ($N = 10,000$)								
	$\rho = -0.2$		$\rho = 0$		$\rho = 0.2$		$\rho = 0.8$	
M	Estimates	Time (s)	Estimates	Time (s)	Estimates	Time (s)	Estimates	Time (s)
1	0.1702	223	0.2613	214	0.3302	219	0.4643	209
2	0.1683	373	0.2646	357	0.3316	354	0.4696	326
5	0.1719	616	0.2735	584.4	0.3353	434	0.4798	360
10	0.1684	1659	0.2681	1572	0.3409	1510	0.4876	1326
Crude Monte Carlo ($N = 50,000$)								
	$\rho = -0.2$		$\rho = 0$		$\rho = 0.2$		$\rho = 0.8$	
M	Estimates	Time (s)	Estimates	Time (s)	Estimates	Time (s)	Estimates	Time (s)
1000	0.1545 (0.0006)	259	0.256 (0.0016)	259	0.3312 (0.0008)	259	0.4806 (0.0005)	259
5000	0.1622 (0.0001)	1237	0.2594 (0.0011)	1238	0.3359 (0.0019)	1239	0.4848 (0.0001)	1240
7000	0.1624 (0.0007)	1733	0.2615 (0.0001)	1734	0.3384 (0.0006)	1735	0.4884 (0.0012)	1737
15000	0.1649 (0.0012)	3886	0.2654 (0.0013)	3890	0.337 (0.0012)	3891	0.4881 (0.0013)	3894
30000	0.1641 (0.0018)	7638	0.2654 (0.0026)	11952	0.3392 (0.0012)	12429	0.4893 (0.0015)	10235

former method uses smaller number of subintervals and requires fewer simulation runs due to the application of Quasi-Monte Carlo method.

As we increase the number of components of the basket, we notice that the computational time exhibits a moderate growth, which is shown in Figure 4.1. In this case, the number of subintervals was one and the number of simulations runs was $N = 4,000$, but we expect that the linearity will hold also for different numbers of subintervals.

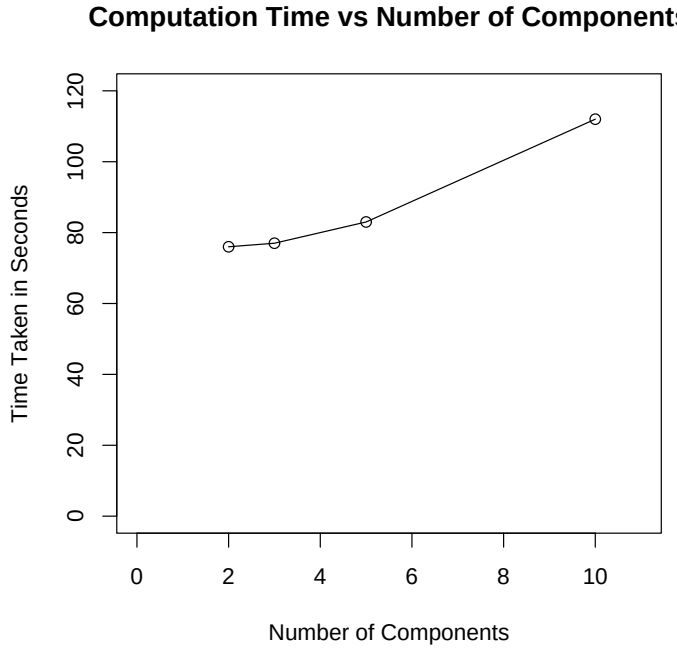

Figure 4.1: Computational Time vs Number of Components in the sum

4.3.2 Sum of Jump-Diffusions

In this section, we assume that the components of the basket follow a multivariate jump-diffusion process as described in Section 4.2. The parameterizations of the diffusion components are shown in Table 4.5.

We also assume that the correlation structure is given by

$$\begin{bmatrix} 1 & -0.2 & -0.2 & -0.1 & -0.1 \\ -0.2 & 1 & -0.2 & -0.1 & -0.1 \\ -0.2 & -0.2 & 1 & -0.1 & -0.1 \\ -0.1 & -0.1 & -0.1 & 1 & -0.1 \\ -0.1 & -0.1 & -0.1 & -0.1 & 1 \end{bmatrix}. \tag{4.78}$$

For the jump terms, which are common shocks to all the underlying components

Table 4.5: Parameters of Diffusion Components for Stock Price Processes

Component	Initial Value	Growth Rate	σ^2
S_1	190.6519	0.02	0.04
S_2	41.2913	0.05	0.10
S_3	61.2880	0.08	0.16
S_4	105.0834	0.10	0.18
S_5	101.6853	0.12	0.21

of the basket, we assume that they follow a Poisson process with $\lambda = 0.7$. The magnitude of the jumps has a double exponential distribution with $p = q = 0.5$, $\eta_1 = 25$, and $\eta_2 = 25$.

By using the simulation method described in Section 4.2, we have obtained the probability that the basket crosses the barrier level of 490 to be 0.4132. This result is based on 10,000 Quasi-Monte Carlo simulations. For the Crude Monte Carlo method, the estimate converges to the true value as the number of subintervals increases. For 10,000 Monte Carlo paths, we have obtained estimates of 0.3867, 0.3932, 0.3986, 0.4085, 0.4102, and 0.4132 with the number of subintervals of 500, 1000, 3000, 5000, 6000, and 7000, respectively. As before, the low discrepancy sequence cannot be used in conjunction with the Crude Monte Carlo method, since the dimensionality of the problem is large due to the large number of subintervals used. We can see that the proposed method allows us to obtain accurate estimates with a very small number of subintervals.

4.4 Application: Path-Dependent Utility Function

In Sections 4.1-4.3, we have developed an efficient method of computing a barrier crossing probability of a basket of stocks. In this section, we examine a particular problem where this method can be applied. We incorporate the concept of barrier crossing into the problem of a portfolio selection. The portfolio selection criteria that take account of the barrier crossing probability can better reflect preferences of an investor who is not willing to lose more than a certain amount of money during a given time horizon.

The portfolio selection problems are typically addressed in two different approaches: risk-criterion minimization and utility maximization. The risk-criterion minimization approach was first explored by a seminal paper by Markowitz (1952). In his pioneering work, he developed a model that fully takes into account the covariance between asset returns and constructs an efficient portfolio by minimizing variance of the portfolio. Alternatively, other risk criteria such as Value-at-Risk (VaR) or Conditional Tail Expectations (CTE) can be minimized in determining an optimal portfolio. In the existing literature, there are approaches that incorporate barrier crossing probability in finding an optimal portfolio. Stutzer (2003) selects an asset allocation so that the probability that the terminal portfolio value goes below a certain threshold level is minimized. Stutzer (2003) further shows that his criterion is consistent with maximizing a power utility function. In a continuous-time setting with dynamic portfolio rebalancing, Bielski et al. (2005) find the efficient mean-

variance frontier of a portfolio with the constraint that the portfolio value is never allowed to be below a bankruptcy level of zero during the given time horizon. For their results to hold, the completeness of the market model is essential. Lamantia and Rossello (2004) introduce the concept of *dynamic Value-at-Risk*, which considers the loss value not only at the end of the time horizon but also during the time horizon. The authors show that the standard VaR measure can be inadequate in addressing the liquidity of a firm.

In the utility maximization approach, we find an optimal portfolio that maximizes the expected value of a utility function $U(x)$ where x represents the amount of the agent's wealth. The utility is assumed to be strictly increasing and concave so that $U^{'}(x) > 0$ and $U^{''}(x) \leq 0$. There is existing literature related to the path-dependent utility function. In Bouchard and Pham (2004) and Blanchet-Scalliet et al. (2005), the authors discuss maximizing the expected utility when the time horizon is uncertain in a continuous time. The time horizon is given by $T \wedge \tau$, where τ is a stopping time given by an exogenous or endogenous variable. This uncertainty of the time horizon may reflect additional factors such as changes in the investor's position (retirement or death, exogenous endowment) or behaviour.

In this section, we focus on the utility maximization approach. In Section 4.4.1, we propose a path-dependent utility function and show that its expectation can be represented as a sum of many barrier crossing probabilities. In Section 4.4.2, we modify the algorithm presented in Section 4.2 and discuss how the expected utility function can be evaluated in a simulation framework. We can then find an optimal portfolio that maximizes the path-dependent utility. In Section 4.4.3, we

demonstrate numerical examples of the portfolio selection.

4.4.1 Path-Dependent Utility Function and Risk Criterion

A possible extension of a utility function that depends only on the terminal wealth to the one that takes into account the way wealth evolved during a given time horizon is

$$U^C(x_{0\leq t\leq T}) = 1_{A(x_{0\leq t\leq T})}U(x_T) + 1_{\overline{A}(x_{0\leq t\leq T})}\nu, \tag{4.79}$$

where x_t denotes wealth at time t, $t \in [0,T]$, and $A(x_{0\leq t\leq T}) = \{\inf_{0\leq t\leq T} x_t > b\}$ is the event that wealth amount does not become equal or lower than a certain threshold value b during the given time horizon T. $\overline{A}$ denotes the complement of A. We refer to this utility function $U^C(.)$ as a path-dependent utility function. Also, the utility function $U(.)$ is strictly increasing and concave so that $U^{'}(x) > 0$ and $U^{''}(x) \leq 0$. From the definition it follows that the utility at time T will be the same as the standard one-period utility if the wealth process does not go below a threshold value during the time horizon. Otherwise, the utility will be equal to a fixed residual value denoted by ν. This path-dependent utility reflects better the investor's utility, since it incorporates the fact that the investor can afford to take only a certain amount of financial loss during a given time horizon.

In the utility maximization approach, we are looking for a portfolio that maximizes the expected utility, $E(U^C(x_{0\leq t\leq T}))$. Below we demonstrate that for $U^C(.)$ the expected utility approach is related to a certain form of barrier crossing probability. As discussed in Section 1.3.2, in a one-period model, Gardiol et al. (2000) show

that any expected utility function can be represented as a weighted sum of tail probabilities to any desired degree by

$$E(U(X_T)) \approx \sum_{k=1}^{K} a_k P(X_T > b_k) \tag{4.80}$$

where a_k and b_k are suitably chosen constants. This implies that the optimal portfolio may be obtained by maximizing a sum of tail probabilities. This can be very helpful in risk management if the tail probabilities can be easily computed. When $K = 1$, we have a degenerate utility function where the investor is satisfied only if $X_T > b_1$. We derive similar results for the expected path-dependent utility $U^C(X_T)$.

We have

$$\begin{aligned} & E(U^C(X_{0\le t\le T})) \\ = \; & E(1_{A(X_{0\le t\le T})}U(X_T)) + E(1_{\overline{A}(X_{0\le t\le T})}\nu) \\ = \; & E(1_{A(X_{0\le t\le T})}U(X_T)) + \nu P(\overline{A}(X_{0\le t\le T})). \end{aligned} \tag{4.81}$$

The first term in (4.81) can be rewritten as follows,

$$\begin{aligned} & E(1_{A(X_{0\le t\le T})}U(X_T)) \\ = \; & E(E(1_{A(X_{0\le t\le T})}|X_T)U(X_T)) \\ = \; & \int_{u:u>b} E(1_{A(X_{0\le t\le T})}|X_T = u)U(u)f(u)du \\ = \; & \int_{u:u>b} P(A(X_{0\le t\le T})|X_T = u)U(u)f(u)du \\ = \; & \int_{u:u>b} g(u)U(u)du \end{aligned}$$

where $f(.)$ is a density function of X_T and $g(u) = P(A(X_{0\leq t\leq T})|X_T = u)f(u)$. We define $G(u)$ to be an antiderivative of $g(u)$ such that

$$\begin{aligned} G(x) &= \int_0^x g(u)du \\ &= \int_0^x P(A(X_{0\leq t\leq T})|X_T = u)f(u)du. \end{aligned}$$

Hence $G(x)$ is the probability that the terminal wealth X_T is less than x and the wealth process $\{X_t, 0 \leq t \leq T\}$ has not crossed the threshold level. Suppose that R is a sufficiently large number such that $\int_{u:u>b} g(u)U(u) \approx \int_b^R g(u)U(u)$. We make use of R in order to avoid subtracting ∞ from ∞ in the steps shown below. Noting that $G(u) = 0$ for $u \leq b$ and $G(R) \approx P(A(X_{0\leq t\leq T}))$, we have

$$\begin{aligned} & E(1_{A(X_{0\leq t\leq T})}U(X_T)) \\ = & \int_b^R g(u)U(u)du + Error1 \\ = & U(u)G(u)|_b^R - \int_b^R G(u)U'(u)du + Error1 \\ = & U(R)G(R) - U(b)G(b) - \int_b^R G(u)U'(u)du + Error1 \\ = & U(R)G(R) - \int_b^R G(u)U'(u)du + Error1 \\ = & U(R)G(R) - [\int_b^R G(R)U'(u)du - \int_b^R (G(R) - G(u))U'(u)du] + Error1 \\ = & U(R)G(R) - [G(R)U(R) - G(R)U(b) - \int_b^R (G(R) - G(u))U'(u)du] + Error1 \\ = & \int_b^R (G(R) - G(u))U'(u)du + G(R)U(b) + Error1 \\ = & \int_0^R (G(R) - G(u))U'(u)du - \int_0^b (G(R) - G(u))U'(u)du + G(R)U(b) + Error1 \\ = & \int_0^R (G(R) - G(u))U'(u)du - \int_0^b G(R)U'(u)du + G(R)U(b) + Error1 \end{aligned}$$

$$= \int_0^R (G(R) - G(u))U'(u)du + Error1 \tag{4.82}$$

$$= \sum_{k=1}^{K} a_k(P(A(X_{0\le t\le T}) - G(u_k)) + Error1 + Error2 \tag{4.83}$$

$$= \sum_{k=1}^{K} a_k H(u_k) + Error1 + Error2, \tag{4.84}$$

where we obtain (4.83) by taking a Riemann sum approximation of the integral in (4.82) with $a_k = U'(u_k)(u_k - u_{k-1})$. $Error1$ can be removed by setting a sufficiently large number for R, and $Error2$ can be removed by taking very fine discretizations of the integral in (4.82). We also let $H(u) = P(A(X_{0\le t\le T})) - G(u)$ which is the probability that the terminal wealth X_T is greater than u and the wealth process $\{X_t, 0 \le t \le T\}$ has not crossed the threshold level b. Now, by substituting (4.84) into (4.81) and assuming $b \in \{u_1, \dots u_K\}$, we obtain

$$\begin{aligned} E(U^C(X_{0\le t\le T})) &\approx \sum_{k=1}^{K} a_k H(u_k) + \nu P(\bar{A}(X_{0\le t\le T})) \\ &= \sum_{k=1}^{K} a_k H(u_k) + \nu H(b) \\ &= \sum_{k=1}^{K} \tilde{a_k} H(u_k), \end{aligned} \tag{4.85}$$

where $\tilde{a_k} = a_k + \nu$ when $u_k = b$, and $\tilde{a_k} = a_k$ otherwise.

This shows that the expected path-dependent utility $E(U^C(X_{0\le t\le T}))$ can be expressed as a linear combination of $H(u_k)$'s. This gives us an alternative way of evaluating the expected utility, which can be useful when methods of rapid evaluation of $H(u_k)$'s are available. A numerical example of this approximation is provided in Section 4.4.3. In the extreme case when $K = 1$, an investor is satisfied

when the terminal value is above a certain required value u_1 and the wealth process has not gone below the threshold value b. Hence, a single $H(.)$ can be used as an alternative criterion for the portfolio selection.

4.4.2 Evaluation of Utility Function

In this section, we build upon our methodology discussed in Sections 4.1-4.3, and propose methods for evaluating the quantities $H(u_k)$'s and $E(U^C(X_{0\leq t\leq T}))$ in (4.85). We suppose that our portfolio comprises of d assets so that we have

$$X(t) = X_1(t) + \ldots + X_d(t),$$

where $X_1, \ldots, X_d$ are assumed to follow a multivariate Geometric Brownian Motion.

Evaluation of $\mathbf{H(u_k)}$'s

We write $H(u_k)$ as $H(X, u_k, b)$ for $k = 1, \ldots K$ to emphasize that these are probabilities that the terminal portfolio value $X(T)$ is greater than a certain level u_k and the process $\{X(t), 0 \leq t \leq T\}$ did not breach the barrier b. Here we denote by K the number of $H(u_k)$'s to be summed in (4.85). Let $J(X, u_k, b) = 1 - H(X, u_k, b)$ be the probability that $X(T)$ is less than u_k or $\{X(t), 0 \leq t \leq T\}$ breached the barrier b. We use the following procedures in order to evaluate $J(X, u_k, b)$'s for $k = 1, \ldots, K$.

1. We initialize $W_k = 0$ for $k = 1, \ldots, K$.

2. We generate terminal values of the underlying variables $X_1(T), \ldots, X_d(T)$ by assuming that they follow a multivariate Geometric Brownian Motion.

3. Suppose that the generated terminal portfolio value $X(T) = X_1(T) + \ldots + X_d(T)$ is x_T. For each $k = 1, \ldots, K$, if x_T does not exceed the level u_k, we set $W_k = W_k + 1$. Otherwise we compute $R = Prob(\inf_{0 \le t \le T} X_t \le b | X(T) = x_T)$. This quantity can be efficiently approximated by the Large Deviations based method discussed in Sections 4.1-4.3. Then we set $W_k = W_k + R$.

4. We repeat Steps 2 and 3 N times.

5. Our estimate for $J(X, u_k, b)$ is $\frac{W_k}{N}$ for $k = 1, \ldots, K$.

In this procedure, we use the same set of simulated values to evaluate all $J(X, u_k, b)$'s for $k = 1, \ldots, K$. Hence, the time to perform this procedure is of the same magnitude regardless of the value of K.

Direct Evaluation of Expected Path-Dependent Utility

Instead of using the relation given by (4.85), the expected path-dependent utility, $E(U^C(X_{0 \le t \le T}))$, can also be directly evaluated in a similar way as follows.

1. We initialize $W = 0$.

2. We generate terminal values of the underlying variables $X_1(T), \ldots, X_d(T)$ by assuming that they follow a multivariate Geometric Brownian Motion, and obtain the portfolio value $X(T)$.

3. With the fixed terminal value of $X(T) = x_T$, we compute $R = Prob(\inf_{0 \le t \le T} X_t > b | X(T) = x_T)$, the probability that the path does not breach the barrier. Then we set $W = W + RU(x_T) + (1 - R)\nu$, where the notations, $U(.)$ and ν are introduced in (4.79).

4. We repeat Steps 2 and 3 N times.

5. Our estimate for $E(U^C(X_{0\leq t\leq T}))$ is $\frac{W}{N}$.

We note that the time needed to perform direct evaluation of the expected path-dependent utility is approximately the same as the time needed to evaluate the sum of $H(.)$'s because both procedures involve computing the barrier crossing probability R over one set of simulated values.

4.4.3 Numerical Examples

In this section, we present some numerical examples of the concepts related to the path-utility function. We show that the approximation in (4.85) holds and demonstrate a portfolio selection using the path-dependent utility.

We suppose that an investor has 500 to invest. There are 5 risky assets, each of which follows a Geometric Brownian Motion with parameters as specified in Table 4.6.

Table 4.6: Parameters of Geometric Brownian Motions for Risky Asset Price Processes

Component	Growth Rate	σ
X_1	0.02	0.04
X_2	0.05	0.10
X_3	0.08	0.16
X_4	0.10	0.18
X_5	0.12	0.21

The instantaneous correlations among these processes are given by

$$\begin{bmatrix} 1 & 0.2 & 0.2 & -0.1 & -0.1 \\ 0.2 & 1 & 0.2 & -0.1 & -0.1 \\ 0.2 & 0.2 & 1 & -0.1 & -0.1 \\ -0.1 & -0.1 & -0.1 & 1 & -0.1 \\ -0.1 & -0.1 & -0.1 & -0.1 & 1 \end{bmatrix}. \tag{4.86}$$

Utility Function Approximation

We verify that the path-dependent utility function can be approximated by the sum of $H(u_k)$'s as shown in (4.85). We assume that the utility is a power utility function with $\alpha = \frac{1}{2}$, so that is $U(X) = 2\sqrt{X}$, and the barrier level b is 485. Also, since both (4.81) and (4.85) contain the term $\nu P(\overline{A}(X_{0\leq t\leq T}))$, we do not need to compare the value of this term. Hence, we can set ν to be 0. With the number of simulations N being 2000, we directly evaluate $E(U^C(X_{0\leq t\leq T}))$. We also obtain approximations based on the right hand side of (4.85) using different number of points evenly distributed between 0 and 700. The methods of evaluating $E(U^C(X_{0\leq t\leq T}))$ and $H(u_k)$'s are described in Section 4.4.2. Table 4.7 shows the results. In this table, the column "Number of Points" refers to K in (4.85), which is the number of terms used for approximation.

The direct evaluation of $E(U^C(X_{0\leq t\leq T}))$ with $N = 2000$ gives 36.6346. As the number of points increases, the approximations using sums of $H(u_k)$'s approach the value obtained from the direct evaluation of the expected path-dependent utility.

Portfolio Selection by Maximization of the Expected Path-Dependent Utility

Table 4.7: Utility Approximation

Number of Points	Estimates
140	34.068
280	34.8202
560	35.3514
1120	35.7274
2240	35.9932

Suppose that we have a one-period static portfolio selection problem to find an optimal asset allocation that maximizes the expected path dependent utility function. We want to find a portfolio that maximizes $E(U^C(X_{0\leq t\leq T}))$, where $U(X) = 2\sqrt{X}$ is a power utility and $\nu = 0$. We adopt the direct evaluation method of $E(U^C(X_{0\leq t\leq T}))$ described in Section 4.4.2. We use $N = 2000$ and $M = 1$ for evaluating expectation of the path-dependent utility functions, where N is the number of simulations and M is the number of subintervals used.

Table 4.8: Results of Optimal Portfolios

Barrier Level	Optimal Allocation of Initial Wealth					Function Value
	X_1	X_2	X_3	X_4	X_5	
475	219.9659	114.9595	60.302	60.0943	44.6783	45.7268
480	269.6661	94.4447	58.2421	43.0824	34.5647	45.477
485	315.7673	85.9466	43.2356	29.4364	25.6141	44.5112
490	307.1396	126.5466	38.0489	20.8944	7.3706	44.4578
495	179.1686	80.837	141.2856	94.1618	4.5231	42.1476

We see from Table 4.8 that the optimal portfolio is different as we vary the barrier level. The column "Function Value" shows the values of the expected utility of the

optimal portfolio. This value decreases as we increase the barrier level. We can observe that as the barrier is lower, the optimal portfolio allocates more toward riskier assets. The lower threshold barrier means that one can afford to lose more money, and hence the portfolio composition can be riskier. As the barrier level gets smaller, the optimal portfolio will converge to a portfolio that maximizes a non-path-dependent expected utility. Hence the path-dependent utility as a criterion selects portfolios differently than the non-path-dependent utility function.

As an alternative portfolio selection criterion, one can also consider using one or more terms of $H(u_k)$'s, and these criteria will give different optimal portfolio selections.

Chapter 5

Directions for Future Research

In this thesis, we have devised efficient methods of computing barrier crossing probabilities for multidimensional processes. In this chapter, we discuss some potential future research topics that constitute natural extensions to the findings presented in this thesis.

We have assumed that the underlying process follows a relatively simple multivariate process, such as a Brownian Motion or a Geometric Brownian Motion. Also, when the underlying process is a one-dimensional general diffusion process, an efficient simulation method for computing an exit probability is presented in Baldi and Caramellino (2002). We would like to further develop our method so that we can compute the barrier crossing probability when the underlying process follows a multivariate general diffusion process or a Levy process.

Moreover, in this thesis, we have assumed that the barrier is a constant or linear function of time. We would like to relax this assumption so that the exit boundary

can be a non-linear function of time..

Also, we can develop a method of estimating the distribution of the exit time when the process follows a correlated multivariate Brownian Motion process. As discussed in Section 3.5, this is important in pricing financial derivatives whose values are dependent upon time of barrier crossing.

In Chapter 4, we examined the problem of computing barrier crossing probabilities when the underlying is a sum of Geometric Brownian Motions. In the future we would like to extend this research on two frontiers. First, instead of assuming that the underlying components follow Geometric Brownian Motions, we can assume general diffusion processes or more general jump-diffusion processes. Second, we can also look at an *inverse* problem. In other words, we can compute *dynamic VaR* of a portfolio where *dynamic VaR* is the maximum loss during a given time period at a specified level of confidence as defined by Lamantia and Rossello (2004).

In Section 4.4, we started looking at a portfolio selection problem that considers level crossing of a portfolio during a given time horizon. The potential research topics in this area include finding a coherent risk measure that incorporates the concept of level crossing. Also, we would like to extend the work of Bielski et al. (2005) so that we can relax the assumption of the market completeness and construct an efficient mean-variance portfolio with bankruptcy prohibition.

In this thesis, we have priced relatively simple financial instruments that are dependent on barrier crossing probabilities. We can devise efficient computational

methods of pricing exotic options with American or Asian features with several underlying instruments. The ability to price derivatives efficiently is of increasing importance because the derivative market is rapidly becoming more complex.

Bibliography

Arthurs, A. (1975) *Calculus of Variations*. London: Routledge & Kegan Paul.

Baldi, P. (1995) Exact asymptotics for the probability of exit from a domain and application to simulation. *The Annals of Probability*, **23**, 1644–1670.

— (1997) Large deviations. Manuscripts.

Baldi, P. and Caramellino, L. (2002) Asymptotics of hitting probabilities for general one-dimensional pinned diffusions. *The Annals of Applied Probability*, **12**, 1071–1095.

Baldi, P., Caramellino, L. and Iovino, M. (1999) Pricing general barrier options: A numerical approach using sharp large deviations. *Mathematical Finance*, **9**, 293–321.

Bielski, T., Jin, H., Pliska, S. and Zhou, X. Y. (2005) Continuous-time mean-variance portfolio selection with bankruptcy prohibition. *Mathematical Finance*, **15**, 213–244.

Black, F. and Cox, J. (1976) Valuing corporate securities: Some effects of bond indenture provisions. *Journal of Finance*, 351–367.

Blanchet-Scalliet, C., El Karoui, N., Jeanblanc, M. and Martellini, L. (2005) Dynamic asset pricing theory with uncertain time-horizon. *Journal of Economic Dynamics and Control*, **29**, 1737–1764.

Bouchard, B. and Pham, H. (2004) Wealth-path dependent utility maximization in incomplete markets. *Finance and Stochastics*, 579–603.

Boyle, P., Tian, W. and Feng, S. (2005) Application of large deviations in finance. In *Handbook of Financial Engineering* (eds. V. Linetsky and J. Birge).

Brigo, D., Mercurio, F., Rapisarda, F. and Scotti, R. (2004) Approximated moment-matching for basket-option pricing. *Quantitative Finance*, **4**, 1–16.

Broadie, M., Glasserman, P. and Kou, S. (1997) A continuity correction for discrete barrier options. *Mathematical Finance*, **7**, 325–348.

Dembo, A. and Zeitouni, O. (1993) *Large Deviations Techniques and Applications*. New York: Springer.

Dionne, G., Gauthier, G., Ouertani, N. and Tahani, N. (2006) Heterogenous basket options pricing using analytical approximations.

Djehiche, B. (1993) A large deviation estimate for ruin probabilities. *Scandinavian Actuarial Journal*, **1**, 42–59.

Gardiol, L., Gibson, R., Bares, P., Cont, R. and Gyger, S. (2000) A large deviation approach to portfolio management. *International Journal of Theoretical and Applied Finance*, **3**, 617–639.

Giesecke, K. (2006) Default and information. *Journal of Economic Dynamics and Control*, **30**, 2281–2303.

Giraudo, M. T., Sacedote, L. and Zucca, C. (2001) A monte carlo method for the simulation of first passage time of diffusion processes. *Methodology and Computing in Applied Probability*, **3**, 215–231.

Giraudo, M. T. and Sacerdote, L. (1999) An improved technique for the simulation of first passage times for diffusion processes. *Commun. Statist. Simula.*, **28**, 1135–1163.

He, H., Keirstead, W. P. and Rebholz, J. (1998) Double lookbacks. *Mathematical Finance*, **8**, 201–228.

Hull, J. and White, A. (2001) Valuing credit default swaps ii: Modelling default correlations. *The Journal of Dervatives*, **8**, 12–31.

Karatzas, I. and Shreve, S. (1991) *Brownian Motion and Stochastic Calculus*. New York: Springer, second edn.

Karlin, S. and Taylor, M. (1981) *A Second Course in Stochastic Process*. New York: Academic Press.

Kolkiewicz, A. (2002) Pricing and hedging more general double-barrier options. *Journal of Computational Finance*, **5**, 21–29.

Kou, S. (2002) A jump-diffusion model for option pricing. *Management Science*, **48**, 1086–1101.

Kou, S. and Wang, H. (2004) Option pricing under a double exponential jump diffusion model. *Management Science*, **50**, 1178–1192.

Lamantia, F. and Rossello, D. (2004) The engineering of dynamic var. *Proceedings to the Second IASTED International Conference.*

Laurent, J. and Gregory, J. (2005) Basket default swaps, cdo's, factor copulas. *The Journal of Risk*, **7**.

Leland, H. E. (1994) Risky debt, bond covenants and optimal capital structure. *Journal of Finance*, **49**, 1213–1252.

Leland, H. E. and Toft, K. B. (1996) Optimal capital structure, endogenous bankruptcy and the term structure of credit spreads. *Journal of Finance*, **51**, 987–1019.

Li, X. (1999) The valuation of basket credit derivatives. *CreditMetrics Monitor*, 34–50.

Longstaff, F. A. and Schwartz, E. S. (1995) A simple approach to credit risk of large corporate bond and loan portfolio. *Journal of Finance*, **50**, 789–819.

Markowitz, H. M. (1952) Portfolio selection. *Journal of Finance*, **7**, 77–91.

Merton, R. C. (1974) On the pricing of corporate debt: the risk structure of interest rates. *The Journal of Finance*, **29**, 449–470.

Milevsky, M. A. and Posner, S. E. (1998) Asian options, the sum of lognormals and the reciprocal gamma distribution. *The Journal of Financial and Quantitative Analysis*, **33**, 409–422.

Pham, H. (2003) A large deviation approach to optimal long term investment. *Finance and Stochastics*, **7**, 169–195.

— (2007) Some applications and methods of large deviations in finance and insurance. Manuscript.

Rockafellar, T. R. (1970) *Convex Analysis*. Princeton: Princeton University Press.

Shevchenko, P. (2003) Addressing the bias in monte carlo pricing for multi-asset options with multiple barriers through discrete sampling. *Journal of Computational Finance*, **6**, 1–20.

Shwartz, A. and Weiss, A. (1995) *Large Deviations for Performance Analysis*. Longon: Chapman & Hall.

Stutzer, M. (2003) Portfolio choice with endogenous utility: A large deviations approach. *Journal of Econometrics*, **116**, 365–386.

Thulin, C. (2006) *Pricing and Hedging of Basket Options*. Master's thesis, KTH.

Will, B. (2003) *Valuation of Multi-Name Credit*. Master's thesis, University of Oxford.

Zhou, C. (1997) A jump-diffusion approach to modelling credit risk and valuing defaultable securities. Federal Reserve Board.

— (2001) The term structure of credit spreads with jump risk. *Journal of Banking and Financs*, **25**, 2015–2040.

Appendix A

Proofs of Lemmas

A.1 Proof of Lemma 2.1.3

Let us denote the transformation matrix $K = \begin{bmatrix} k_1 & k_2 \\ k_2 & k_3 \end{bmatrix}$.

Let $\begin{bmatrix} z_1^{'} \\ z_2^{'} \end{bmatrix}$ be a transformed point of $\begin{bmatrix} z_1 \\ z_2 \end{bmatrix}$ such that

$$\begin{bmatrix} z_1^{'} \\ z_2^{'} \end{bmatrix} = \begin{bmatrix} k_1 & k_2 \\ k_2 & k_3 \end{bmatrix} \begin{bmatrix} z_1 \\ z_2 \end{bmatrix}. \tag{A.1}$$

Then, we obtain

$$\begin{bmatrix} k_1 & k_2 \\ k_2 & k_3 \end{bmatrix}^{-1} \begin{bmatrix} z_1^{'} \\ z_2^{'} \end{bmatrix} = \begin{bmatrix} z_1 \\ z_2 \end{bmatrix} \tag{A.2}$$

$$\frac{1}{k_1k_3 - k_2^2}\begin{bmatrix} k_3 & -k_2 \\ -k_2 & k_1 \end{bmatrix}\begin{bmatrix} z_1^{'} \\ z_2^{'} \end{bmatrix} = \begin{bmatrix} z_1 \\ z_2 \end{bmatrix} \tag{A.3}$$

$$\left[\frac{k_3z_1^{'} - k_2z_2^{'}}{k_1k_3 - k_2^2}, \frac{-k_2z_1^{'} + k_1z_2^{'}}{k_1k_3 - k_2^2}\right]^T = [z_1, z_2]^T. \tag{A.4}$$

We substitute (A.4) into $a_1z_1 + a_2z_2 = c$ which gives the following equation

$$a_1\left[\frac{k_3z_1^{'} - k_2z_2^{'}}{k_1k_3 - k_2^2}\right] + a_2\left[\frac{-k_2z_1^{'} + k_1z_2^{'}}{k_1k_3 - k_2^2}\right] = c \tag{A.5}$$

or equivalently

$$\begin{aligned} &a_1k_3z_1^{'} - a_1k_2z_2^{'} - a_2k_2z_1^{'} + a_2k_1z_2^{'} = c(k_1k_3 - k_2^2) \\ &(a_1k_3 - a_2k_2)z_1^{'} + (a_2k_1 - a_1k_2)z_2^{'} = c(k_1k_3 - k_2^2). \end{aligned} \tag{A.6}$$

Therefore, we obtain a new equation of line $a_1^{'}z_1 + a_2^{'}z_2 = c^{'}$, where $a_1^{'} = a_1k_3 - a_2k_2$, $a_2^{'} = a_2k_1 - a_1k_2$, and $c^{'} = c(k_1k_3 - k_2^2)$. $\square$

A.2 Proof of Lemma 2.1.4

We compute $y^{'}$ that is a mirrored point of y around the linear line B, which is represented as $a_1z_1 + a_2z_2 = c$. The point $y^{'} = (y_1^{'}, y_2^{'})$ can be obtained by solving the following system of equations:

$$a_1 = k(y_1^{'} - y_1) \tag{A.7}$$

$$a_2 = k(y_2^{'} - y_2) \tag{A.8}$$

$$a_1(\frac{y_1^{'} + y_1}{2}) + a_2(\frac{y_2^{'} + y_2}{2}) = c. \tag{A.9}$$

The first two equations, (A.7) and (A.8), impose the condition that the straight line connecting y and $y^{'}$ should be parallel to the projection vector (a_1, a_2). This condition is equivalent to that the straight line from y to $y^{'}$ is perpendicular to the line B. The third equation (A.9) imposes the condition that the point of the intersection of the line between y and $y^{'}$ and the line B should be equidistant to y and $y^{'}$. Solving this system of equations for the unknowns a_1, a_2, and k using $Maple^{TM}$, we obtain the following solution,

$$y_1^{'} = -\frac{a_1^2 y_1 - a_2^2 y_1 + 2a_1 a_2 y_2 - 2a_1 c}{a_1^2 + a_2^2} \tag{A.10}$$

$$y_2^{'} = -\frac{-a_1^2 y_2 + a_2^2 y_2 + 2a_1 a_2 y_1 - 2a_2 c}{a_1^2 + a_2^2}. \tag{A.11}$$

□

A.3 Solution to Optimization Problem from Section 2.1.3

We would like to find t_1^* and t_2^* that minimize the following objective function,

$$\frac{1}{2}\{\frac{\|x-\phi_1\|^2}{t_1-s} + \frac{\|\phi_1-\phi_2\|^2}{t_2-t_1} + \frac{\|y-\phi_2\|^2}{1-t_2} + \frac{\|x-y\|^2}{1-s}\}. \tag{A.12}$$

Since the fourth term in the objective function does not involve neither t_1 nor t_2, the problem is equivalent to finding t_1^* and t_2^* that minimize

$$\{\frac{\|x-\phi_1\|^2}{t_1-s} + \frac{\|\phi_1-\phi_2\|^2}{t_2-t_1} + \frac{\|y-\phi_2\|^2}{1-t_2}\}. \tag{A.13}$$

Hence, more formally, we want to minimize $\{\frac{\|x-\phi_1\|^2}{t_1-s} + \frac{\|\phi_1-\phi_2\|^2}{t_2-t_1} + \frac{\|y-\phi_2\|^2}{1-t_2}\}$ with respect to t_1 and t_2 subject to the constraint $(t_1 - s) + (t_2 - t_1) + (1 - t_2) = 1 - s$.

By setting $u = \|x - \phi_1\|$, $v = \|\phi_1 - \phi_2\|$, $w = \|y - \phi_2\|$, $a = t_1 - s$, $b = t_2 - t_1$, and $c = 1 - t_2$, we have the following problem. We want to minimize

$$\frac{u^2}{a} + \frac{v^2}{b} + \frac{w^2}{c} \tag{A.14}$$

with the constraint that $a + b + c = 1 - s$.

Now we can set up a Lagrange equation,

$$F = \frac{u^2}{a} + \frac{v^2}{b} + \frac{w^2}{c} - \lambda(1 - s - a - b - c). \tag{A.15}$$

The first-order conditions are

$$\frac{\partial F}{\partial a} = -\frac{u^2}{a^2} + \lambda = 0 \tag{A.16}$$

$$\frac{\partial F}{\partial b} = -\frac{v^2}{b^2} + \lambda = 0 \tag{A.17}$$

$$\frac{\partial F}{\partial c} = -\frac{w^2}{c^2} + \lambda = 0 \tag{A.18}$$

$$\frac{\partial F}{\partial \lambda} = a + b + c - 1 + s = 0. \tag{A.19}$$

These first order conditions give us

$$\frac{u}{a} = \frac{v}{b} = \frac{w}{c} \text{ and } a + b + c = 1 - s. \tag{A.20}$$

From these, we get

$$a = (1 - s)\frac{u}{u + v + w},\ b = (1 - s)\frac{v}{u + v + w},\ \text{and } c = (1 - s)\frac{w}{u + v + w}. \tag{A.21}$$

By substituting back the values of u, v, w, a, b, and c, we obtain

$$t_1 - s = (1-s)\frac{\|x-\phi_1\|}{\|x-\phi_1\| + \|\phi_1-\phi_2\| + \|y-\phi_2\|} \tag{A.22}$$

$$t_2 - t_1 = (1-s)\frac{\|\phi_1-\phi_2\|}{\|x-\phi_1\| + \|\phi_1-\phi_2\| + \|y-\phi_2\|} \tag{A.23}$$

$$1 - t_2 = (1-s)\frac{\|y-\phi_2\|}{\|x-\phi_1\| + \|\phi_1-\phi_2\| + \|y-\phi_2\|}. \tag{A.24}$$

By rearranging (A.22) and (A.23), we get the following optimal values for t_1 and t_2,

$$t_1^* = s + (1-s)\frac{\|x-\phi_1\|}{\|x-\phi_1\| + \|\phi_1-\phi_2\| + \|y-\phi_2\|} \tag{A.25}$$

$$t_2^* = s + (1-s)\frac{\|\phi_1-\phi_2\| + \|x-\phi_1\|}{\|x-\phi_1\| + \|\phi_1-\phi_2\| + \|y-\phi_2\|}. \tag{A.26}$$

□

Appendix B

Brownian Motion Conditioned on its State at Time 1

In this section, we provide a brief discussion on conditional diffusion processes. We also apply this concept to a Brownian Motion, so that we can obtain a diffusion process for the Brownian Motion with its value fixed at time 1. Most of the presented results are taken from Section 9.2 of Karlin and Taylor (1981).

Let us consider a regular diffusion process $\{X(t), 0 \leq t \leq 1\}$ with infinitesimal mean $\mu(x)$ and volatility $\sigma(x)$. Also, let $\{X^*(t), 0 \leq t \leq 1\}$ be the same process as $\{X(t), 0 \leq t \leq 1\}$, but confined to the sample paths with $\alpha < X(1) < \beta$. It turns out that X^* also follows a diffusion process with new infinitesimal mean $\mu^*(x)$ and variance $\sigma^*(x)$.

Now consider a constrained Brownian Motion with the condition that

$$\alpha < X(1) < \beta. \tag{B.1}$$

Then the relationships between parameters of regular diffusion process and parameters of conditioned diffusion process are given as follows,

$$\mu^*(x,t) = \mu(x) + \frac{\partial\pi(x,t)/\partial x}{\pi(x,t)}\sigma^2(x) \tag{B.2}$$

$$\sigma^*(x,t) = \sigma(x) \tag{B.3}$$

where $\pi(x,t)$ is the probability that from the initial state value x on the sample path satisfies (B.1) at time 1. This constrained Brownian Motion is also referred to as a Brownian Bridge. We compute $\mu^*(x)$ and $\sigma^*(x)$ under two cases: (1) assuming that the drift term is 0 in the original Brownian Motion (2) assuming a non-zero drift.

B.1 $\mu^*(x)$ and $\sigma^*(x)$ with Zero Drift Assumption

We have

$$\pi(x,t) = \int_\alpha^\beta \frac{1}{\sqrt{2\pi(1-t)}\sigma} e^{(y-x)^2/2(1-t)\sigma^2} dy \tag{B.4}$$

$$\frac{\partial\pi(x,t)}{\partial x} = \int_\alpha^\beta \frac{1}{\sqrt{2\pi(1-t)}\sigma} e^{(y-x)^2/2(1-t)\sigma^2} \left(\frac{2(y-x)}{2(1-t)\sigma^2}\right) dy \tag{B.5}$$

$$\frac{\partial\pi(x,t)/\partial x}{\pi(x,t)} = \frac{\int_\alpha^\beta \frac{1}{\sqrt{2\pi(1-t)}\sigma} e^{(y-x)^2/2(1-t)\sigma^2} \frac{y-x}{(1-t)\sigma^2} dy}{\int_\alpha^\beta \frac{1}{\sqrt{2\pi(1-t)}\sigma} e^{(y-x)^2/2(1-t)\sigma^2} dy}. \tag{B.6}$$

Suppose that we want to condition on $X(1) = a$. We set $\alpha = a - \epsilon$ and $\beta = a + \epsilon$. By letting $\epsilon \to 0$, we get

$$\frac{\partial\pi(x,t)/\partial x}{\pi(x,t)} = \lim_{\epsilon\to 0}\frac{\int_{a-\epsilon}^{a+\epsilon} e^{(y-x)^2/2(1-t)\sigma^2}\frac{y-x}{(1-t)\sigma^2}dy}{\int_{a-\epsilon}^{a+\epsilon} e^{(y-x)^2/2(1-t)\sigma^2}dy}. \tag{B.7}$$

We apply the change of variable technique by letting $r = y - a$. Then we have

$$\frac{\partial\pi(x,t)/\partial x}{\pi(x,t)} = \lim_{\epsilon\to 0}\frac{\int_{-\epsilon}^{\epsilon} e^{(r+a-x)^2/2(1-t)\sigma^2}\frac{r+a-x}{(1-t)\sigma^2}dr}{\int_{-\epsilon}^{\epsilon} e^{(r+a-x)^2/2(1-t)\sigma^2}dr}. \tag{B.8}$$

Since both the numerator and denominator of the right hand side of (B.8) approach 0 as we take the limit of ϵ, l'Hôpital's rule give us

$$\frac{\partial\pi(x,t)/\partial x}{\pi(x,t)} = \lim_{\epsilon\to 0}\frac{e^{(\epsilon+a-x)^2/2(1-t)\sigma^2}\frac{\epsilon+a-x}{(1-t)\sigma^2} + e^{(-\epsilon+a-x)^2/2(1-t)\sigma^2}\frac{-\epsilon+a-x}{(1-t)\sigma^2}}{e^{(\epsilon+a-x)^2/2(1-t)\sigma^2} + e^{(-\epsilon+a-x)^2/2(1-t)\sigma^2}}. \tag{B.9}$$

Now, by taking a limit, we obtain

$$\begin{aligned}\frac{\partial\pi(x,t)/\partial x}{\pi(x,t)} &= \frac{e^{(a-x)^2/2(1-t)\sigma^2}\frac{a-x}{(1-t)\sigma^2}}{e^{(a-x)^2/2(1-t)\sigma^2}} &\text{(B.10)}\\ &= \frac{a-x}{(1-t)\sigma^2}. &\text{(B.11)}\end{aligned}$$

Now, by using (B.2) and (B.3), we obtain the following parameters for the conditioned process,

$$\begin{aligned}u^*(x,t) &= 0 + \frac{a-x}{(1-t)\sigma^2}\sigma^2\\ &= \frac{a-x}{1-t} &\text{(B.12)}\\ \sigma^*(x,t) &= \sigma. &\text{(B.13)}\end{aligned}$$

B.2 $\mu^*(x)$ and $\sigma^*(x)$ with Non-Zero Drift Assumption

We assume that we have a non-zero drift term of the original Brownian Motion given by $\mu(x,t) = \mu$. Then we get

$$\pi(x,t) = \int_\alpha^\beta \frac{1}{\sqrt{2\pi(1-t)}\sigma} e^{(y-(x+\mu(1-t))^2/2(1-t)\sigma^2} dy \tag{B.14}$$

$$\frac{\partial \pi(x,t)}{\partial x} = \int_\alpha^\beta \frac{1}{\sqrt{2\pi(1-t)}\sigma} e^{(y-(x+\mu(1-t))^2/2(1-t)\sigma^2} \frac{2(y-(x+\mu(1-t))}{2(1-t)\sigma^2} dy \tag{B.15}$$

$$\frac{\partial \pi(x,t)/\partial x}{\pi(x,t)} = \frac{\int_\alpha^\beta \frac{1}{\sqrt{2\pi(1-t)}\sigma} e^{(y-(x+\mu(1-t))^2/2(1-t)\sigma^2} \frac{2(y-(x+\mu(1-t))}{2(1-t)\sigma^2} dy}{\int_\alpha^\beta \frac{1}{\sqrt{2\pi(1-t)}\sigma} e^{(y-(x+\mu(1-t))^2/2(1-t)\sigma^2} dy}. \tag{B.16}$$

Suppose that we want to condition on $X(1) = a$. We set $\alpha = a - \epsilon$ and $\beta = a + \epsilon$. Letting $\epsilon \to 0$, we have

$$\frac{\partial \pi(x,t)/\partial x}{\pi(x,t)} = \lim_{\epsilon \to 0} \frac{\int_{a-\epsilon}^{a+\epsilon} e^{(y-(x+\mu(1-t))^2/2(1-t)\sigma^2} \frac{y-(x+\mu(1-t))}{(1-t)\sigma^2} dy}{\int_{a-\epsilon}^{a+\epsilon} e^{(y-(x+\mu(1-t)))^2/2(1-t)\sigma^2} dy}. \tag{B.17}$$

By going through the same arguments in (B.8)-(B.11), we obtain

$$\frac{\partial \pi(x,t)/\partial x}{\pi(x,t)} = \frac{a-(x+\mu(1-t))}{(1-t)\sigma^2}. \tag{B.18}$$

Now, by using (B.2) and (B.3), we obtain the following parameters for the conditioned process:

$$\begin{aligned} u^*(x,t) &= \mu + \frac{a-(x+\mu(1-t))}{(1-t)\sigma^2}\sigma^2 \\ &= \frac{\mu-\mu t+a-x-\mu+\mu t}{1-t} \\ &= \frac{a-x}{1-t} \qquad \text{(B.19)} \\ \sigma^*(x,t) &= \sigma. \qquad \text{(B.20)} \end{aligned}$$

(B.19) and (B.20) are identical to (B.12) and (B.13), indicating that the drift term does not play any role in determining the parameters of the Brownian Bridge process.

In this section, we have shown the relationship between the instantaneous parameters of Brownian Motion and those of Brownian Bridge for one-dimension process. For the multi-dimensional process, similar results are easily obtained by using the same procedures with vectors and matrices.

In particular, in this thesis, when we have a multivariate process, we perform a transformation so that the process becomes an uncorrelated multidimensional process. Hence, we can apply the results of Sections B.1 and B.2 to each component of the multidimensional process.

Suppose that we have a two-dimensional independent Brownian Motion process with drift terms μ_i's and volatility terms σ_i's for $i = 1, 2$. Hence, by (B.19) and

(B.20), for the conditioned process with $X_i(1) = a_i$ for $i = 1, 2$, we have the following parameters for each component

$$u_i^*(x,t) = \frac{a_i - x_i}{1-t} \tag{B.21}$$

$$\sigma_i^*(x,t) = \sigma_i, \tag{B.22}$$

where $i = 1, 2$.

Appendix C

Proof of Expressions (2.66) and (2.67)

In order to make this section self-contained, let us re-state the result that we want to prove here.

Let us consider the case where $a_{r_1}p_1 + a_{r_2}p_2 < 1$. This is the situation where the line connecting $x^{'}_{B_1}$ and $y^{'}_{B_2}$ does not cross neither barriers B_1 nor B_2. In this case,

$$\min_{\epsilon_1 \in B_1, \epsilon_2 \in B_2} [\|x - \epsilon_1\| + \|\epsilon_2 - \epsilon_1\| + \|y - \epsilon_2\|] \tag{C.1}$$

$$= \begin{cases} \min_{\epsilon \in B_1}[\|x - \epsilon\| + \|y - \epsilon\|] & , \quad \text{if path x-}\epsilon^*\text{-y crosses line } B_2 \\ \min_{\epsilon \in B_2}[\|x - \epsilon\| + \|y - \epsilon\|] & , \quad \text{if path x-}\epsilon^*\text{-y crosses line } B_1 \\ \|x - p\| + \|y - p\| & , \quad \text{otherwise} \end{cases} \tag{C.2}$$

$$= \begin{cases} \|x^{'}_{B_1} - y\| & , \quad \text{if path x-}\epsilon^*\text{-y crosses line } B_2 \\ \|x - y^{'}_{B_2}\| & , \quad \text{if path x-}\epsilon^*\text{-y crosses line } B_1 \\ \|x - p\| + \|y - p\| & , \quad \text{otherwise} \end{cases} \tag{C.3}$$

where all the notations are defined in the same way as in Section 2.1.3.

The solutions of this optimization problem consist of three cases. The first two cases are relatively easy to prove, but the third case is more involved. In the first case, consider a path x-ϵ_1^*-y. This is the shortest path that starts at x, touches a point along line B_1, and ends at y. If this path happens to cross the line B_2, this path is the shortest path that touches both B_1 and B_2. Since no other path that starts at x, touches B_1 and ends at y is shorter than x-ϵ_1^*-y, there is no other path that starts at x, touches both B_1 and B_2 and ends at y can be shorter than x-ϵ_1^*-y.

In the second case, basically the same argument as in the first one can be used. In this case, we have a path x-ϵ_2^*-y, which starts at x, touches a point along B_2, and ends at y. If this particular path happens to cross B_1, x-ϵ_2^*-y would be the shortest path that touches both B_1 and B_2.

In the third case, we know that the path x-ϵ_1^*-y does not cross B_2 nor x-ϵ_2^*-y cross B_1 neither. Refer to Figure C.1 for this discussion. Without a loss of generality, we assume that the point x is located near B_1 and the point y near B_2, depicted as in the figure. Now let us compare the paths x-ϵ_1^*-y, x-p-y, and x-$q_1^{'}$-y. These paths all start at x, touch a point along B_1 and ends at y. Since p is located closer to ϵ_1^* than $q_1^{'}$ to ϵ_1^*, the length of x-p-y is shorter than that of x-$q_1^{'}$-y. Notice that both x-p-y and x-$q_1^{'}$-y touch both line B_1 and B_2. Hence x-$q_1^{'}$-y, where $q_1^{'}$ is any point along B_1 to the right to the point p, can not be the minimizing path that touches both B_1 and B_2. By a similar argument, we can also show that x-$q_2^{'}$-y, where $q_2^{'}$ is any point along B_2 to the left to the point p, can not be the minimizing path that

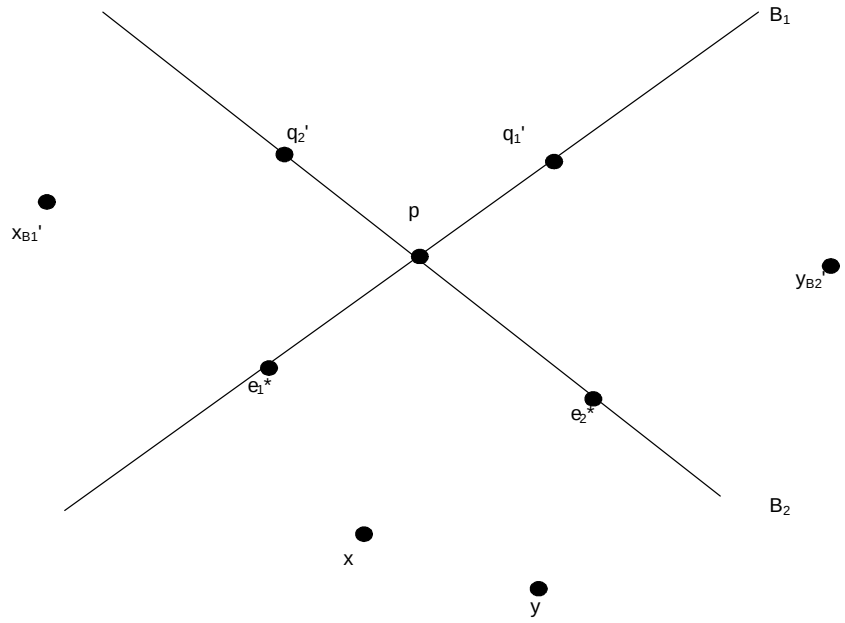

Figure C.1: Finding a length minimizing path

touches both B_1 and B_2.

In the last paragraph, we have shown that we can exclude a certain portion of B_1 and B_2. The portion that we can exclude is denoted as a dotted line in Figure C.2. Hence, as shown in Figure C.2, the solid lines of B_1 and B_2 are a set of points we need to consider to find an optimal trajectory that minimizes its length. x'_{B_1} is a mirrored point of x around B_1, and similarly, y'_{B_2} is a mirrored point of y around B_2.

Recall that $a_{r_1}p_1 + a_{r_2}p_2 < 1$, where $p = [p_1, p_2]^T$ is the point of the intersection of B_1 and B_2, and a_{p_1} and a_{p_2} are defined in such a way that $a_{p_1}z_1 + a_{p_2}z_2 = 1$ is the equation of the line connecting x'_{B_1} and y'_{B_2}. This is the situation where the

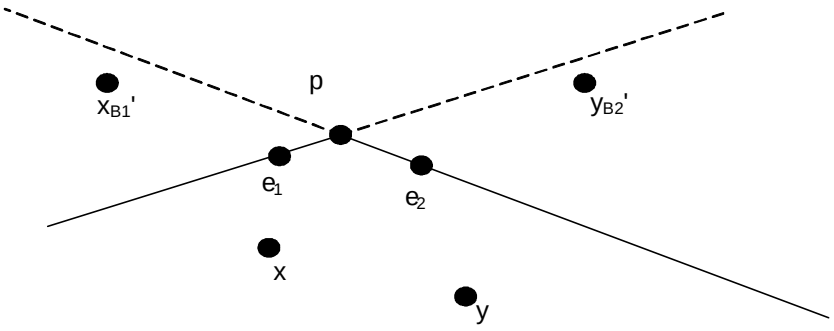

Figure C.2: Finding a length minimizing path

line connecting x'_{B_1} and y'_{B_2} does not cross neither barriers B_1 nor B_2, as shown in Figure C.2.

We want to find the shortest path that starts at x, touches both B_1 and B_2, and ends at y. This is equivalent to finding the shortest path that starts at x'_{B_1}, touches both B_1 and B_2, and ends at y'_{B_2}. In Figure C.2, ϵ_1 is any point along B_1 that is left of p, and ϵ_2 is any point along B_2 that is right of p. Then we can easily see that any possible path x'_{B_1}-ϵ_1-ϵ_2-y'_{B_2} cannot be shorter than the path x'_{B_1}-p-y'_{B_2}. Therefore, under the third case, x-p-y is the shortest path that starts at x, touches both B_1 and B_2, and ends at y. $\square$

Appendix D

Results of Numerical Study

In this section, we show the tables which contain the results of "Detailed Numerical Study 1" in Section 2.3.2.

Table D.1: LDT Approximations Case 1

	True Value	LDT	Difference	Relative Error	Baldi's
$T = 0.25$					
VCV1	0.028118	0.025756	-0.002362	0.084003	0.025646
VCV2	0.031223	0.029445	-0.001778	0.056945	0.025646
VCV3	0.032199	0.031284	-0.000915	0.028417	0.025646
VCV4	0.032624	0.032138	-0.000486	0.014897	0.025646
VCV5	0.033115	0.0033073	-4.2E-05	0.001268	0.025646
VCV6	0.033172	0.033165	-7E-06	0.000211	0.025646
VCV7	0.033196	0.033202	6E-06	0.000181	0.025646
VCV8	0.033238	0.033259	2.1E-05	0.000632	0.025646
VCV9	0.03335	0.033364	1.4E-05	0.00042	0.025646
VCV10	0.033369	0.033375	6E-06	0.00018	0.025646
VCV11	0.033379	0.033381	2E-06	5.99E-05	0.025646
VCV12	0.033382	0.033383	1E-06	3E-05	0.025646
VCV13	0.033184	0.033184	0	0	0.025646
$T = 0.5$					
VCV1	0.18136	0.16077	-0.02059	0.113531	0.16014
VCV2	0.20662	0.18535	-0.02127	0.102943	0.16014
VCV3	0.21708	0.20229	-0.01479	0.068132	0.16014
VCV4	0.22284	0.21282	-0.01002	0.044965	0.16014
VCV5	0.23211	0.23049	-0.00162	0.006979	0.16014
VCV6	0.23365	0.23334	-0.00031	0.001327	0.16014
VCV7	0.23438	0.23466	0.00028	0.001195	0.16014
VCV8	0.23577	0.23697	0.0012	0.000509	0.16014
VCV9	0.24138	0.24376	0.00238	0.00986	0.16014
VCV10	0.24339	0.24539	0.002	0.008217	0.16014
VCV11	0.24554	0.24676	0.00122	0.004969	0.16014
VCV12	0.24728	0.24769	0.00041	0.001658	0.16014
VCV13	0.23402	0.23402	0	0	0.16014
$x = [0.784, 0.778]^T$, $y = [0.788, 0.781]^T$, $B = [1, 1]^T$					

Table D.2: LDT Approximations Case 1 Continued

	True Value	LDT	Difference	Relative Error	Baldi's
$T = 0.75$					
VCV1	0.33439	0.29584	-0.03855	0.115285	0.299
VCV2	0.37865	0.33477	-0.04388	0.115885	0.299
VCV3	0.39824	0.36465	-0.03359	0.084346	0.299
VCV4	0.40969	0.3851	-0.02459	0.060021	0.299
VCV5	0.42981	0.42499.	-0.00482	0.011214	0.299
VCV6	0.43346	0.43251	-0.00095	0.002192	0.299
VCV7	0.43524	0.43616	0.00092	0.002114	0.299
VCV8	0.43873	0.44283	0.0041	0.009345	0.299
VCV9	0.45457	0.46606	0.01149	0.025277	0.299
VCV10	0.46151	0.47323	0.01172	0.025395	0.299
VCV11	0.47062	0.48053	0.00991	0.021057	0.299
VCV12	0.48174	0.48714	0.0054	0.011209	0.299
VCV13	0.43435	0.43435	0	0	0.299
$T = 1$					
VCV1	0.45137	0.40124	-0.05013	0.111062	0.40018
VCV2	0.50588	0.44625	-0.05963	0.117874	0.40018
VCV3	0.53051	0.48273	-0.04778	0.090064	0.40018
VCV4	0.5452	0.50891	-0.03629	0.066563	0.40018
VCV5	0.57185	0.56405	-0.0078	0.01364	0.40018
VCV6	0.57684	0.57527	-0.00157	0.002722	0.40018
VCV7	0.5793	0.58083	0.00153	0.002641	0.40018
VCV8	0.58416	0.59125	0.00709	0.012137	0.40018
VCV9	0.6073	0.63086	0.02356	0.038795	0.40018
VCV10	0.61824	0.64467	0.02643	0.04275	0.40018
VCV11	0.6339	0.66016	0.02626	0.041426	0.40018
VCV12	0.65731	0.67644	0.01913	0.029103	0.40018
VCV13	0.57807	0.57807	0	0	0.40018
$x = [0.784, 0.778]^T$, $y = [0.788, 0.781]^T$, $B = [1, 1]^T$					

Table D.3: LDT Approximation Case 2

	True Value	LDT	Difference	Relative Error	Baldi's
$T = 0.25$					
VCV1	0.061071	0.055434	-0.005637	0.092302	0.055279
VCV2	0.068578	0.063575	-0.005003	0.072953	0.055279
VCV3	0.071255	0.068333	-0.002922	0.041008	0.055279
VCV4	0.07255	0.070829	-0.001721	0.023722	0.055279
VCV5	0.074273	0.074079	-0.000194	0.002612	0.055279
VCV6	0.074506	0.074473	-3.3E-05	0.000443	0.055279
VCV7	0.074611	0.07464	2.9E-0.5	0.000389	0.055279
VCV8	0.0748	0.074908	0.000108	0.001444	0.055279
VCV9	0.075395	0.07551	0.000115	0.001525	0.055279
VCV10	0.075535	0.075603	6.8E-05	0.0009	0.055279
VCV11	0.075635	0.07566	2.5E-05	0.000331	0.055279
VCV12	0.07568	0.075683	3E-06	3.96E-05	0.055279
VCV13	0.074559	0.074559	0	0	0.055279
$T = 0.5$					
VCV1	0.26538	0.23566	-0.02972	0.11199	0.23512
VCV2	0.30129	0.26791	-0.03338	0.11079	0.23512
VCV3	0.31689	0.29222	-0.02467	0.07785	0.23512
VCV4	0.32583	0.30827	-0.01756	0.053893	0.23512
VCV5	0.34106	0.33786	-0.0032	0.009383	0.23512
VCV6	0.34373	0.34312	-0.00061	0.001775	0.23512
VCV7	0.34503	0.34561	0.00058	0.001681	0.23512
VCV8	0.34754	0.35006	0.00252	0.007251	0.23512
VCV9	0.35846	0.36466	0.0062	0.017296	0.23512
VCV10	0.36292	0.36878	0.00586	0.016147	0.23512
VCV11	0.36833	0.37269	0.00436	0.011837	0.23512
VCV12	0.39396	0.39588	0.00192	0.004874	0.23512
VCV13	0.34439	0.34439	0	0	0.23512
$x = [0.884, 0.878]^T$, $y = [0.688, 0.681]^T$, $B = [1, 1]^T$					

Table D.4: LDT Approximations Case 2 Continued

	True Value	LDT	Difference	Relative Error	Baldi's
$T = 1$					
VCV1	0.5414	0.4856	-0.0558	0.103066	0.48489
VCV2	0.60024	0.5311	-0.06914	0.115187	0.48489
VCV3	0.62699	0.57001	-0.05698	0.090879	0.48489
VCV4	0.64308	0.59884	-0.044236	0.068788	0.48489
VCV5	0.67259	0.66258	-0.01001	0.014883	0.48489
VCV6	0.67819	0.67617	-0.00202	0.002979	0.48489
VCV7	0.68097	0.68294	0.00197	0.002893	0.48489
VCV8	0.68646	0.69578	0.00932	0.013577	0.48489
VCV9	0.71317	0.74745	0.03428	0.048067	0.48489
VCV10	0.72613	0.76694	0.04081	0.056202	0.48489
VCV11	0.74550	0.79019	0.04469	0.059945	0.48489
VCV12	0.77769	0.81710	0.03941	0.050679	0.48489
VCV13	0.67958	0.67958	0	0	0.48489
$x = [0.884, 0.878]^T$, $y = [0.688, 0.681]^T$, $B = [1, 1]^T$					

Table D.5: LDT Approximations Case 3

	True Value	LDT	Difference	Relative Error	Baldi's
$T = 0.25$					
VCV1	0.91365	0.88891	-0.02474	0.027078	0.88891
VCV2	0.94201	0.89358	-0.04843	0.051411	0.88891
VCV3	0.95407	0.90889	-0.04518	0.047352	0.88891
VCV4	0.96091	0.92346	-0.03745	0.039873	0.88891
VCV5	0.97248	0.96345	-0.00903	0.009286	0.88891
VCV6	0.97452	0.97272	-0.0018	0.001847	0.88891
VCV7	0.9755	0.9773	0.0018	0.001845	0.88891
VCV8	0.97741	0.98638	0.00897	0.009177	0.88891
VCV9	0.98584	1	0.01416	0.014363	0.88891
VCV10	0.98938	1	0.01062	0.010734	0.88891
VCV11	0.99387	1	0.00613	0.006168	0.88891
VCV12	0.99891	1	0.00109	0.001091	0.88891
VCV13	0.97501	0.97501	0	0	0.88891
$T = 0.5$					
VCV1	0.96100	0.94282	-0.01818	0.018918	0.94282
VCV2	0.97747	0.94548	-0.03199	0.032727	0.94282
VCV3	0.98371	0.95425	-0.02946	0.029948	0.94282
VCV4	0.98702	0.96266	-0.02436	0.02468	0.94282
VCV5	0.99214	0.98623	-0.00591	0.005957	0.94282
VCV6	0.99296	0.99178	-0.00118	0.001188	0.94282
VCV7	0.99335	0.99454	0.00119	0.001198	0.94282
VCV8	0.9941	1	0.0059	0.005935	0.94282
VCV9	0.99705	1	0.00295	0.002959	0.94282
VCV10	0.99810	1	0.0019	0.001904	0.94282
VCV11	0.99919	1	0.00081	0.000811	0.94282
VCV12	1	1	0	0	0.94282
VCV13	0.99316	0.99316	0	0	0.94282
$x = [0.954, 0.948]^T$, $y = [0.968, 0.951]^T$, $B = [1, 1]^T$					

Table D.6: LDT Approximations Case 3 Continued

	True Value	LDT	Difference	Relative Error	Baldi's
$T = 1$					
VCV1	0.98284	0.97099	-0.01185	0.012057	0.97099
VCV2	0.99151	0.97241	-0.0191	0.019264	0.97099
VCV3	0.99441	0.97710	-0.01731	0.017407	0.97099
VCV4	0.99584	0.98162	-0.01422	0.014279	0.97099
VCV5	0.99785	0.99441	-0.00344	0.003447	0.97099
VCV6	0.99814	0.99745	-0.00069	0.000691	0.97099
VCV7	0.99828	0.99897	0.00069	0.000691	0.97099
VCV8	0.99853	1	0.00147	0.001472	0.97099
VCV9	0.99942	1	0.00058	0.00058	0.97099
VCV10	0.99968	1	0.00032	0.00032	0.97099
VCV11	0.99990	1	1E-04	0.0001	0.97099
VCV12	1	1	0	0	0.97099
VCV13	0.99821	0.67958	0	0	0.97099
$x = [0.954, 0.948]^T$, $y = [0.968, 0.951]^T$, $B = [1, 1]^T$					

Table D.7: Result of Numerical Study 4

	True Value	LDT	Difference	Relative Error	Baldi's
$T = 0.5$					
VCV1	0.010835	0.010134	-0.000701	0.064698	0.010103
VCV2	0.011777	0.011322	-0.000455	0.038635	0.010103
VCV3	0.012031	0.011831	-0.0002	0.016624	0.010103
VCV4	0.012128	0.012034	-9.4E-05	0.007751	0.010103
VCV5	0.012221	0.012215	-6E-06	0.000491	0.010103
VCV6	0.012230	0.012229	-1E-06	8.18E-05	0.010103
VCV7	0.012233	0.012339	0.000106	0.008665	0.010103
VCV8	0.012239	0.012241	2.1E-06	0.000172	0.010103
VCV9	0.012251	0.012252	1E-06	8.16E-05	0.010103
VCV10	0.012253	0.012253	0	0	0.010103
VCV11	0.012253	0.012253	0	0	0.010103
VCV12	0.012253	0.012253	0	0	0.010103
VCV13	0.012231	0.012231	0	0	0.010103
$T = 1$					
VCV1	0.11266	0.10085	-0.01181	0.10486	0.10052
VCV2	0.12781	0.11636	-0.01145	0.089586	0.10052
VCV3	0.13371	0.12633	-0.00738	0.055194	0.10052
VCV4	0.13679	0.13208	-0.00471	0.034432	0.10052
VCV5	0.14136	0.14071	-0.00065	0.004598	0.10052
VCV6	0.14206	0.14194	-0.000117	0.000824	0.10052
VCV7	0.14238	0.14285	0.00047	0.003301	0.10052
VCV8	0.14298	0.1434	0.00042	0.002937	0.10052
VCV9	0.14517	0.1458	0.00063	0.00434	0.10052
VCV10	0.14583	0.14628	0.00045	0.003086	0.10052
VCV11	0.14641	0.14663	0.00022	0.001503	0.10052
VCV12	0.14677	0.14682	5E-05	0.000341	0.10052
VCV13	0.14222	0.14222	0	0	0.10052
$x = [0.654, 0.648]^T$, $y = [0.668, 0.651]^T$, $B = [1, 1]^T$					

Appendix E

Computing the Barrier Crossing Probability by Simulation

In Section 3.1.1, we have described an algorithm for computing a barrier crossing probability by simulation, which uses the Large Deviations method. Particularly, in the case where we take a single step for simulating the terminal value of the underlying variable, we have described the six step method for approximating the barrier crossing probability. In this section, we formally justify our approach in Section 3.1.1 using probability theory.

We define the following events:

$$\begin{aligned} A &= \{\text{At least one barrier is breached within the time horizon 1.}\} \\ A_1 &= \{\text{The value at time 1 of at least one component is below the barrier.}\} \\ A_2 &= \bar{A_1} \cap A. \end{aligned}$$

The ultimate goal of the algorithm in Section 3.1.1 is to compute $P(A)$, which can be represented in the following way,

$$\begin{aligned} P(A) &= E(I_A) \\ &= E(I_{A_1} + I_{A_2}) \\ &= E(I_{A_1}) + E(I_{A_2}) \\ &= P(A_1) + P(A_2) \\ &= P(A_1) + P(\bar{A}_1 \cap A), \end{aligned} \tag{E.1}$$

where I is an indicator variable.

In this section, we describe how to obtain an approximation for $P(A)$ using simulations. For the underlying variable, we generate N observations of its terminal value and denote them as $x^1, x^2, \ldots, x^N$. Let s be the number of paths where the terminal value of at least one component is lower than its corresponding barrier. By the Law of Large Numbers, we have

$$P(A_1) \approx \frac{s}{N}. \tag{E.2}$$

We also have

$$P(\bar{A}_1 \cap A) = E(I_{\bar{A}_1} I_A).$$

From the N simulations above, we can also obtain the simulated values of $I_{\bar{A}_1}$. Let p_i be the specific instance of $I_{\bar{A}_1}$ in the i^{th} simulation.

Hence, the following approximation can be obtained. Let X be a vector of terminal values of all components. We have

$$\begin{aligned} P(\bar{A}_1 \cap A) &= E[E[I_A I_{\bar{A}_1}|X]] \\ &= E[I_{\bar{A}_1} E[I_A|X]] \\ &= \int_{x\text{: all components above the barrier}} P(A|X=x) dP_x(x) \\ &\approx \sum_{i|p_i=1} \frac{P(A|x^i)}{N}. \end{aligned} \tag{E.3}$$

We note that $P(A|x^i)$ is the barrier crossing probability for the stochastic process with a fixed terminal value of x^i. We can approximate this quantity using Large Deviations Theory. Now, combining (E.1), (E.2), and (E.3), we obtain the following expression that approximates the barrier crossing probability, $P(A)$,

$$P(A) \approx \frac{s}{N} + \sum_{i|p_i=1} \frac{P(A|x^i)}{N}. \tag{E.4}$$

Now it is easy to see that the algorithm in Section 3.1.1 is consistent with the approximation obtained in (E.4).

Appendix F

Proof that Baldi's Approach is Sharp Large Deviations Estimate

In this section, we show that the Large Deviations Estimate for $P(E_1 \cup, \ldots, \cup E_d)$ described in Section 2.1.2, is indeed a Sharp Large Deviations Estimate. This will imply, by Theorem 2.1 by Baldi(1999), that we can express

$$P^{\epsilon}_{\mathbf{X},0}\{\tau \leq 1\} = \exp(-\frac{u(\mathbf{x},0)}{\epsilon})(1 + o(\epsilon^m)), \tag{F.1}$$

where m is an arbitrary positive number and τ is defined as the exit time from the region D defined by a set of linear boundaries. We would refer to these boundaries as $B_1, B_2, \ldots, B_d$.

In order to show (F.1), we need to show that, in our problem, $\omega(x,s) = 1$ and $\psi_i(x,s), i = 1, \ldots,$ vanish in the expression given by Theorem 1.2.2. Without loss of generality, we can assume that the underlying multivariate Brownian Bridge

process is an uncorrelated one because, as shown in Section 2.1.2, we can transform a correlated process to an uncorrelated one.

According to Baldi (1995), the theory of Large Deviations states that when the most likely path γ of breaching a barrier is unique, the barrier crossing probability, $P^{\varepsilon}\{\tau \leq T\}$ is asymptotically the same as $P^{\varepsilon}\{\tau \leq T\, X^{\varepsilon} \in B_{\delta}(\gamma))\}$ where $B_{\delta}(\gamma))$ denotes the neighbourhood (a tube) of radius δ of γ and τ is the first time the barrier is breached. Since D is defined by a set of linear boundaries, $B_1, \ldots, B_d$, let B_i^* denote the linear boundary that the most likely path γ touches and let E_i^* be the half-space defined by B_i^*.

Assume that B_i^* is unique. This is a reasonable assumption in our application because the probability that we have non-unique B_i^* is 0 due to the fact that the terminal values are generated from a continuous distribution. Under this assumption, we have

$$\begin{aligned} & P^{\epsilon}_{x,0}\{\tau \leq 1\} && \text{(F.2)} \\ = \;& P^{\epsilon}_{x,0}\{\tau \leq 1, X^{\epsilon} \in B_{\delta}(\gamma)\} && \text{(F.3)} \\ = \;& P^{\epsilon}_{x,0,E_i^*}\{\tau \leq 1\}, && \text{(F.4)} \end{aligned}$$

where (F.4) is the probability that the process $X(t)$ exits the half-space E_i^*. Note that the equalities refer to the asymptotic equality as $\epsilon \to 0$.

By Theorem 1.2.2 and (1.14), we have

$$P^{\epsilon}_{x,0,E_i^*}\{\tau \leq 1\} = \exp(-\frac{u(\mathbf{x}, 0)}{\epsilon})(1 + o(\epsilon^m)) \qquad \text{(F.5)}$$

for all $m > 0$, as shown by Example 4.5 of Baldi et al. (1999). Combining (F.5) and (F.4), we can conclude that

$$P^{\epsilon}_{x,0}\{\tau \leq 1\} = \exp(-\frac{u(\mathbf{x}, 0)}{\epsilon})(1 + o(\epsilon^m)) \tag{F.6}$$

for every $m > 0$. Hence, the Large Deviations estimate for the exit probability from the region D is a Sharp Large Deviations estimate.